doi.org/10.26434/chemrxiv.12084672.v1

Stereoselective Synthesis of Unnatural α-Amino Acids through Photoredox Catalysis

Andrey Shatskiy, Anton Axelsson, Björn Blomkvist, Jian-Quan Liu, Peter Dinér, Markus Kärkäs

Submitted date: 05/04/2020 • Posted date: 07/04/2020

Citation information: Shatskiy, Andrey; Axelsson, Anton; Blomkvist, Björn; Liu, Jian-Quan; Dinér, Peter; Kärkäs, Markus (2020): Stereoselective Synthesis of Unnatural α-Amino Acids through Photoredox Catalysis. ChemRxiv. Preprint. https://doi.org/10.26434/chemrxiv.12084672.v1

A protocol for stereoselective C-radical addition to a chiral glyoxylate-derived sulfinyl imine was developed through visible light-promoted photoredox catalysis, providing a convenient method for the synthesis of unnatural α-amino acids. The developed protocol allows the use of ubiquitous carboxylic acids as radical precursors without prior derivatization. The protocol utilizes near-stoichiometric amounts of the imine and the acid radical precursor in combination with a catalytic amount of an organic acridinium-based photocatalyst. The mechanism for the developed transformation is discussed and the stereodetermining radical addition step was studied by the DFT calculations.

Stereoselective Synthesis of Unnatural α-Amino Acids through Photoredox Catalysis

Andrey Shatskiy,[†] Anton Axelsson,[†] Björn Blomkvist,[†] Jian-Quan Liu,[†] Peter Dinér,[†] and Markus D. Kärkäs[,†]*

[†] Department of Chemistry, KTH Royal Institute of Technology, SE-100 44 Stockholm, Sweden

Abstract

A protocol for stereoselective *C*-radical addition to a chiral glyoxylate-derived sulfinyl imine was developed through visible light-promoted photoredox catalysis, providing a convenient method for the synthesis of unnatural α-amino acids. The developed protocol allows the use of ubiquitous carboxylic acids as radical precursors without prior derivatization. The protocol utilizes near-stoichiometric amounts of the imine and the acid radical precursor in combination with a catalytic amount of an organic acridinium-based photocatalyst. The mechanism for the developed transformation is discussed and the stereodetermining radical addition step was studied by the DFT calculations.

Keywords: *amino acids, carboxylic acids, decarboxylation, organic photocatalyst, photoredox catalysis, stereoselective synthesis*

Introduction

Unnatural α-amino acids constitute an important class of biologically relevant compounds that are widely used in both pharmaceutical industry and fundamental research.[1] A number of pharmaceuticals based on unnatural α-amino acids are currently on the market, including ACE inhibitors for the treatment of cardiovascular and renal diseases,[2] antiviral medicines,[3] and others.[4] Most recently, several drug target studies addressing the globally threatening respiratory disease COVID-19 caused by the SARS-CoV-2 coronavirus were released.[5] Therein, a number of unnatural α-amino acid-based drug candidates were identified, in particular peptidomimetic α-ketoamide inhibitors, demonstrating the high demand for such building blocks in the present time.

A variety of synthetic strategies to access unnatural amino acid derivatives have been developed over the years, with some notable methods being the catalytic asymmetric Strecker-type reactions, asymmetric hydrogenation of dehydroamino acids, and electrophilic and nucleophilic alkylation of glycine derivatives (Figure 1).[6] Among these, functionalization or reduction of α-imino esters offers a straightforward route to various enantiomerically enriched α-amino acids.[7] Traditionally, these strategies have employed polar retrosynthetic disconnections, which often require the use of (super)stoichiometric amounts of toxic and highly sensitive reagents at low temperatures, thereby limiting the substrate scope and practicality for scale up of these reactions. These limitations have recently been challenged by re-introduction of free radical reaction manifolds, aided by developments in base-metal catalysis,[8] electrosynthesis[9] and photoredox catalysis.[10] Radical addition to imines through photoredox catalysis was recently demonstrated in symmetric[11] and asymmetric[12] fashion. In 2017, Alemán and co-workers reported a protocol for asymmetric radical addition to imines mediated by visible light.[12] The developed catalytic system made use of a chiral sulfoxide auxiliary group, commonly employed in the synthesis of chiral amines.[13] Here, the *C*-centered radical was generated through visible light-mediated reductive cleavage of the N–O bond in a redox-active phthalimide ester, followed by radical addition to the sulfinyl imine. The reductive nature of the

protocol necessitates a stoichiometric amount of a reducing agent (Hanztsch ester) to be used. More recently, a related Ni-based catalytic system was described by Baran and co-workers.[14] This protocol also employed a redox-active ester as the radical precursor, with Zn as a stoichiometric reducing agent and a Ni-based catalyst for mediating the C–C bond formation. Although this protocol displayed an impressive substrate scope, it is associated with moderate atom-economy, limiting its applicability for large-scale synthesis.

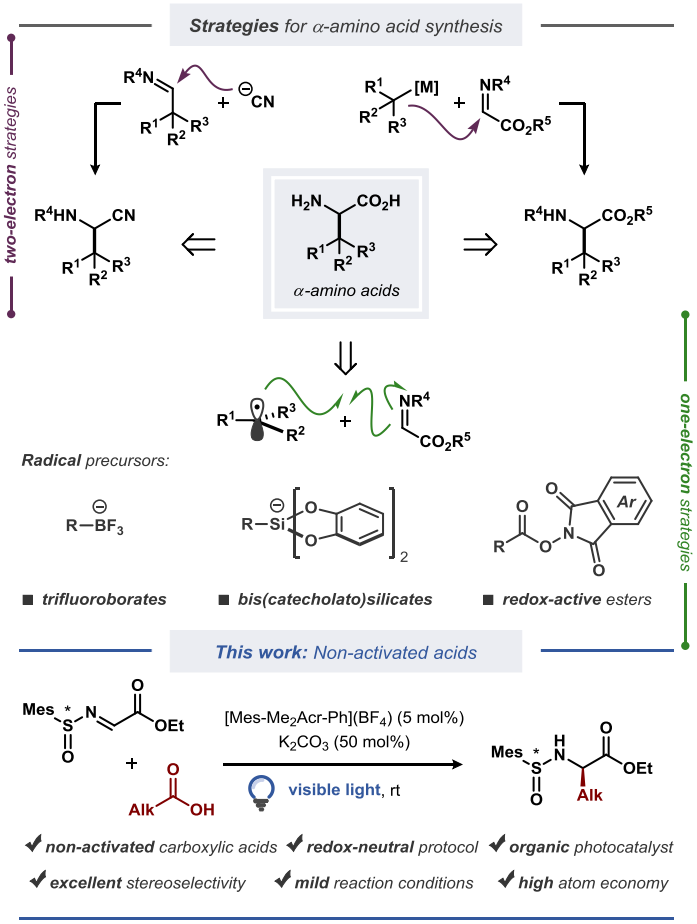

Figure 1. Strategies for synthesis of unnatural α-amino acids (top), and diastereoselective decarboxylative alkylation of sulfinyl imines with non-activated carboxylic acids (bottom).

Results and Discussion

Inspired by the catalytic systems developed by the Alemán,[12] Ye,[11a] and Baran[13] groups, we sought to realize a protocol for diastereoselective decarboxylative radical addition to chiral sulfinyl imines that

would utilize ubiquitous non-activated carboxylic acids as radical precursors.[15] A related direct decarboxylative addition process was attempted by the Alemán group for a benzaldehyde-derived sulfinyl imine under reaction conditions reported by MacMillan;[16] however, no formation of the desired product was observed (see the Supporting Information to ref. 12). Similarly, we observed no desired product with pivalic acid **2a** as the radical precursor and sulfinyl imine **1** as the radical acceptor when the reaction was conducted in DMSO with $[Ir(dF(CF_3)ppy)_2(dtbbpy)](PF_6)$ as photocatalyst (Table 1, entry 1), presumably due to fast decomposition of sulfinyl imine **1**. Gratifyingly, changing the solvent to α,α,α-trifluorotoluene ($PhCF_3$) furnished the desired product **3a** in fairly good yield of 65%, although with poor diastereoselectivity (Table 1, entry 2). Using other bases in place of Cs_2CO_3 completely prohibited the reaction (for details on the optimization studies, see the Supporting Information), and the highly-oxidizing photocatalyst 4CzIPN[17] failed to deliver the radical addition product (Table 1, entry 3). Fortunately, the highly-oxidizing organic acridinium-based photocatalyst $[Mes\text{-}Acr\text{-}Me](BF_4)$ delivered product **3a** with excellent diastereoselectivity, although in poor yield (Table 1, entry 4). Increasing the catalyst loading from 1 to 5 mol% and switching to the more stable *N*-phenyl-substituted photocatalysts $[Mes\text{-}Acr\text{-}Ph](BF_4)$ and $[Mes\text{-}Me_2Acr\text{-}Ph](BF_4)$[18] dramatically increased the yield of the stereoselective radical addition product up to 78% (Table 1, entries 5–7). Changing the base to K_2CO_3 and increasing the base loading further improved the yield up to 85% (Table 1, entry 11). Finally, utilizing a slight excess of the acid radical precursor **2a** delivered the desired product **3a** in excellent yields (91% and 95% for 1.2 and 1.5 equiv. of **2a**, respectively; Table 1, entries 13 and 14). Consistently with the previous reports on radical additions to sulfinyl imines, the *tert*-butyl- and *para*-tolyl-substituted sulfinyl imines **4** and **5** proved to be inefficient as radical acceptors (Table 1, entries 15 and 16).[12,14] In case of *tert*-butyl-substituted sulfinyl imine **4**, it is likely that the transiently formed

Table 1. Optimization of the reaction conditions for the decarboxylative radical addition to a glyoxylate-derived sulfinyl imine.[a]

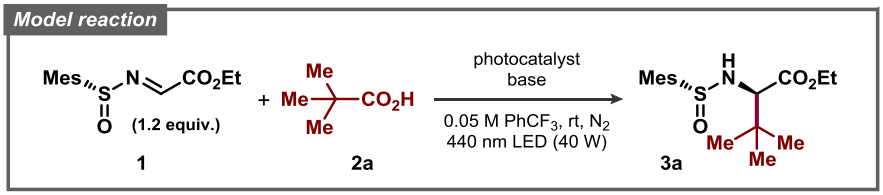

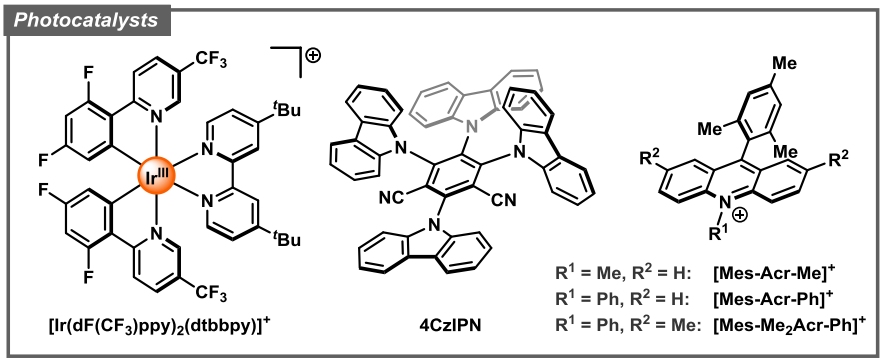

entry	*photocatalyst*	*base*	*time*	*yield*[b]	*dr*[b]
1[c]	[Ir(dF(CF$_3$)ppy)$_2$(dtbbpy)](PF$_6$), 1 mol%	Cs$_2$CO$_3$, 0.2 equiv.	20 min	< 5%	–
2	[Ir(dF(CF$_3$)ppy)$_2$(dtbbpy)](PF$_6$), 1 mol%	Cs$_2$CO$_3$, 0.2 equiv.	20 min	65%	**4 : 1**
3	4CzIPN, 1 mol%	Cs$_2$CO$_3$, 0.2 equiv.	20 min	< 5%	—
4	[Mes-Acr-Me](BF$_4$), 1 mol%	Cs$_2$CO$_3$, 0.2 equiv.	20 min	27%	> 95 : 5
5	[Mes-Acr-Me](BF$_4$), 5 mol%	Cs$_2$CO$_3$, 0.2 equiv.	20 min 60 min	48% 66%	> 95 : 5 > 95 : 5
6	[Mes-Acr-Ph](BF$_4$), 5 mol%	Cs$_2$CO$_3$, 0.2 equiv.	60 min	73%	> 95 : 5
7	[Mes-Me$_2$Acr-Ph](BF$_4$), 5 mol%	Cs$_2$CO$_3$, 0.2 equiv.	60 min	78%	> 95 : 5
8	[Mes-Me$_2$Acr-Ph](BF$_4$), 5 mol%	K$_3$PO$_4$, 0.2 equiv.	60 min	80%	> 95 : 5
9	[Mes-Me$_2$Acr-Ph](BF$_4$), 5 mol%	K$_2$CO$_3$, 0.2 equiv.	60 min	84%	> 95 : 5
10	[Mes-Me$_2$Acr-Ph](BF$_4$), 5 mol%	K$_2$CO$_3$, 0.05 equiv.	20 min	< 5%	—
11	[Mes-Me$_2$Acr-Ph](BF$_4$), 5 mol%	K$_2$CO$_3$, 0.5 equiv.	60 min	85%	> 95 : 5
12[d]	[Mes-Me$_2$Acr-Ph](BF$_4$), 5 mol%	K$_2$CO$_3$, 0.5 equiv.	60 min	77%	> 95 : 5
13[e]	**[Mes-Me$_2$Acr-Ph](BF$_4$), 5 mol%**	**K$_2$CO$_3$, 0.5 equiv.**	**60 min**	**91%**	**> 95 : 5**
14[f]	[Mes-Me$_2$Acr-Ph](BF$_4$), 5 mol%	K$_2$CO$_3$, 0.5 equiv.	60 min	95%	> 95 : 5
15	As **entry 13**, but with ^{t}Bu-sulfinyl imine **4**		60 min	< 5%	—
16	As **entry 13**, but with *p*-Tol-sulfinyl imine **5**		60 min	50%	7 : 1
	deviations from the conditions in entry 13				
17	under air		60 min	12%	> 95 : 5
18	no photocatalyst		60 min	< 5%	—
19	no light		60 min	< 5%	—

[a] The reactions were performed on 0.1 mmol scale: stock solutions of the pivalic acid **2** and the photocatalyst (each in 1 mL of the solvent) were mixed with the sulfinyl imine **1** and the base under anhydrous conditions, and stirred under irradiation with 440 nm blue LED light at room temperature (for details, see the Supporting Information). [b] Determined by ^{1}H NMR of a crude reaction mixture with 1,3,5-trimethoxybenzene as an internal standard. [c] 0.1 M DMSO. [d] 0.1 M PhCF$_3$. [e] 1.0 equiv. of sulfinyl imine **1** and 1.2 equiv. of pivalic acid **2**. [f] 1.0 equiv. of sulfinyl imine **1** and 1.5 equiv. of pivalic acid **2**.

aminyl radical intermediate underwent decomposition to form an iminosulfanone (–N=S=O), thereby disrupting the catalytic cycle.[19]

The substrate scope of the developed transformation was evaluated with a variety of commercially available tertiary, secondary, and primary carboxylic acids (Figure 2). For all of the amino acid derivatives, except product **3f**, excellent diastereoselectivity at the α-position was observed (>95:5 *dr*). The unfunctionalized tertiary carboxylic acids **2a** and **2c** delivered the radical addition products **3a** and **3c** in high yields (81% and 87%, respectively). The potentially oxidatively sensitive gemfibrozil-derived product **3b** could also be accessed, although in lower yield (44%). Surprisingly, *N*-Boc-piperidine-derived product **3d** was obtained in relatively low yield (33%), while oxetane- and cyclopropyl-containing carboxylic acids **2e** and **2f** delivered the corresponding products **3e** and **3f** in moderate yields (54% and 52%, respectively). The cyclohexyl radical addition adduct **3h** was obtained in high yield (73%), while other non-stabilized secondary and primary carboxylic acids **2l–k** provided lower yields compared to the tertiary acids, consistent with previous reports featuring secondary and primary free radical intermediates under related conditions.[20] Further optimization of the reaction conditions for the primary acids **2j** and **2k** did not result in improved yields (Tables S2 and S3), illustrating the intrinsic instability of the respective radical intermediates and/or the photocatalyst under the employed conditions.

Next, we surveyed carboxylic acid radical precursors that furnish stabilized α-heteroatom *C*-radicals. Gratifyingly, *N*-Boc-protected α-amino acid radical precursors based on pipecolic acid, proline, valine, and phenylalanine provided the expected amino acid derivatives **3l–o** in generally excellent yields (up to >99%), exemplifying a prominent synthetic route to biologically active α,β-diamino acids.[21] The α-*O*-substituted radicals derived from tetrahydro-2-furonic and methoxymandelic acids provided the expected radical addition products **3p** and **3q** in 45% and 60% yields, respectively. A tertiary α-*O*-substituted radical derived from clofibric acid **2g** delivered product **3g** in excellent yield (90%). Interestingly, products **3n–q** were obtained not only with

excellent diastereoselectivity at the α-position (>95:5 *dr*), but also with a slight diastereoselectivity at the β-position (up to 1.5:1 *dr*). In general, the acids with strong electron-withdrawing substituents at the α-position (CF_3, benzyl, and benzoyl) did not provide the desired products, likely due to the insufficient nucleophilic character of the formed *C*-radicals (see the unsuccessful substrates in Figure 2). The α-H and α-Me-substituted cyclopropanecarboxylic acids were also inefficient, despite successful reaction with the analogous α-Ph-substituted substrate **2f**.

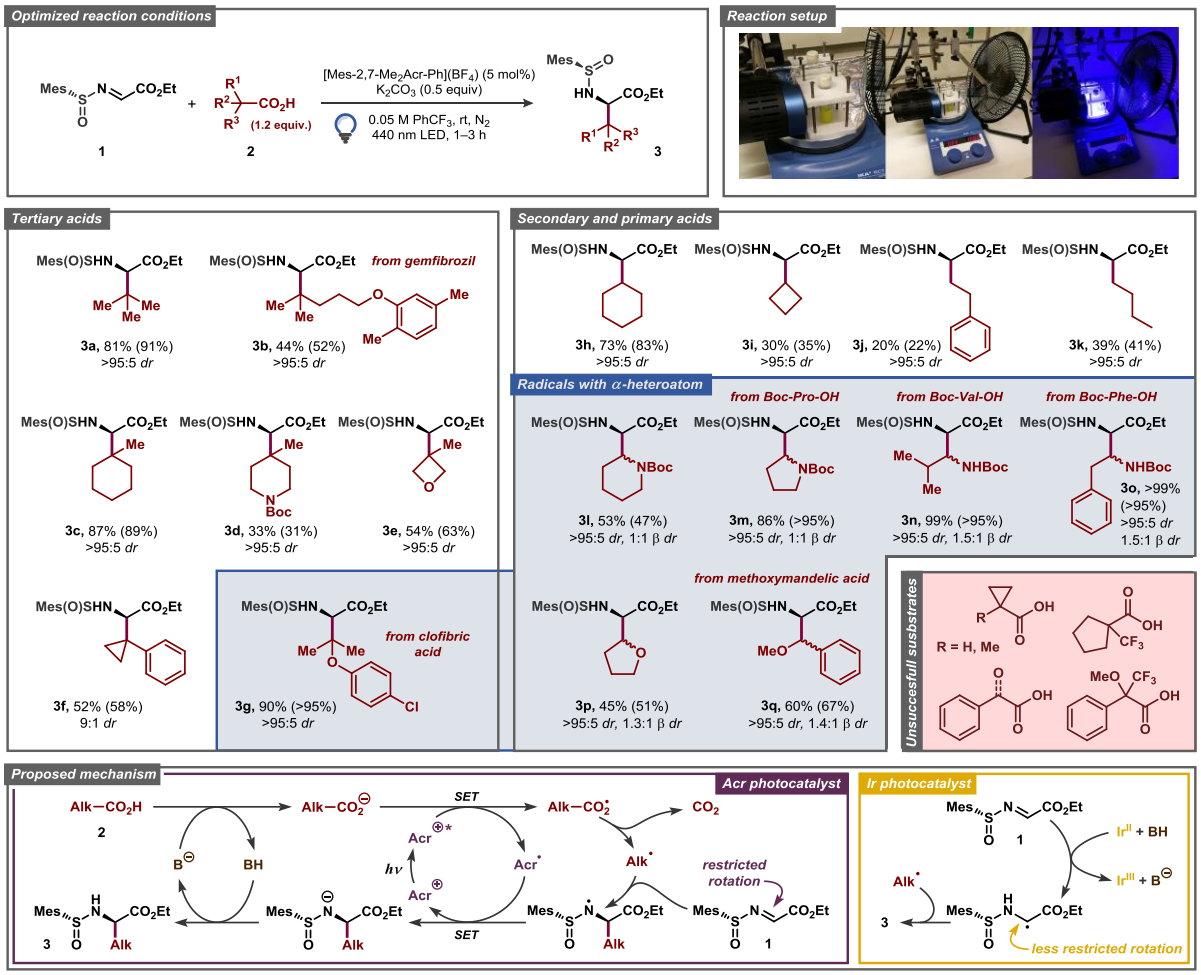

Figure 2. Substrate scope for the decarboxylative radical addition to glyoxylate-derived sulfinyl imine **1** to furnish the unnatural amino acid precursors **3**. The isolated yields of the products and NMR-yields from the crude reaction mixtures (in parenthesis) are reported (see the Supporting Information for details). [a] 1 mmol scale reaction.

Based on previous literature precedents, a mechanism for the developed transformation was proposed (Figure 2, bottom).[12,22] Initially, the acridinium photocatalyst [Mes-Me_2Acr-Ph](BF_4) (Acr^+) is excited by visible light (λ_{max} ≈ 425 nm) to a highly oxidizing excited state Acr^+* ($E(Acr^+*/Acr^\bullet)$ ≈ 2.09 V vs. SCE).[23] In this state, the photocatalyst can abstract an electron from the deprotonated carboxylic acid *via* a single-electron transfer (SET) event to generate a carboxylate radical while being reduced to the acridinium radical $Acr^\bullet$. The carboxyl radical then extrudes CO_2 to form a *C*-centered radical, which undergoes addition to the sulfinyl imine **1** in the key step of the reaction, forming an α-alkylated *N*-centered radical. Finally, the *N*-centered radical is reduced by $Acr^\bullet$, closing the photocatalytic cycle and furnishing the desired product **3** upon protonation.

An alternative mechanism for a related radical addition process to imine derivatives was proposed by Ooi and co-workers.[24] Here, the key C–C bond-forming step was found to proceed through radical-radical coupling between a *C*-centered radical and an azaketyl-type radical. However, under our conditions such a mechanistic pathway seems unlikely due to weak reducing ability of the one-electron reduced form of the employed acridinium photocatalyst ($E(Acr^+/Acr^\bullet)$ ≈ −0.58 V vs. SCE). As opposed to the conditions reported by Ooi and co-workers, where strongly reducing $[Ir(ppy)_2(bpy)]^+$-type photocatalysts ($E(Ir^{III}/Ir^{II})$ ≈ −1.5 V vs. SCE) were used, electron transfer from $Acr^\bullet$ to sulfinyl imine **1** (E_p ≈ −1.1 V vs. SCE, as determined by cyclic voltammetry) should not be favored. Notably, a shift to an Ooi-type radical-radical coupling pathway could explain the low diastereoselectivity (4:1 *dr*) during formation of product **3a** when the reaction was conducted with the $[Ir(dF(CF_3)ppy)_2(dtbbpy)](PF_6)$ photocatalyst (Table 1, entry 2; Figure 2, bottom right). The low diastereoselectivity could also be explained by product epimerization during the reaction; however, no epimerization was observed when product **3a** was subjected to the comparable reaction conditions.

In order to gain better understanding of the stereodetermining C–C bond forming step in the proposed mechanism with acridinium-based photocatalyst DFT calculations were performed on the

M062X-D3/6-311+G(d,p) level of theory (see the Supporting Information for details). First, the structure of the sulfinyl imine radical acceptor **1** was evaluated. Previously, Alemán and co-workers tentatively suggested an *s-cis* conformation around the N–S bond as being more stable in this compound due to the hydrogen bonding between the imine proton and the sulfoxide oxygen (Figure 3).[12] Such a conformational preference would then lead to the α-(*R*) product when the S(*R*)-sulfinyl imine is employed as the radical acceptor. This stereochemical outcome was indeed observed for both Alemán´s and our catalytic system. The calculations confirmed that the *s-cis* conformer is more stable compared to the *s-trans* by 3.8 kcal/mol, corresponding to >99.8:0.2 ratio between the conformers from the Boltzmann distribution at room temperature. In the *s-cis* conformer the expected constructive orbital overlap was observed between the imine hydrogen and the sulfoxide oxygen, while for the *s-trans* conformer the constructive, but weaker, orbital overlap was found between the imine hydrogen and the carbonyl oxygen of the ester group (for a detailed discussion, see the Supporting Information).

Subsequently, the radical addition step was evaluated with the *tert*-butyl radical donor producing product **3a**, and the computed Gibbs free energy diagram for the reaction is presented in Figure 3. The formation of (*R*,*R*)-diastereomer of **3a** was found to be favored both kinetically and thermodynamically and the computed activation barrier was found to be 3.8 kcal/mol smaller for the *re*-addition compared to the *si*-addition, while the (*R*,*R*)-diastereomer product is 2.5 kcal/mol more stable compared to the (*R*,*S*)-diastereomer. The better stabilization of the *re*-TS is in part due to the stronger hydrogen bonding between the imine hydrogen and the sulfoxide oxygen for this transition state, as evident from the calculated bond distances and the visualized molecular orbitals (Figure S3). Additionally, significant sterical crowding occurs in the *si*-TS, where the incoming *tert*-butyl radical requires the mesityl group to become almost completely coplanar to the sulfoxide S=O bond. In contrast, the mesityl group and the S=O bond in the *re*-TS are out of plane by 50° while the incoming *tert*-butyl radical experiences no sterical crowding (Figure 3).

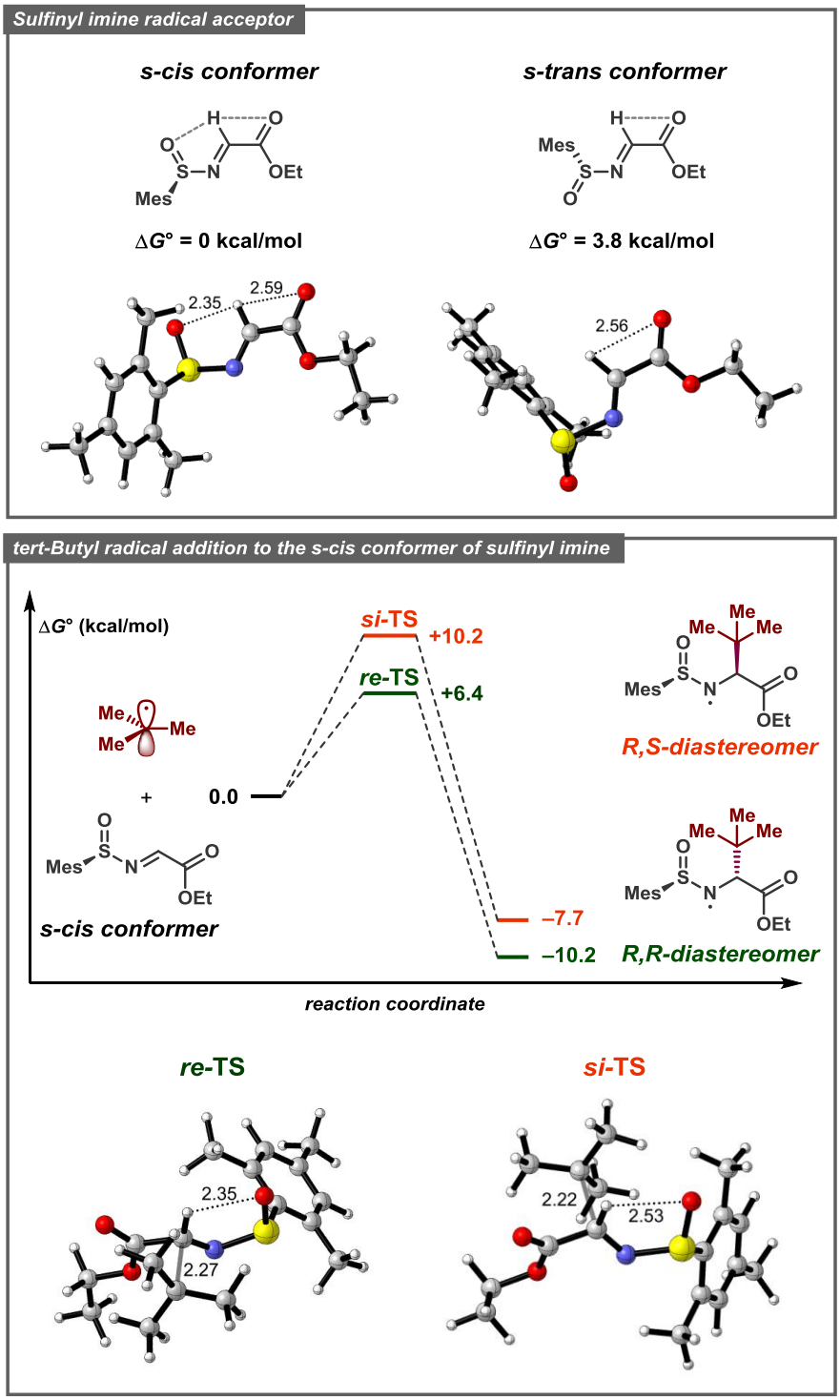

Figure 3. Calculated structures with selected bond distances (Å) for the *s-cis* and *s-trans* isomers of sulfinyl imine **1** (*top*), Gibbs free energy diagram for *tert*-butyl radical addition to **1** (*middle*), and calculated structures for the *re*-TS and *si*-TS transition states (*bottom*).

Conclusions

A practical protocol for stereoselective synthesis of various α-amino acids has been developed, employing ubiquitous carboxylic acids as radical precursors and an organic photocatalyst under visible light irradiation. This protocol allows for synthesis of highly functionalized α-amino acids, which are challenging to prepare through traditional two-electron reaction manifolds. The protocol utilizes near-stoichiometric amounts of reagents and does not produce large quantities of waste, which is an intrinsic disadvantage of the previously described systems utilizing redox-active esters as radical precursors.

ORCID

Andrey Shatskiy: 0000-0002-7249-7437

Anton Axelsson: 0000-0003-0899-2852

Björn Blomkvist: 0000-0001-6026-1921

Jian-Quan Liu: 0000-0002-5533-2075

Peter Dinér: 0000-0001-6782-6622

Markus D. Kärkäs: 0000-0002-6089-5454

Notes

The authors declare no competing financial interest.

Acknowledgements

Financial support from KTH Royal Institute of Technology to M.D.K. is gratefully acknowledged. The Olle Engkvists Stiftelse and the Wenner-Gren Foundations are kindly acknowledged for postdoctoral fellowships to A.S. and J.L., respectively. P.D. acknowledges financial support from the Carl Trygger Foundation for a postdoctoral fellowship to A.A.

References

(1) (a) Ravikumar, Y.; Nadarajan, S. P.; Yoo, T. H.; Lee, C.; Yun, H. Unnatural Amino Acid Mutagenesis-Based Enzyme Engineering. *Trends in Biotechnology* **2015**, *33*, 462–470. (b) Blaskovich, M. A. T. Unusual Amino Acids in Medicinal Chemistry. *J. Med. Chem.* **2016**, *59*, 10807−10836. (c) Neumann-Staubitz, P.; Neumann, H. The Use of Unnatural Amino Acids to Study and Engineer Protein Function. *Current Opinion in Structural Biology* **2016**, *38*, 119–128.

(2) Arora, P. K.; Chauhan, A. ACE Inhibitors: A Comprehensive Review. *International Journal of Pharmaceutical Sciences and Research* **2013**, *3*, 532–549.

(3) De Clercq, E.; Li, G. Approved Antiviral Drugs over the Past 50 Years. *Clinical Microbiology Reviews* **2016**, *29*, 695–747.

(4) (a) Miller, L. M.; Pritchard, J. M.; Macdonald, S. J. F.; Jamieson, C.; Watson, A. J. B. Emergence of Small-Molecule Non-RGD-Mimetic Inhibitors for RGD Integrins. *J. Med. Chem.* **2017**, *60*, 3241–3251. (b) Giraud, I.; Rapp, M.; Maurizis, J.-C.; Madelmont, J.-C. Synthesis and in vitro Evaluation of Quaternary Ammonium Derivatives of Chlorambucil and Melphalan, Anticancer Drugs Designed for the Chemotherapy of Chondrosarcoma. *J. Med. Chem.* **2002**, *45*, 2116–2119. (c) Ankersen, M.; Johansen, N. L.; Madsen, K.; Hansen, B. S.; Raun, K.; Nielsen, K. K.; Thøgersen, H.; Hansen, T. K.; Peschke, B.; Lau, J.; Lundt, B. F.; Andersen, P. H. A New Series of Highly Potent Growth Hormone-Releasing Peptides Derived from Ipamorelin. *J. Med. Chem.* **1998**, *41*, 3699–3704.

(5) (a) Gordon, D. E.; Jang, G. M.; Bouhaddou, M.; Xu, J.; Obernier, K.; O'Meara, M. J.; Guo, J. Z.; Swaney, D. L.; Tummino, T. A.; Huettenhain, R.; Kaake, R. M.; Richards, A. L.; Tutuncuoglu, B.; Foussard, H.; Batra, J.; Haas, K.; Modak, M.; Kim, M.; Haas, P.; Polacco, B. J.; Braberg, H.; Fabius, J. M.; Eckhardt, M.; Soucheray, M.; Bennett, M. J.; Cakir, M.; McGregor, M. J.; Li, Q.; Naing, Z. Z. C.; Zhou, Y.; Peng, S.; Kirby, I. T.; Melnyk, J. E.; Chorba, J. S.; Lou, K.; Dai, S. A.; Shen, W.; Shi, Y.; Zhang, Z.; Barrio-Hernandez, I.; Memon, D.; Hernandez-Armenta, C.; Mathy, C. J. P.; Perica, T.; Pilla, K. B.; Ganesan, S. J.; Saltzberg, D. J.; Ramachandran, R.; Liu, X.; Rosenthal, S. B.; Calviello,

L.; Venkataramanan, S.; Liboy-Lugo, J.; Lin, Y.; Wankowicz, S. A.; Bohn, M.; Sharp, P. P.; Trenker, R.; Young, J. M.; Cavero, D. A.; Hiatt, J.; Roth, T. L.; Rathore, U.; Subramanian, A.; Noack, J.; Hubert, M.; Roesch, F.; Vallet, T.; Meyer, B.; White, K. M.; Miorin, L.; Rosenberg, O. S.; Verba, K. A.; Agard, D.; Ott, M.; Emerman, M.; Ruggero, D.; García-Sastre, A.; Jura, N.; von Zastrow, M.; Taunton, J.; Ashworth, A.; Schwartz, O.; Vignuzzi, M.; d'Enfert, C.; Mukherjee, S.; Jacobson, M.; Malik, H. S.; Fujimori, D. G.; Ideker, T.; Craik, C. S.; Floor, S.; Fraser, J. S.; Gross, J.; Sali, A.; Kortemme, T.; Beltrao, P.; Shokat, K.; Shoichet, B. K.; Krogan, N. J. A SARS-CoV-2-Human Protein-Protein Interaction Map Reveals Drug Targets and Potential Drug-Repurposing. *bioRxiv* **2020**, DOI:10.1101/2020.03.22.002386. (b) Zhang, L.; Lin, D.; Sun, X.; Curth, U.; Drosten, C.; Sauerhering, L.; Becker, S.; Rox, K.; Hilgenfeld, R. Crystal Structure of SARS-CoV-2 Main Protease Provides a Basis for Design of Improved α-Ketoamide Inhibitors. *Science* **2020**, DOI:10.1126/science.abb3405. (c) Zhang, L.; Lin, D.; Kusov, Y.; Nian, Y.; Ma, Q.; Wang, J.; von Brunn, A.; Leyssen, P.; Lanko, K.; Neyts, J.; de Wilde, A.; Snijder, E. J.; Liu, H.; Hilgenfeld, R. α-Ketoamides as Broad-Spectrum Inhibitors of Coronavirus and Enterovirus Replication: Structure-Based Design, Synthesis, and Activity Assessment. *J. Med. Chem.* **2020**, DOI: 10.1021/acs.jmedchem.9b01828. (d) Liu, C.; Zhou, Q.; Li, Y.; Garner, L. V.; Watkins, S. P.; Carter, L. J.; Smoot, J.; Gregg, A. C.; Daniels, A. D.; Jervey, S.; Albaiu, D. Research and Development on Therapeutic Agents and Vaccines for COVID-19 and Related Human Coronavirus Diseases. *ACS Cent. Sci.* **2020**, *6*, 315–331.

(6) (a) Nájera, C.; Sansano, J. M. Catalytic Asymmetric Synthesis of α-Amino Acids. *Chem. Rev.* **2007**, *107*, 4584–4671. (b) Liu, J.-Q.; Shatskiy, A.; Matsuura, B. S.; Kärkäs, M. D. Recent Advances in Photoredox Catalysis Enabled Functionalization of α-Amino Acids and Peptides: Concepts, Strategies and Mechanisms. *Synthesis* **2019**, *51*, 2759–2791. (c) Ma, J.-A. Recent Developments in the Catalytic Asymmetric Synthesis of α- and β-Amino Acids. *Angew. Chem., Int. Ed.* **2003**, *42*, 4290–4299.

(7) Eftekhari-Sis, B.; Zirak, M. α-Imino Esters in Organic Synthesis: Recent Advances. *Chem. Rev.* **2017**, *117*, 8326–8419.

(8) (a) Weix, D. J. Methods and Mechanisms for Cross-Electrophile Coupling of Csp^2 Halides with Alkyl Electrophiles. *Acc. Chem. Res.* **2015**, *48*, 1767–1775. (b) Gandeepan, P.; Müller, T.; Zell, D.; Cera, G.; Warratz, S.; Ackermann, L. 3d Transition Metals for C–H Activation. *Chem. Rev.* **2019**, *119*, 2192–2452. (c) Kaga, A.; Chiba, S. Engaging Radicals in Transition Metal-Catalyzed Cross-Coupling with Alkyl Electrophiles: Recent Advances. *ACS Catal.* **2017**, *7*, 4697–4706. (d) Milan, M.; Salamone, M.; Costas, M.; Bietti, M. The Quest for Selectivity in Hydrogen Atom Transfer Based Aliphatic C–H Bond Oxygenation. *Acc. Chem. Res.* **2018**, *51*, 1984–1995.

(9) For leading reviews on organic electrosynthesis, see: (a) Shatskiy, A.; Lundberg, H.; Kärkäs, M. D. Organic Electrosynthesis: Applications in Complex Molecule Synthesis. *ChemElectroChem* **2019**, *6*, 4067–4092. (b) Möhle, S.; Zirbes, M.; Rodrigo, E.; Gieshoff, T.; Wiebe, A.; Waldvogel, S. R. Modern Electrochemical Aspects for the Synthesis of Value-Added Organic Products. *Angew. Chem., Int. Ed.* **2018**, *57*, 6018–6041. (c) Yan, M.; Kawamata, Y.; Baran, P. S. Synthetic Organic Electrochemical Methods Since 2000: On the Verge of a Renaissance. *Chem. Rev.* **2017**, *117*, 13230–13319. (d) Kärkäs, M. D. Electrochemical Strategies for C–H Functionalization and C–N Bond Formation. *Chem. Soc. Rev.* **2018**, *47*, 5786–5865.

(10) For leading reviews on photoredox catalysis, see: (a) Shaw, M. H.; Twilton, J.; MacMillan, D. W. C. Photoredox Catalysis in Organic Chemistry. *J. Org. Chem.* **2016**, *81*, 6898–6926. (b) Kärkäs, M. D.; Porco Jr, J. A.; Stephenson, C. R. J. Photochemical Approaches to Complex Chemotypes: Applications in Natural Product Synthesis. *Chem. Rev.* **2016**, *116*, 9683–9747. (c) Romero, N. A.; Nicewicz, D. A. Organic Photoredox Catalysis. *Chem. Rev.* **2016**, *116*, 10075–10166.

(11) (a) Wu, G.; Wang, J.; Liu, C.; Sun, M.; Zhang, L.; Ma, Y.; Cheng, R.; Ye, J. Transition Metal-Free, Visible-Light-Mediated Construction of α,β-Diamino Esters via Decarboxylative Radical Addition at Room Temperature. *Org. Chem. Front.* **2019**, *6*, 2245–2249. (b) Yoshimi, Y.; Kobayashi, K.; Kamakura, H.; Nishikawa, K.; Haga, Y.; Maeda, K.; Morita, T.; Itou, T.; Okada, Y.; Hatanaka, M.

Addition of Alkyl Radicals, Generated from Carboxylic Acids via Photochemical Decarboxylation, to Glyoxylic Oxime Ether: A Mild and Efficient Route to α-Substituted α-Aminoesters. *Tetrahedron Lett*. **2010**, *51*, 2332–2334.

(12) Garrido-Castro, A. F.; Choubane, H.; Daaou, M.; Maestro, M. C.; Alemán, J. Asymmetric Radical Alkylation of *N*-Sulfinimines under Visible Light Photocatalytic Conditions. *Chem. Commun.* **2017**, *53*, 7764–7767.

(13) For selected reviews on the use of chiral sulfoxides in asymmetric synthesis, see: (a) Han, J.; Soloshonok, V. A.; Klika, K. D.; Drabowicz, J.; Wzorek, A. Chiral Sulfoxides: Advances in Asymmetric Synthesis and Problems with the Accurate Determination of the Stereochemical Outcome. *Chem. Soc. Rev.* **2018**, *47*, 1307–1350. (b) Carreño, M. C.; Hernández-Torres, G.; Ribagorda, M.; Urbano, A. Enantiopure Sulfoxides: Recent Applications in Asymmetric Synthesis. *Chem. Commun.* **2009**, 6129–6144.

(14) Ni, S.; Garrido-Castro, A. F.; Merchant, R. R.; deGruyter, J. N.; Schmitt, D. C.; Mousseau, J. J.; Gallego, G. M.; Yang, S.; Collins, M. R.; Qiao, J. X.; Yeung, K.-S.; Langley, D. R.; Poss, M. A.; Scola, P. M.; Qin, T.; Baran, P. S. A General Amino Acid Synthesis Enabled by Innate Radical Cross-Coupling. *Angew. Chem., Int. Ed.* **2018**, *57*, 14560–14565.

(15) Yoshimi, Y. Photoinduced Electron Transfer-Promoted Decarboxylative Radical Reactions of Aliphatic Carboxylic Acids by Organic Photoredox System. *J. Photochem. Photobiol. A: Chemistry* **2017**, *342*, 116–130.

(16) Chu, L.; Ohta, C.; Zuo, Z.; MacMillan, D. W. C. Carboxylic Acids as a Traceless Activation Group for Conjugate Additions: A Three-Step Synthesis of (±)-Pregabalin. *J. Am. Chem. Soc.* **2014**, *136*, 10886–10889.

(17) Shang, T.-Y.; Lu, L.-H.; Cao, Z.; Liu, Y.; He, W.-M.; Yu, B. Recent Advances of 1,2,3,5-Tetrakis(carbazol-9-yl)-4,6-dicyanobenzene (4CzIPN) in Photocatalytic Transformations. *Chem. Commun.* **2019**, *55*, 5408–5419.

(18) Margrey, K. A.; Nicewicz, D. A. A General Approach to Catalytic Alkene Anti-Markovnikov Hydrofunctionalization Reactions via Acridinium Photoredox Catalysis. *Acc. Chem. Res*. **2016**, *49*, 1997–2006.

(19) (a) Huang, W.; Ye, J.-L.; Zheng, W.; Dong, H.-Q.; Wei, B.-G. Radical Migration–Addition of *N*-tert-Butanesulfinyl Imines with Organozinc Reagents. *J. Org. Chem.* **2013**, *78*, 11229–11237. (b) Matos, J.L.M.; Vásquez-Céspedes, S.; Gu, J.; Oguma, T.; Shenvi, R.A. Branch-Selective Addition of Unactivated Olefins into Imines and Aldehydes. *J. Am. Chem. Soc.* **2018**, *140*, 16976–16981.

(20) (a) Kammer, L. M.; Rahman, A.; Opatz, T. A Visible Light-Driven Minisci-Type Reaction with *N*-Hydroxyphthalimide Esters. *Molecules* **2018**, *23*, 764. (b) Davies, J.; Angelini, L.; Alkhalifah, M. A.; Malet Sanz, L.; Sheikh, N. S.; Leonori, D. Photoredox Synthesis of Arylhydroxylamines from Carboxylic Acids and Nitrosoarenes. *Synthesis* **2018**, *50*, 821–830.

(21) (a) Viso, A.; Fernández de la Pradilla, R.; García, A.; Flores, A. α,β-Diamino Acids: Biological Significance and Synthetic Approaches. *Chem. Rev.* **2005**, *105*, 3167–3196. (b) Wang, J.; Zhang, L.; Jiang, H.; Liu, H. Most Efficient Routes for the Synthesis of α,β-Diamino Acid-Derived Compounds. *Current Pharmaceutical Design* **2010**, *16*, 1252–1259.

(22) Fernández-Salas, J. A.; Maestro, M. C.; Rodríguez-Fernández, M. M.; García-Ruano, J. L.; Alonso, I. Intermolecular Alkyl Radical Additions to Enantiopure *N-tert*-Butanesulfinyl Aldimines. *Org. Lett*. **2013**, *15*, 1658–1661.

(23) Note, that the excited state of the acridinium photocatalyst is a biradical and is better represented as $Acr^{\bullet}$–$Mes^{\bullet}$*, see the following paper for details: Fukuzumi, S.; Ohkubo, K. Organic Synthetic Transformations Using Organic Dyes as Photoredox Catalysts. *Org. Biomol. Chem.* **2014**, *12*, 6059–6071.

(24) (a) Uraguchi, D.; Kinoshita, N.; Kizu, T.; Ooi, T. Synergistic Catalysis of Ionic Brønsted Acid and Photosensitizer for a Redox Neutral Asymmetric α-Coupling of *N*-Arylaminomethanes with Aldimines. *J. Am. Chem. Soc.* **2015**, *137*, 13768–13771. (b) Kizu, T.; Uraguchi, D.; Ooi, T.

Independence from the Sequence of Single-Electron Transfer of Photoredox Process in Redox-Neutral Asymmetric Bond-Forming Reaction. *J. Org. Chem.* **2016**, *81*, 6953–6958.

Supporting Information

Stereoselective Synthesis of Unnatural α-Amino Acids through Photoredox Catalysis

Andrey Shatskiy,[†] Anton Axelsson,[†] Björn Blomkvist,[†] Jian-Quan Liu,[†] Peter Dinér,[†] and Markus D. Kärkäs[,†]*

[†] Department of Chemistry, KTH Royal Institute of Technology, SE-100 44 Stockholm, Sweden

E-mail: karkas@kth.se

Table of Contents

1. *Experimental*

Commercial anhydrous α,α,α-trifluorotoluene (Sigma-Aldrich, Art. No. 547948-100ML) was used without further purification. When needed, CH_2Cl_2, MeCN, and Et_3N were dried by refluxing over CaH_2 for several hours followed by distillation, and the dried solvents were used immediately after preparation. 2,2,2-Trifluoroethanol (TFE) and PhF were dried over activated 3 Å molecular sieves. The 4CzIPN photocatalyst was synthesized according to the previously published procedure.[1]

The radical addition reactions were carried out in 4 mL vials (VWR, Screw neck vials N13, Art. No. MANA702962) equipped with a stirring bar (VWR, Art. No. 442-0401) and a septum (VWR, Art. No. 217-0183). The reaction vials were placed in a holder (distance between the reaction vial and the lamp is ca. 2 cm, Figure S1) and illuminated with 440 nm LED (Kessil PR160, set to maximum intensity) with continuous stirring at 1000 rpm. The isolated radical addition products were purified by column chromatography (15–20 cm height, 2 cm inner diameter) with silica gel (high-purity grade, 60 Å, 130–270 mesh, Sigma-Aldrich, Art. No. 288608-1KG) or by preparative TLC (PLC Silica gel 60 F_{254}, 1 mm, 20 x 20 cm, Merck, Art. No. 1.13895).

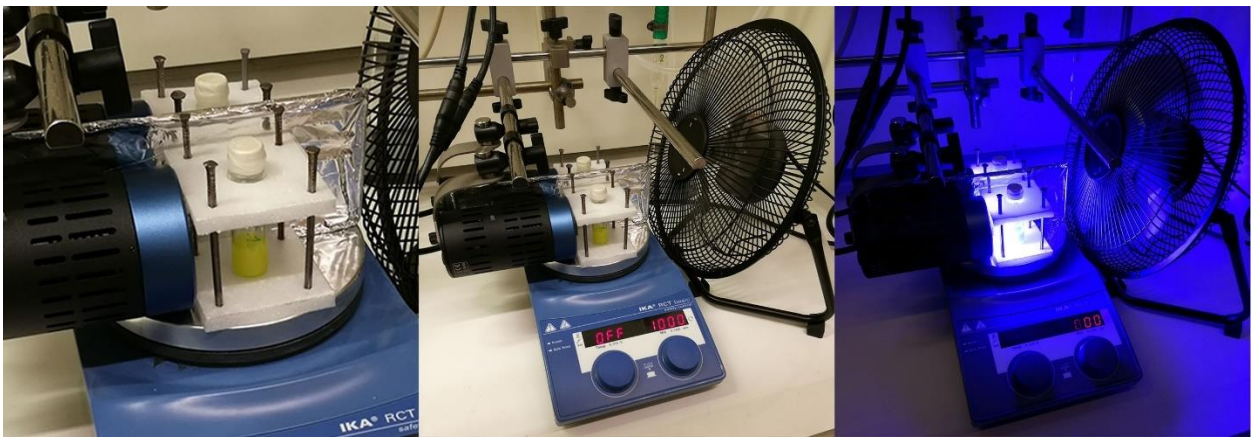

Figure S1. The reaction setup for optimization of the reaction conditions and substrate scope evaluation.

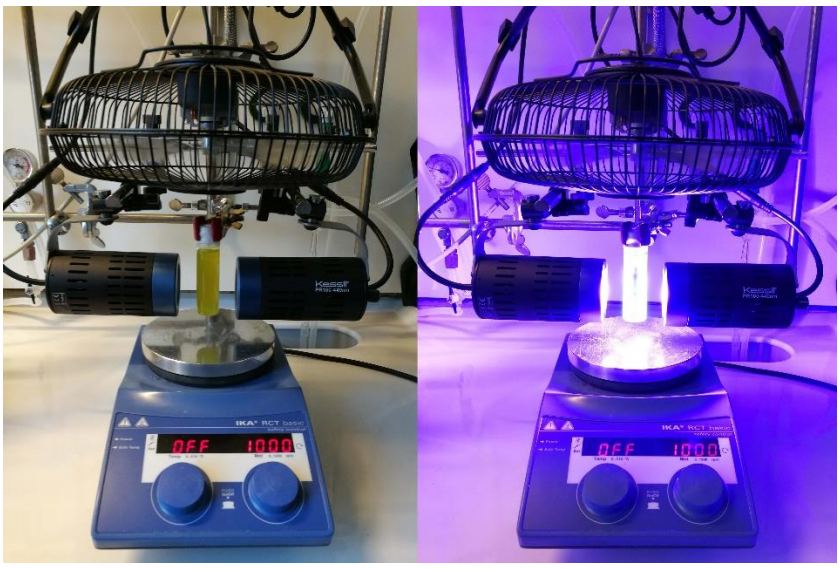

Figure S2. The reaction setup for 1 mmol scale synthesis.

NMR spectra were recorded in $CDCl_3$ on Bruker Avance DMX 500 MHz or Bruker Ascend 400 MHz NMR spectrometers and internally calibrated against the residual undeuterated solvent peaks ($CHCl_3$: δ 7.26 for ^1H NMR and δ 77.16 for ^{13}C NMR). The chemical shifts are reported in ppm and the peak multiplicities are designated as: s (singlet), d (doublet), t (triplet), q (quadruplet), dd (doublet of doublets), td (triplet of doublets), m (multiplet).

2. *General procedure for the synthesis of sulfinyl imines*

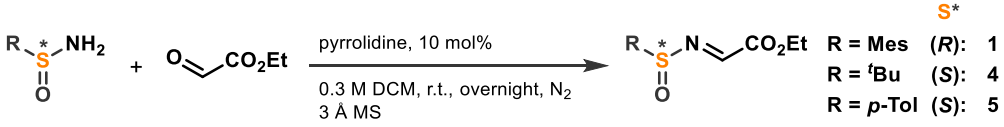

Sulfinyl imines **1**, **4**, and **5** were synthesized according to a procedure adapted from reference [2]. Sulfinyl amide (1 equiv.) and 4 Å activated molecular sieves (2 g per 1 mmol of sulfinyl amide) were placed in a dry 25 mL round-bottom flask equipped with a stirring bar and a septum and evacuated and back-filled with N_2 three times. Anhydrous DCM (0.03 M), ethyl glyoxalate (1 equiv., 50% solution in toluene), and pyrrolidine (10 moil%) were added and the reaction mixture was stirred at room temperature under N_2 balloon. After 19 h the reaction mixture was filtered through celite washing with DCM, and concentrated on rotary evaporator resulting in a crude product as a yellow oil. The crude product was purified by column chromatography (silica gel, hexane/ethyl acetate 4:1) and the fractions containing the desired product were combined, concentrated on rotary evaporator, and dried under vacuo overnight, resulting in the desired product.

3. *Optimization of the reaction conditions*

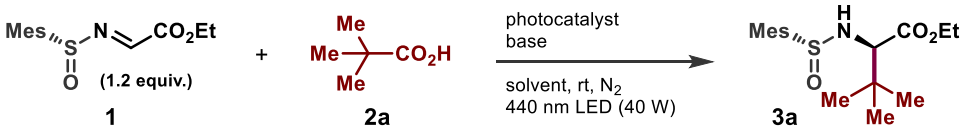

The reactions were typically performed on 0.1 mmol scale (relative to the limiting starting material). The sulfinyl imine **1**, photocatalyst, and the base were placed in the reaction vial equipped with a stirring bar and a septum. The solids were evacuated and back-filled with N_2 three times, followed by addition of a stock solution of pivalic acid **2a** in deaerated anhydrous $PhCF_3$ and short sonication. Thereafter, the reaction mixture was placed ca. 2 cm from the light source (440 nm LED, see Figure S1) and stirred with a fan cooling. The reactions were monitored by ^1H NMR with 1,3,5-trimethoxybenzene as an internal standard. Typically, 0.5 mL of the reaction mixture was taken at a time, filtered through a silica plug eluting with hexane/ethyl acetate 1:1, concentrated on rotary evaporator, dissolved in a stock solution of the internal standard in $CDCl_3$, and analyzed by ^1H NMR (500 MHz). Note, when performing the reactions with small amounts of the photocatalysts (Table S1, entries 1–8), both photocatalyst and the acid were added as stock solutions.

Table S1. Optimization of the reaction conditions with pivalic acid **2a** as the radical precursor.

entry	*photocatalyst*	*base*	*solvent*	*time*	*yield*[a]	*dr*[a]
1	[Ir(dF(CF$_3$)ppy)$_2$(dtbbpy)](PF$_6$), 1 mol%	Cs$_2$CO$_3$, 0.2 equiv.	DMSO, 0.1 M	20 min	< 5%	–
2	[Ir(dF(CF$_3$)ppy)$_2$(dtbbpy)](PF$_6$), 1 mol%	Cs$_2$CO$_3$, 0.2 equiv.	PhCF$_3$, 0.05 M	20 min	65%	4 : 1
3	[Ir(dF(CF$_3$)ppy)$_2$(dtbbpy)](PF$_6$), 1 mol%	2,6-lutidine, 0.2 equiv.	PhCF$_3$, 0.05 M	20 min	< 5%	—
4	[Ir(dF(CF$_3$)ppy)$_2$(dtbbpy)](PF$_6$), 1 mol%	DIPEA, 0.2 equiv.	PhCF$_3$, 0.05 M	20 min	< 5%	—
5	[Ir(dF(CF$_3$)ppy)$_2$(dtbbpy)](PF$_6$), 1 mol%	K$_3$PO$_4$, 0.2 equiv.	PhCF$_3$, 0.05 M	20 min	< 5%	—
6	[Ir(dF(CF$_3$)ppy)$_2$(dtbbpy)](PF$_6$), 1 mol%	Bu$_4$NH$_2$PO$_4$, 0.2 equiv.	PhCF$_3$, 0.05 M	20 min	< 5%	—
7	4CzIPN, 1 mol%	Cs$_2$CO$_3$, 0.2 equiv.	PhCF$_3$, 0.05 M	20 min	< 5%	—
8	[Mes-Acr-Me](BF$_4$), 1 mol%	Cs$_2$CO$_3$, 0.2 equiv.	PhCF$_3$, 0.05 M	20 min	27%	> 95 : 5
9	[Mes-Acr-Me](BF$_4$), 5 mol%	Cs$_2$CO$_3$, 0.2 equiv.	PhCF$_3$, 0.05 M	20 min	48%	> 95 : 5
				60 min	66%	> 95 : 5
10	[Mes-Acr-Me](BF$_4$), 5 mol%	Cs$_2$CO$_3$, 0.2 equiv.	MeCN, 0.05 M	20 min	15%	> 95 : 5
11	[Mes-Acr-Me](BF$_4$), 5 mol%	Cs$_2$CO$_3$, 0.2 equiv.	CH$_2$Cl$_2$, 0.05 M	20 min	24%	> 95 : 5
12	[Mes-Acr-Ph](BF$_4$), 5 mol%	Cs$_2$CO$_3$, 0.2 equiv.	PhCF$_3$, 0.05 M	60 min	73%	> 95 : 5
13	[Mes-2,7-Me$_2$Acr-Ph](BF$_4$), 5 mol%	Cs$_2$CO$_3$, 0.2 equiv.	PhCF$_3$, 0.05 M	60 min	78%	> 95 : 5
14	[Mes-2,7-Me$_2$Acr-Ph](BF$_4$), 5 mol%	Cs$_2$CO$_3$, 0.2 equiv.	PhF, 0.05 M	20 min	10%	> 95 : 5
15	[Mes-2,7-Me$_2$Acr-Ph](BF$_4$), 5 mol%	Cs$_2$CO$_3$, 0.2 equiv.	TFE, 0.05 M	20 min	< 5%	—
16	[Mes-2,7-Me$_2$Acr-Ph](BF$_4$), 5 mol%	2,6-lutidine, 0.2 equiv.	PhCF$_3$, 0.05 M	20 min	< 5%	—
17	[Mes-2,7-Me$_2$Acr-Ph](BF$_4$), 5 mol%	Li$_2$CO$_3$, 0.2 equiv.	PhCF$_3$, 0.05 M	60 min	< 5%	—
18	[Mes-2,7-Me$_2$Acr-Ph](BF$_4$), 5 mol%	K$_3$PO$_4$, 0.2 equiv.	PhCF$_3$, 0.05 M	60 min	80%	> 95 : 5
19	[Mes-2,7-Me$_2$Acr-Ph](BF$_4$), 5 mol%	K$_2$CO$_3$, 0.2 equiv.	PhCF$_3$, 0.05 M	60 min	84%	> 95 : 5
20	[Mes-2,7-Me$_2$Acr-Ph](BF$_4$), 5 mol%	K$_2$CO$_3$, 0.05 equiv.	PhCF$_3$, 0.05 M	20 min	< 5%	—
21	[Mes-2,7-Me$_2$Acr-Ph](BF$_4$), 5 mol%	K$_2$CO$_3$, 0.5 equiv.	PhCF$_3$, 0.05 M	60 min	85%	> 95 : 5
22	[Mes-2,7-Me$_2$Acr-Ph](BF$_4$), 5 mol%	K$_2$CO$_3$, 0.5 equiv.	PhCF$_3$, 0.1 M	60 min	77%	> 95 : 5
23[b]	[Mes-2,7-Me$_2$Acr-Ph](BF$_4$), 5 mol%	K$_2$CO$_3$, 0.5 equiv.	PhCF$_3$, 0.05 M	60 min	91%	> 95 : 5
24[c]	[Mes-2,7-Me$_2$Acr-Ph](BF$_4$), 5 mol%	K$_2$CO$_3$, 0.5 equiv.	PhCF$_3$, 0.05 M	60 min	95%	> 95 : 5

[a] Determined by ^{1}H NMR of the crude reaction mixture with 1,3,5-trimethoxybenzene as an internal standard. [b] 1.0 equiv. of sulfinyl imine **1** and 1.2 equiv. of pivalic acid **2a**. [c] 1.0 equiv. of sulfinyl imine **1** and 1.5 equiv. of pivalic acid **2a**.

Table S2. Optimization of the reaction conditions with hydrocinnamic acid **2j** as the radical precursor.

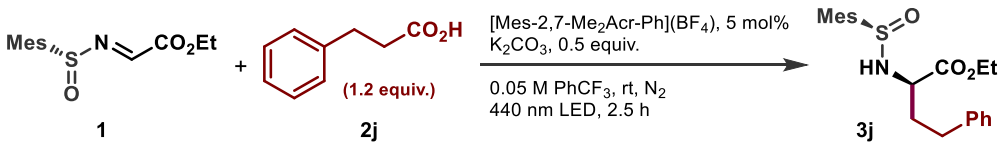

entry	*deviations from standard conditions*	*time*	*remaining imine*[a]	*yield*[a]
1	***none***	60 min	0.67 equiv.	19%
		150 min	0.45 equiv.	22%
2	***solvent:*** $PhCF_3$/TFE 19:1, 0.05 M	60 min	0.47 equiv.	< 5%
3	***solvent:*** $PhCF_3$/HFIP 19:1, 0.05 M	60 min	0.46 equiv.	12%
4	***solvent:*** $PhCF_3$/toluene 1:1, 0.05 M	20 min	0.82 equiv.	7%
5	***base:*** Bu_4NOAc, 0.5 equiv.	20 min	0.74 equiv.	11%
		60 min	0.54 equiv.	20%
6	***base:*** Bu_4NOBz, 0.5 equiv.	20 min	0.70 equiv.	9%
		60 min	0.49 equiv.	16%
7	***base:*** $Bu_4NOP(O)(OBu)_2$, 0.5 equiv.	60 min	0.75 equiv.	9%
		270 min	0.35 equiv.	15%
8	***base:*** CsF, 0.5 equiv.	60 min	0.65 equiv.	15%
9	***light:*** two LEDs (double intensity)	60 min	0.55 equiv.	20%
10	***additive:*** Bu_4NPF_6, 0.5 equiv.	60 min	0.62 equiv.	13%
11	***additive:*** Bu_4NOTf, 0.5 equiv.	60 min	0.66 equiv.	11%

[a] Determined by ^1H NMR of the crude reaction mixture with 1,3,5-trimethoxybenzene as an internal standard.

Table S3. Optimization of the reaction conditions with valeric acid **2k** as the radical precursor.

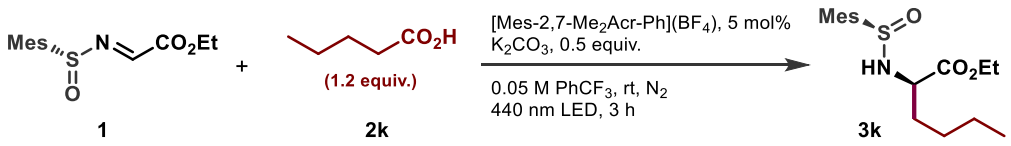

entry	*deviations from standard conditions*	*time*	*remaining imine*[a]	*yield*[a]
1	***none***	60 min	0.49 equiv.	32%
		180 min	0.34 equiv.	41%
2	***solvent:*** $PhCF_3$, 0.025 M	60 min	0.62 equiv.	20%
		180 min	0.52 equiv.	21%
3	***acid:*** 2.0 equiv.	60 min	0.18 equiv.	38%
		180 min	0 equiv.	38%
4	***light:*** half intensity	180 min	0.37 equiv.	39%
		360 min	0.22 equiv.	45%
5	***photocatalyst:*** 1 mol%	60 min	0. 56 equiv.	21%
6	***temperature:*** −20 °C	180 min	0.80 equiv.	11%
7	***temperature:*** 70 °C	60 min	0.41 equiv.	21%

[a] Determined by ^1H NMR of a crude reaction mixture with 1,3,5-trimethoxybenzene as an internal standard.

4. *General procedure for the decarboxylative addition to sulfinyl imine 1*

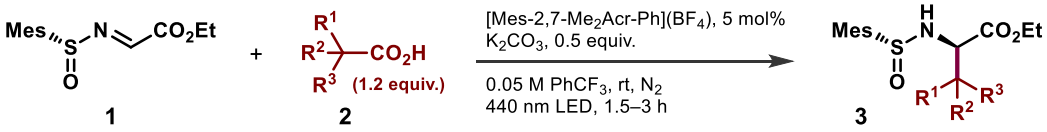

The sulfinyl imine **1** (1 equiv.), [Mes-2,7-Me_2Acr-Ph](BF_4) photocatalyst (5 mol%), K_2CO_3 (0.5 equiv.), and acid **2** (1.2 equiv.) were placed in the reaction vial equipped with a stirring bar and a septum. The solids were evacuated and back-filled with N_2 three times, followed by addition of deaerated anhydrous $PhCF_3$ (0.05 M relative to sulfinyl imine **1**) and short sonication to obtain a fine suspension (acids that are liquid at room temperature were added as solutions in $PhCF_3$). Thereafter, the reaction mixture was placed ca. 2 cm from the light source (440 nm LED) and stirred under illumination with a fan cooling (see Figure S1). After the reaction was complete the mixture was filtered through a silica plug eluting with hexane/ethyl acetate 1:1, concentrated on rotary evaporator (40 °C), and the crude product **3** was purified by column chromatography or preparative TLC.

Important! Products 3 slowly epimerize in chloroform. When used, chloroform should be removed from the samples directly after column chromatography or NMR experiments to avoid epimerization.

5. *Procedure for the 1 mmol scale synthesis of compound 3a*

The sulfinyl imine **1** (267.4 mg, 1 mmol, 1 equiv.), [Mes-2,7-Me_2Acr-Ph](BF_4) photocatalyst (24.5 mg, 0.05 mmol, 5 mol%), K_2CO_3 (69.1 mg, 0.5 mmol, 0.5 equiv.), and pivalic acid (122.6 mg, 1.2 mmol, 1.2 equiv.) were placed in the reaction vial (VWR, 24.0 mL sample vial, Art. No. 218-2226) equipped with a stirring bar and a septum. The solids were evacuated and back-filled with N_2 three times, followed by addition of deaerated anhydrous $PhCF_3$ (20 mL, 0.05 M) and short sonication to obtain a fine suspension. Thereafter, the reaction mixture was placed between **two** 440 nm LED lamps and stirred under illumination with a fan cooling (see Figure S2). After 2.5 h the reaction mixture was filtered through silica eluting with hexane/ethyl acetate 1:1, concentrated on rotary evaporator (40 °C), and the crude product was purified by column chromatography with chloroform/ethyl acetate 35:1 as eluent. The purified product was dried in vacuo overnight, resulting in **3a** as white solid (247.2 mg, 76% yield, >95:5 α dr).

6. *Computational studies*

Synthesis of product **3a** from the sulfinyl imine **1** and pivalic acid **2a** was selected as the model reaction for the computational studies. All calculations were performed on the M062X-D3/6-311+G(d,p)[3] level of theory using Gaussian 16 package, revision B.01.[4] The effect of the solvent (chlorobenzene) was modeled implicitly using the Solvation Model based on Density (SMD) method.[5] Vibrational analysis confirmed that all reported structures either represents true minima (no imaginary frequencies), or the true first order saddle points (for transition states, one imaginary frequency) on the potential energy surface. Free energies were obtained by adding the thermal correction term from the frequency analysis to the electronic energy. To account for the change in the standard state (1 atm → 1 M) an entropic correction term of 1.89 kcal/mol (−RTlnQ) was added to all considered species.

6.1. *Conformation analysis for sulfinyl imine 1*

Previously, Alemán and co-workers suggested that the *s-cis* conformer of sulfinyl imine **1** should be more stable compared to the *s-trans* conformer due to the hydrogen bonding between the imine hydrogen and sulfoxide oxygen.[6] To confirm this, we performed a relaxed scan for the O–S–N–C dihedral angle with 30° increment on the M062X-3D/631+G(d)/SMD(chlorobenzene) level of theory (Figure S3). The identified minimum (*D* = 0°) indeed corresponded to the *s-cis* conformation, which was then re-optimized on the M062X-D3/6-311+G(d,p)/SMD(chlorobenzene) level of theory. For comparison, the *s-trans* conformer (*D* = 150°) was also re-calculated at same level of theory. The structures of the two conformers, their HOMO-3 orbitals and the relative free energies are presented in Figures 3 and S3. The *s-cis* conformer was found to be favored by 3.8 kcal/mol compared to the *s-trans* conformer, an energy difference representing a >99.8:0.2 ratio considering a 1:1 Boltzmann distribution at room temperature (298.15 K). This result is in good agreement with the previous report investigating *N-t*-Bu-sulfinyl imines, where the *s-cis* conformer was calculated to be 4.0 kcal/mol more stable than the *s-trans* conformer.[7] However, sulfinyl imine from the previous report did not include an additional potential hydrogen bond acceptor, i.e. the carbonyl oxygen present in sulfinyl imine **1**. The hydrogen bond interaction can be

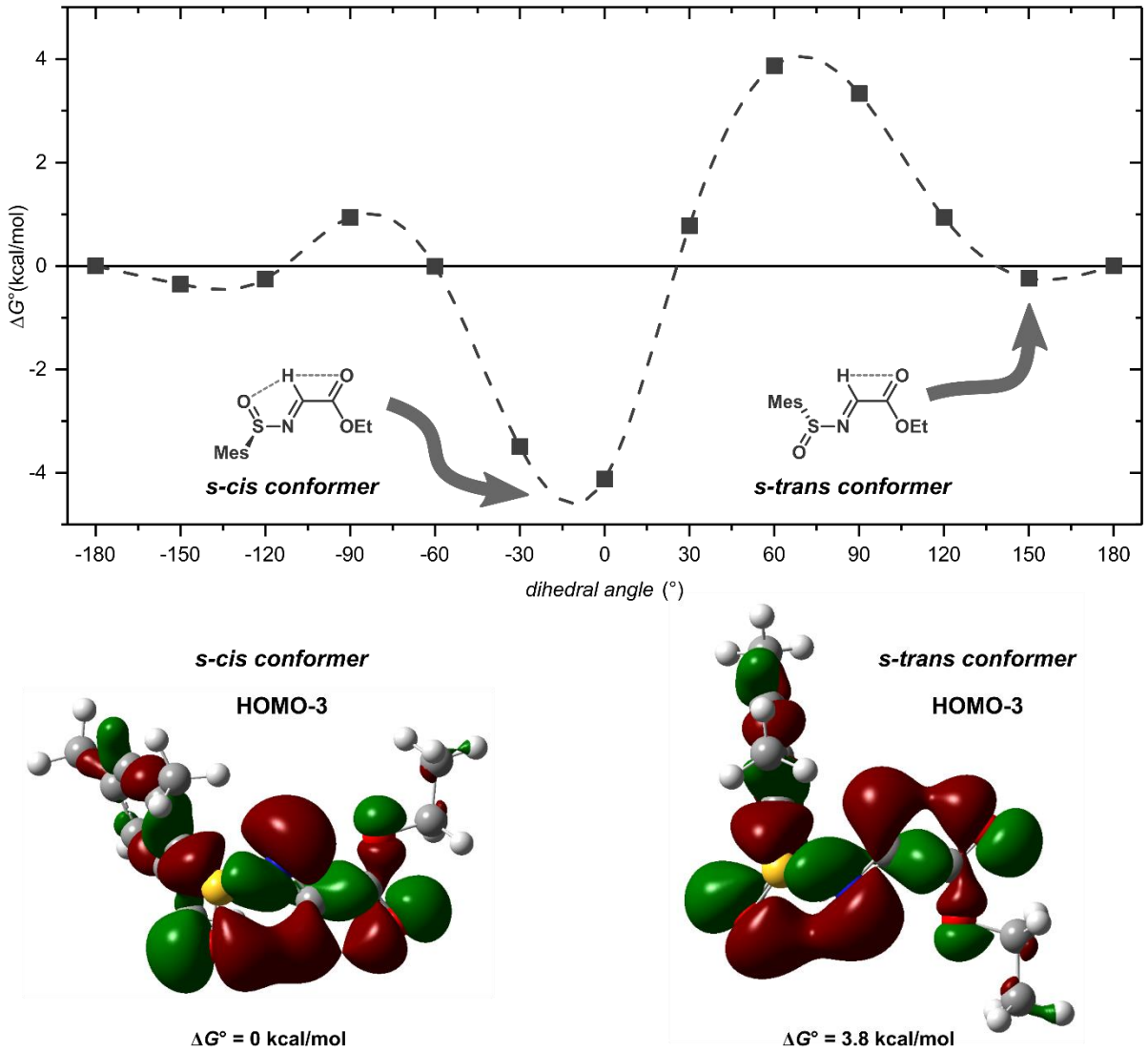

Figure S3. *Top:* Potential energy curve as derived from a relaxed scan of the O-S-N-C dihedral angle. Calculations performed on the M062X-3D/631+G(d)/SMD(chlorobenzene) level of theory. *Bottom:* HOMO-3 orbitals and the relative free energies (kcal/mol) of the *s-cis* and the *s-trans* conformations of the *N*-sulfinyl imine **1**.

visualized for the HOMO-3 orbitals of the two conformers. For the *s-cis* conformer, a constructive overlap between the imine hydrogen and the sulfoxide oxygen was observed, while for the *s-trans* conformer a constructive overlap was instead found between the imine hydrogen and the carbonyl oxygen.

To estimate the strength of the intramolecular hydrogen bonding, the relative stabilities of the corresponding conformers of *N*-sylfinyl imidoylfluoride were evaluated at the M062X-D3/6-311+G(d,p)/ SMD(chlorobenzene) level of theory (Figure S4). The comparison demonstrated that the *s-trans* conformer is 0.6 kcal/mol more stable compared to the *s-cis* conformer, indicating that the intramolecular hydrogen bond in the *N*-sylfinyl imine **1** is worth approximately 4.4 kcal/mol.

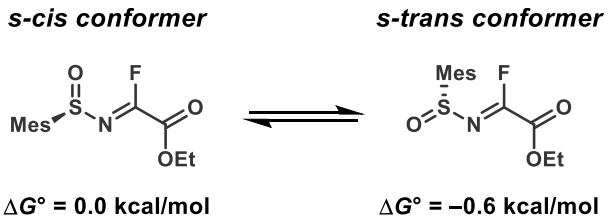

Figure S4. The relative free energies of the *s-cis* and *s-trans* conformers of the *N*-sulfinyl imidoyl fluoride.

6.2. *Addition of the tert-butyl radical to sulfinyl imine 1*

Next, the stereodetermining radical addition of the *tert*-butyl radical derived from **2a** to the *N*-sulfinyl imine **1** was investigated. The computed free energy surface of the reaction is presented in Figure 3. The activation barriers for the *re*- and *si*-additions were found to be 6.4 and 10.2 kcal/mol, respectively. In both cases, addition of the *tert*-butyl radical to the imine is exergonic, presumably due to the formation of a more stable radical. However, the formation of the experimentally observed *R,R*-diastereomer is 2.5 kcal/mol more favored compared to the *R,S*-diastereomer. Hence, the formation of the *R,R*-diastereomer is favored both kinetically and thermodynamically.

The structure, selected distances and relative free energies of both *re*-TS and *si*-TS can be seen in Figure 3. The C–C distance and the incoming angle is similar for both transition states, *re*-TS having a slightly longer C–C distance (2.27 Å vs. 2.22 Å) and a slightly wider incoming angle (∠ NCC, 109.7° vs. 108.6°). The geometries agree qualitatively with a transition state for the addition of an isopropyl radical to glyoxylate oxime methyl ether reported previously by Jørgensen and co-workers.[8] In Jørgensen's work a lower energy barrier of 1.6 kcal/mol was predicted, presumably a result of smaller stability of the isopropyl radical as compared to the *tert*-butyl radical.

Two reasons for the energetic ordering of the located transition states can be seen reasoned. Firstly, the distance between the imine hydrogen and the sulfoxide oxygen is significantly longer in the *si*-TS compared to the *re*-TS (2.53 Å vs. 2.35 Å), indicating a weaker hydrogen bond. The weaker hydrogen bond interaction can also be seen in the HOMO-3 of the two transition states (Figure S5). For the *re*-TS, a constructive overlap between the imine hydrogen and the sulfoxide oxygen can be observed, while this interaction is absent in the *si*-TS. It should be noted, however, that there is a constructive overlap between the imine hydrogen and the sulfoxide oxygen in HOMO-4 for both structures, indicating that the hydrogen bond is present in both structures but that the interaction is stronger in the *re*-TS. Secondly, there is significant steric crowding between one of the methyl groups of the mesityl substituent in the *si*-TS, which is not present in the *re*-TS. This is an effect of a rotation of the mesityl group in *si*-TS, which occurs to make room for the incoming *tert*-butyl radical. The O–S–C–C dihedral angle then becomes −50° in the *re*-TS and −2° in the *si*-TS, making the methyl group and the sulfoxide oxygen in *si*-TS almost completely coplanar.

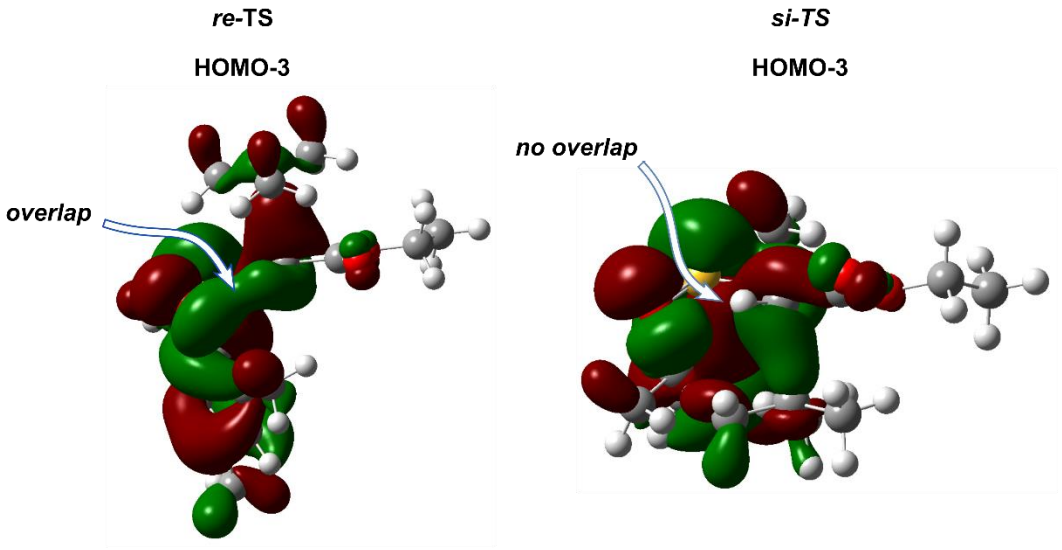

Figure S5. Plot of the HOMO-3 orbitals of the *re*-TS and *si*-TS.

6.3. Evaluation of different functionals

To evaluate the accuracy of the M062X-D3 functional, the single point energies of the *re*-TS and *si*-TS were recalculated using B3LYP-D3[9] and wB97XD functionals (Table S4).[10] It is worth noting that the wB97XD-functional is using the D2 version of Grimme's empirical dispersion,[11] instead of the D3 version that is used for the other two. As seen in Table S4, the three functionals are in excellent agreement with each other. The largest difference is between the M062X-D3 and the wB97XD functional (0.4 kcal/mol), which is to be expected since they are using different models for the empirical dispersion. Nonetheless, the tested functionals all predict that the *re*-TS is favored by 3.4–3.8 kcal/mol compared to the *si*-TS.

Table S4. Relative free energy of activation for the *re*-TS and *si*-TS computed with different functionals for the single point electronic energy.

structure	**M062X-D3 $\Delta\Delta G^{\ddagger}$**	**B3LYP-D3 $\Delta\Delta G^{\ddagger}$**	**wB97XD $\Delta\Delta G^{\ddagger}$**
re-TS	0.0 kcal/mol	0.0 kcal/mol	0.0 kcal/mol
si-TS	3.8 kcal/mol	3.7 kcal/mol	3.4 kcal/mol

7. Analytical data

Compound **1** (ethyl (*R,E*)-2-((mesitylsulfinyl)imino)acetate)

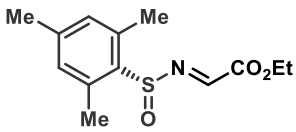

Synthesized according to the general procedure described in **Section 2** on 2.73 mmol scale. The product is a white solid (0.621 g, **85% yield**). The NMR spectra agree with the previously reported data.[2]

^{1}H NMR (500 MHz, $CDCl_3$) δ 8.24 (s, 1H), 6.86 (s, 3H), 4.45–4.30 (m, 2H), 2.45 (s, 9H), 2.28 (s, 4H), 1.37 (t, *J* = 7.1 Hz, 3H).

^{13}C NMR (126 MHz, $CDCl_3$) δ 161.53, 154.05, 142.63, 138.93, 133.17, 131.19, 62.76, 21.26, 19.02, 14.21.

***R*$_f$** = 0.53 (hexane/ethyl acetate 4:1).

Compound **4** (ethyl (*S,E*)-2-((*tert*-butylsulfinyl)imino)acetate)

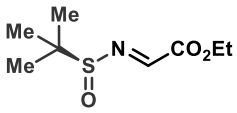

Synthesized according to the general procedure described in **Section 2** on 4.13 mmol scale. The product is a yellow oil (0.629 g, **74% yield**). The NMR spectra agree with the previously reported data.[12]

^{1}H NMR (400 MHz, $CDCl_3$) δ 8.00 (s, 1H), 4.38 (q, *J* = 6.6 Hz, 2H), 1.38 (t, *J* = 6.6 Hz, 3H), 1.27 (s, 9H).

^{13}C NMR (101 MHz, $CDCl_3$) δ 161.26, 155.74, 62.59, 59.05, 22.87, 14.20.

***R*$_f$** = 0.43 (hexane/ethyl acetate 4:1).

Compound **5** (ethyl (*R,E*)-2-((*p*-tolylsulfinyl)imino)acetate)

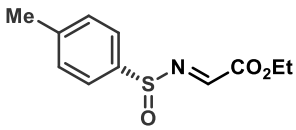

Synthesized according to the general procedure described in **Section 2** on 3.22 mmol scale. The product is a colorless oil (0.327 g, **42% yield**). The NMR spectra agree with the previously reported data.[13]

^{1}H NMR (400 MHz, $CDCl_3$) δ 8.14 (s, 1H), 7.60 (d, *J* = 7.1 Hz, 2H), 7.33 (d, *J* = 7.6 Hz, 2H), 4.43–4.26 (m, 2H), 2.41 (s, 3H), 1.35 (t, *J* = 6.9 Hz, 3H).

^{13}C NMR (101 MHz, $CDCl_3$) δ 161.39, 153.22, 142.69, 139.33, 62.75, 21.61, 14.17.

***R*$_f$** = 0.39 (hexane/ethyl acetate 4:1).

Compound **3a** (ethyl (*R*)-2-(((*R*)-mesitylsulfinyl)amino)-3,3-dimethylbutanoate)

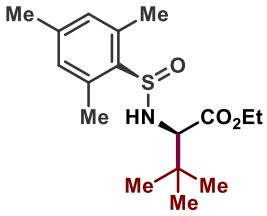

Synthesized according to the general procedure described in **Section 3** on 0.3 mmol scale and 1.5 h reaction time (1 h reaction time for NMR yield). The crude product was purified by column chromatography using hexane/ethyl acetate 9:1 as eluent. The product is a white solid (79.1 mg, **81% yield**, >95:5 α dr). The NMR spectra agree with the previously reported data.[13]

^{1}H NMR (500 MHz, $CDCl_3$) δ 6.87 (s, 2H), 5.05 (d, *J* = 10.0 Hz, 1H), 4.34–4.14 (m, 2H), 3.60 (d, *J* = 10.1 Hz, 1H), 2.57 (s, 6H), 2.29 (s, 3H), 1.31 (t, *J* = 7.1 Hz, 3H), 0.97 (s, 9H).

^{13}C NMR (126 MHz, $CDCl_3$) δ 172.84, 140.99, 138.24, 136.90, 130.92, 66.63, 61.44, 35.16, 26.62, 21.19, 19.45, 14.32.

R_f = 0.33 (hexane/ethyl acetate 4:1)

Compound **3b** (ethyl (*R*)-6-(2,5-dimethylphenoxy)-2-(((*R*)-mesitylsulfinyl)amino)-3,3-dimethylhexanoate)

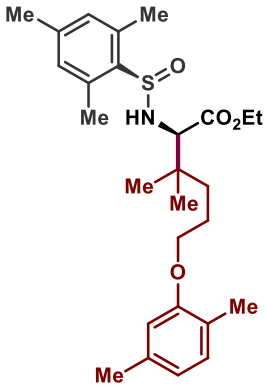

Synthesized according to the general procedure described in **Section 3** on 0.15 mmol scale and 2 h reaction time (2 h reaction time for NMR yield). The crude product (after filtration through silica plug and removal of the solvent) was dissolved in 20 mL of ethyl acetate and washed with 0.1 M aq. NaOH (5 x 10 mL) and water (10 mL), dried over anhydrous Na_2SO_4, concentrated, and purified by column chromatography using petroleum ether/CH_2Cl_2/ethyl acetate 8:1:1 as eluent. The product is a pale-yellow oil (31.3 mg, **44% yield**, >95:5 α dr).

^{1}H NMR (500 MHz, $CDCl_3$) δ 7.00 (d, *J* = 7.4 Hz, 1H), 6.87 (s, 2H), 6.66 (d, *J* = 7.4 Hz, 1H), 6.61 (s, 1H), 5.07 (d, *J* = 10.1 Hz, 1H), 4.31–4.18 (m, 2H), 3.90 (t, *J* = 6.4 Hz, 2H), 3.74 (d, *J* = 10.1 Hz, 1H), 2.57 (s, 6H), 2.30 (d, *J* = 8.4 Hz, 6H), 2.14 (s, 3H), 1.91–1.70 (m, 2H), 1.57–1.41 (m, 2H), 1.31 (t, *J* = 7.2 Hz, 3H), 0.97 (s, 6H).

^{13}C NMR (126 MHz, $CDCl_3$) δ 172.79, 157.09, 141.07, 138.17, 136.92, 136.61, 130.95, 130.45, 123.73, 120.88, 112.17, 68.41, 65.20, 61.54, 37.60, 35.80, 24.15, 23.87, 23.70, 21.55, 21.19, 19.43, 15.88, 14.32.

R_f = 0.24 (petroleum ether/CH_2Cl_2/ethyl acetate 8:1:1)

Compound **3c** ((*R*)-*N*-((*R*)-2-(ethylperoxy)-1-(1-methylcyclohexyl)-2λ^2-ethyl)-2,4,6-trimethylbenzenesulfinamide)

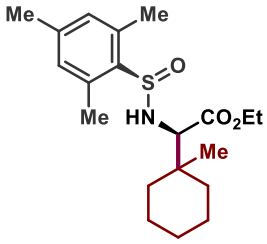

Synthesized according to the general procedure described in **Section 3** on 0.2 mmol scale and 1.5 h reaction time (1 h reaction time for NMR yield). The crude product was purified by column chromatography using chloroform/ethyl acetate 30:1 as eluent. The product is a pale-yellow oil (63.7 mg, **87% yield**, >95:5 α dr). The NMR spectra agree with the previously reported data.[13]

^{1}H NMR (500 MHz, $CDCl_3$) δ 6.86 (s, 2H), 5.01 (d, *J* = 10.1 Hz, 1H), 4.32–4.14 (m, 2H), 3.83 (d, *J* = 10.1 Hz, 1H), 2.57 (s, 6H), 2.29 (s, 3H), 1.68–1.38 (m, 7H), 1.38–1.22 (m, 3H), 1.30 (t, *J* = 7.2 Hz, 3H), 0.84 (s, 3H).

^{13}C NMR (126 MHz, $CDCl_3$) δ 172.87, 140.94, 138.29, 136.86, 130.90, 64.85, 61.36, 37.73, 34.96, 34.89, 26.08, 21.70, 21.66, 21.17, 20.73, 19.43, 14.32.

R_f = 0.20 (chloroform/ethyl acetate 30 :1)

Compound **3d** (*tert*-butyl 4-((*R*)-2-(ethylperoxy)-1-(((*R*)-mesitylsulfinyl)amino)-2λ^2-ethyl)-4-methylpiperidine-1-carboxylate)

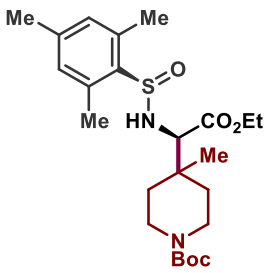

Synthesized according to the general procedure described in **Section 3** on 0.2 mmol scale and 2 h reaction time (1 h reaction time for NMR yield). The crude product was purified by column chromatography using hexane/CH_2Cl_2/ethyl acetate 6:1:1 as eluent. The product is a pale-yellow oil (30.6 mg, **33% yield**, >95:5 α dr).

^{1}H NMR (500 MHz, $CDCl_3$) δ 6.87 (s, 2H), 5.04 (*d*, *J* = 10.0 Hz, 1H), 4.31–4.15 (m, 2H), 3.77 (d, *J* = 9.9 Hz, 1H), 3.80–3.60 (m, 2H), 3.20–3.06 (m, 2H), 2.56 (s, 6H), 2.29 (s, 3H), 1.72–1.61 (m, 1H), 1.60–1.51 (m, 1H), 1.45 (s, 9H), 1.43–1.37 (m, 1H), 1.30 (t, *J* = 7.1 Hz, 3H), 1.33–1.23 (m, 1H), 0.91 (s, 3H).

^{13}C NMR (126 MHz, $CDCl_3$) δ 172.20, 154.98, 141.20, 137.95, 136.88, 130.99, 79.67, 64.89, 61.72, 36.47, 34.07, 33.96, 31.73, 28.58, 22.79, 21.18, 19.45, 19.02, 14.31, 14.26.

R_f = 0.16 (hexane/CH_2Cl_2/ethyl acetate 4:1:1)

Compound **3e** (ethyl (*R*)-2-(((*R*)-mesitylsulfinyl)amino)-2-(3-methyloxetan-3-yl)acetate)

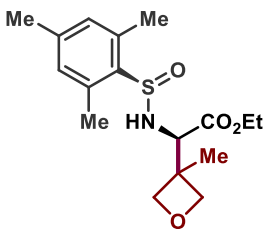

Synthesized according to the general procedure described in **Section 3** on 0.2 mmol scale and 3 h reaction time (2 h reaction time for NMR yield). The crude product was purified by column chromatography using petroleum ether/CH_2Cl_2/ethyl acetate 2:1:1 as eluent. The product is a pale-orange oil (36.7 mg, **54% yield**, >95:5 α dr). The NMR spectra agree with the previously reported data.[2]

^{1}H NMR (500 MHz, $CDCl_3$) δ 6.88 (s, 2H), 5.21 (d, *J* = 8.2 Hz, 1H), 4.84 (d, *J* = 6.3 Hz, 1H), 4.74 (d, *J* = 6.1 Hz, 1H), 4.44 (d, *J* = 8.1 Hz, 1H), 4.31 (d, *J* = 6.3 Hz, 1H), 4.28–4.23 (m, 2H), 4.23–4.15 (m, 1H), 2.58 (s, 6H), 2.29 (s, 3H), 1.27 (t, *J* = 7.1 Hz, 3H), 1.22 (s, 3H).

^{13}C NMR (126 MHz, $CDCl_3$) δ 171.48, 141.33, 137.73, 136.88, 131.03, 80.37, 80.32, 62.21, 62.18, 42.90, 21.17, 19.45, 19.31, 14.28.

***R*$_f$** = 0.28 (petroleum ether/CH_2Cl_2/ethyl acetate 2:1:1)

Compound **3f** (ethyl (*R*)-2-(((*R*)-mesitylsulfinyl)amino)-2-(1-phenylcyclopropyl)acetate)

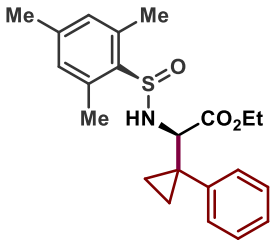

Synthesized according to the general procedure described in **Section 3** on 0.15 mmol scale and 3 h reaction time (3 h reaction time for NMR yield). The crude product was purified by column chromatography using hexane/CH_2Cl_2/ethyl acetate 8:1:1 as eluent. The product is a pale-red oil (30.0 mg, **52% yield**, 9:1 α dr). The NMR spectra agree with the previously reported data.[2]

^{1}H NMR (500 MHz, $CDCl_3$) δ 7.25–7.15 (m, 5H), 6.86 (s, 2H), 6.81 (s, 2H, *minor diastereomer*), 5.09 (d, *J* = 7.8 Hz, 1H), 4.71 (d, *J* = 10.1 Hz, 1H, *minor diastereomer*), 4.24–4.06 (m, 2H), 3.77 (d, *J* = 7.7 Hz, 1H), 3.54 (d, *J* = 10.1 Hz, 1H, *minor diastereomer*), 2.55 (s, 6H), 2.29 (s, 3H), 1.24 (t, *J* = 7.1 Hz, 3H), 1.27–1.17 (m, 1H), 1.07–1.00 (m, 1H), 1.00–0.93 (m, 1H), 0.93–0.86 (m, 1H). *Mixture of two diastereomers is reported*.

^{13}C NMR (126 MHz, $CDCl_3$) δ 171.63, 140.95, 140.78, 140.76, 140.10, 137.96, 137.42, 137.18, 136.85, 131.08, 131.02, 130.94, 130.62, 128.24, 128.20, 127.49, 127.34, 65.10, 64.27, 61.74, 61.45, 29.83, 29.63, 21.18, 21.11, 19.67, 19.43, 14.31, 14.23, 12.77, 12.35, 11.67, 11.51. *Mixture of two diastereomers is reported*.

***R*$_f$** = 0.38 (hexane/CH_2Cl_2/ethyl acetate 8:1:1)

Compound **3g** (ethyl (*R*)-3-(4-chlorophenoxy)-2-(((*R*)-mesitylsulfinyl)amino)-3-methylbutanoate)

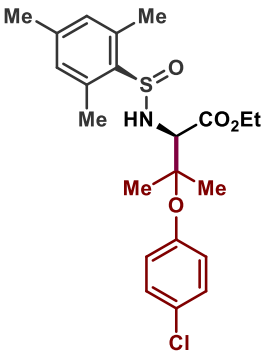

Synthesized according to the general procedure described in **Section 3** on 0.15 mmol scale and 1.5 h reaction time (1 h reaction time for NMR yield). The crude product was purified by column chromatography with neutralized silica (prior to loading of the crude product the column was washed with the eluent containing 2% Et_3N, followed by pristine eluent) using petroleum ether/CH_2Cl_2/ethyl acetate 8:1:1 as eluent. The product is a pale-yellow oil (59.3 mg, **90% yield**, >95:5 α dr). The NMR spectra agree with the previously reported data.[2]

^{1}H NMR (500 MHz, $CDCl_3$) δ 7.23–7.17 (m, 2H), 6.90–6.84 (m, 4H), 5.33 (d, *J* =

9.9 Hz, 1H), 4.37–4.19 (m, 2H), 4.01 (d, *J* = 9.8 Hz, 1H), 2.58 (s, 6H), 2.29 (s, 3H), 1.36–1.25 (m, 9H).

^{13}C NMR (126 MHz, $CDCl_3$) δ 171.43, 152.97, 141.18, 137.89, 136.98, 131.00, 129.43, 129.19, 125.52, 81.87, 65.58, 61.89, 24.29, 23.85, 21.18, 19.46, 14.29.

R_f = 0.16 (petroleum ether/CH_2Cl_2/ethyl acetate 8:1:1)

Compound **3h** (ethyl (*R*)-2-cyclohexyl-2-(((*R*)-mesitylsulfinyl)amino)acetate)

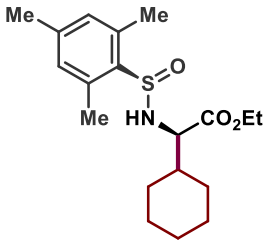

Synthesized according to the general procedure described in **Section 3** on 0.15 mmol scale and 3 h reaction time (2 h reaction time for NMR yield). The crude product was purified by preparative TLC using chloroform/ethyl acetate 12:1 as eluent. The product is a pale-yellow oil (38.7 mg, **73% yield**, >95:5 α dr).

^{1}H NMR (500 MHz, $CDCl_3$) δ 6.87 (s, 2H), 5.01 (d, *J* = 9.3 Hz, 1H), 4.31–4.15 (m, 2H), 3.76 (dd, *J* = 9.3, 5.4 Hz, 1H), 2.59 (s, 6H), 2.29 (s, 3H), 1.79–1.55 (m, 5H), 1.30 (t, *J* = 7.1 Hz, 3H), 1.26–0.95 (m, 6H).

^{13}C NMR (126 MHz, $CDCl_3$) δ 173.26, 140.94, 138.32, 136.82, 130.91, 62.74, 61.61, 41.83, 29.73, 27.99, 26.13, 25.99, 21.17, 19.51, 14.32.

R_f = 0.39 ($CHCl_3$/ethyl acetate 10:1)

Compound **3i** (ethyl (*R*)-2-cyclobutyl-2-(((*R*)-mesitylsulfinyl)amino)acetate)

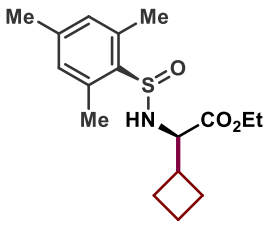

Synthesized according to the general procedure described in **Section 3** on 0.2 mmol scale and 3 h reaction time (2.5 h reaction time for NMR yield). The crude product was purified by column chromatography using chloroform/ethyl acetate 35:1 as eluent. The product is a pale-pink oil (19.1 mg, **30% yield**, >95:5 α dr).

^{1}H NMR (500 MHz, $CDCl_3$) δ 6.87 (s, 2H), 5.04 (d, *J* = 8.9 Hz, 1H), 4.29–4.09 (m, 2H), 3.86 (dd, *J* = 8.9, 7.7 Hz, 1H), 2.66–2.53 (m, 1H), 2.59 (s, 6H), 2.28 (s, 3H), 2.07–1.91 (m, 3H), 1.91–1.72 (m, 3H), 1.27 (t, *J* = 7.1 Hz, 3H).

^{13}C NMR (126 MHz, $CDCl_3$) δ 172.88, 140.98, 138.18, 136.87, 130.93, 61.61, 61.31, 38.99, 24.94, 24.91, 21.16, 19.49, 18.02, 14.31.

R_f = 0.20 (chloroform/ethyl acetate 35:1)

Compound **3j** (ethyl (*R*)-2-(((*R*)-mesitylsulfinyl)amino)-4-phenylbutanoate)

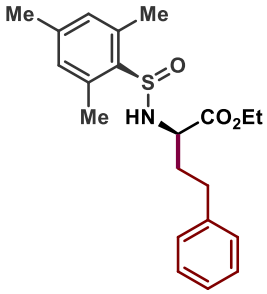

Synthesized according to the general procedure described in **Section 3** on 0.2 mmol scale and 3 h reaction time (2.5 h reaction time for NMR yield). The crude product was purified by column chromatography using chloroform/ethyl acetate 35:1 as eluent. The product is a pale-orange oil (14.8 mg, **20% yield**, >95:5 α dr).

^{1}H NMR (500 MHz, $CDCl_3$) δ 7.32–7.26 (m, 2H), 7.23–7.13 (m, 3H), 6.89 (s, 2H), 5.15 (d, *J* = 8.4 Hz, 1H), 4.26–4.13 (m, 2H), 4.04–3.96 (m, 1H), 2.79–2.67 (m, 2H), 2.62 (s, 6H), 2.30 (s, 3H), 2.19–2.07 (m, 1H), 2.00–1.89 (m, 1H), 1.28 (t, *J* = 7.1 Hz, 3H).

^{13}C NMR (126 MHz, $CDCl_3$) δ 173.45, 141.14, 140.86, 138.05, 136.89, 131.01, 128.67, 128.59, 126.34, 61.90, 56.85, 35.79, 31.75, 21.19, 19.51, 14.28.

R_f = 0.22 (chloroform/ethyl acetate 35:1)

Compound **3k** (ethyl (*R*)-2-(((*R*)-mesitylsulfinyl)amino)hexanoate)

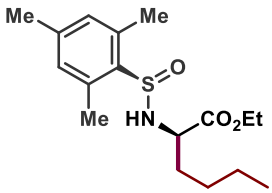

Synthesized according to the general procedure described in **Section 3** on 0.2 mmol scale and 3 h reaction time (3 h reaction time for NMR yield). The crude product was purified by column chromatography using chloroform/ethyl acetate 35:1 as eluent. The product is a pale-orange oil (25.2 mg, **39% yield**, >95:5 α dr).

^{1}H NMR (500 MHz, $CDCl_3$) δ 6.87 (s, 2H), 5.04 (*d*, J = 8.5 Hz, 1H), 4.29–4.13 (m, 2H), 3.95 (td, *J* = 8.3, 4.8 Hz, 1H), 2.59 (s, 6H), 2.28 (s, 3H), 1.85–1.75 (m, 1H), 1.68–1.57 (m, 1H), 1.43–1.30 (m, 4H), 1.29 (t, *J* = 7.2 Hz, 3H), 0.92–0.85 (m, 3H).

^{13}C NMR (126 MHz, $CDCl_3$) δ 173.75, 140.99, 138.10, 136.82, 131.05, 130.94, 61.72, 57.39, 33.84, 27.59, 22.31, 21.16, 19.44, 14.27, 14.01.

R_f = 0.24 (chloroform/ethyl acetate 30:1)

Compound **3l** (*tert*-butyl (*R*)-2-((*R*)-2-ethoxy-1-(((*R*)-mesitylsulfinyl)amino)-2-oxoethyl)piperidine-1-carboxylate)

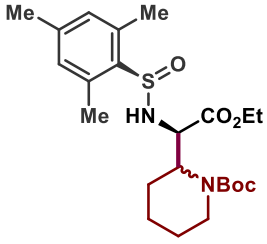

Synthesized according to the general procedure described in **Section 3** on 0.2 mmol scale and 1.5 h reaction time (1 h reaction time for NMR yield). The crude product was purified by column chromatography using hexane/CH_2Cl_2/ethyl acetate 6:1:1 as eluent. The product is a pale-yellow oil (48.3 mg, **53% yield**, >95:5 α dr; 1:1 β dr).

^{1}H NMR (500 MHz, $CDCl_3$) δ 6.88–6.72 (m, 4H), 5.20 (d, *J* = 10.8 Hz, 1H), 4.85 (d, *J* = 9.0 Hz, 1H), 4.46 (d, *J* = 10.7 Hz, 1H), 4.35–4.00 (m, 8H), 3.91 (d, *J* = 13.7 Hz,

1H), 2.79 (t, *J* = 13.3 Hz, 1H), 2.70–2.59 (m, 1H), 2.53 (s, 12H), 2.23 (s, 6H), 1.75–1.50 (m, 12H), 1.29 (dt, *J* = 29.6, 7.0 Hz, 6H), 1.22–0.97 (m, 18H). *Mixture of two diastereomers is reported*.

^{13}C NMR (126 MHz, $CDCl_3$) δ 173.07, 172.27, 156.32, 155.16, 141.02, 140.73, 139.33, 138.70, 137.68, 137.18, 136.76, 130.80, 130.67, 81.47, 79.76, 62.78, 61.84, 61.57, 57.73, 57.50, 52.98, 51.53, 39.98, 38.64, 29.79, 28.54, 28.26, 28.23, 28.13, 28.08, 27.93, 25.76, 25.62, 25.44, 25.07, 24.94, 23.09, 21.04, 21.02, 20.84, 19.41, 19.23, 19.14, 14.14, 13.88. *Mixture of two diastereomers is reported*.

***R*$_f$** = 0.28 (hexane/CH_2Cl_2/ethyl acetate 4:1:1)

Compound **3m** (*tert*-butyl (*R,S*)-2-((*R*)-2-ethoxy-1-(((*R*)-mesitylsulfinyl)amino)-2-oxoethyl)pyrrolidine-1-carboxylate)

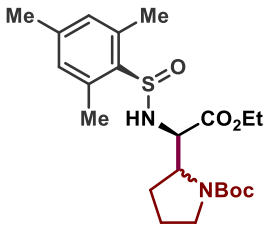

Synthesized according to the general procedure described in **Section 3** on 0.2 mmol scale and 1.5 h reaction time (1 h reaction time for NMR yield). The crude product was purified by column chromatography using hexane/ethyl acetate 7:1 as eluent. The product is a colorless oil (0.0758 g, **86% yield**, >95:5 α dr, 1:1 β dr). Two rotamers for each diastereomer at β-position (1:1) were observed by NMR. The NMR spectra agree with the previously reported data.[2]

^{1}H NMR (500 MHz, $CDCl_3$) δ 6.85 (d, *J* = 14.0 Hz, 4H), 5.48 (d, *J* = 8.4 Hz, 1H), 5.39 (d, *J* = 7.6 Hz, 1H), 5.27 (d, *J* = 7.0 Hz, 1H), 5.11 (d, *J* = 8.7 Hz, 1H), 4.82 (dd, *J* = 7.6, 4.0 Hz, 1H), 4.73 (dd, *J* = 7.0, 3.8 Hz, 1H), 4.36 (s, 1H), 4.31–4.15 (m, 4H), 4.15–4.07 (m, 2H), 4.07–3.98 (m, 1H), 3.63–3.30 (m, 2H), 3.30–3.18 (m, 1H), 3.18–3.07 (m, 1H), 2.67–2.47 (m, 12H), 2.36–2.18 (m, 6H), 2.01–1.90 (m, 1H), 1.90–1.75 (m, 4H), 1.75–1.59 (m, 3H), 1.59–1.34 (m, 18H), 1.34–1.18 (m, 6H). *Mixture of two rotamers for each of two diastereomers is reported*.

^{13}C NMR (126 MHz, $CDCl_3$) δ 172.19, 171.99, 171.77, 155.30, 154.39, 154.06, 153.89, 140.97, 140.74, 138.62, 138.29, 137.72, 136.92, 136.64, 136.47, 130.84, 80.46, 80.22, 79.74, 62.12, 62.01, 61.66, 60.09, 59.43, 59.16, 58.75, 57.79, 57.32, 47.55, 47.37, 47.17, 46.69, 28.56, 28.49, 28.38, 27.71, 26.82, 26.07, 24.25, 23.78, 23.67, 22.76, 21.09, 21.05, 20.89, 19.45, 19.31, 14.20, 14.05. *Mixture of two rotamers for each of two diastereomer is reported*.

***R*$_f$** = 0.26 (hexane/ethyl acetate 7:1)

Compound **3n** (ethyl (2*R*,3*S*)-3-((*tert*-butoxycarbonyl)amino)-2-(((*R*)-mesitylsulfinyl)amino)-4-methylpentanoate)

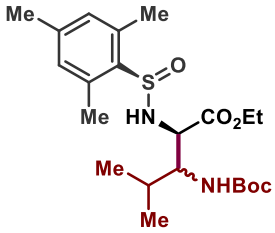

Synthesized according to the general procedure described in **Section 3** on 0.2 mmol scale and 1 h reaction time (0.5 h reaction time for NMR yield). The crude product was purified by column chromatography using chloroform/ethyl acetate 20:1 as eluent. The product is pale-orange oil (87.4 mg, **99% yield**, >95:5 α dr, 1.5:1 β dr).

^{1}H NMR (500 MHz, $CDCl_3$) δ 6.94–6.80 (m, 4H), 5.31 (d, *J* = 7.4 Hz, 1H), 5.11 (d, *J* = 9.6 Hz, 1H, *minor diastereomer*), 4.69 (d, *J* = 10.3 Hz, 1H, *minor diastereomer*), 4.39 (d, *J* = 10.5 Hz, 1H), 4.30–4.13 (m, 5H), 4.03 (dd, *J* = 9.6, 6.6 Hz, 1H, *minor diastereomer*), 3.85–3.74 (m, 2H), 2.63–2.54 (m, 12H), 2.32–2.26 (m, 6H), 1.90–1.81 (m, 1H, *minor diastereomer*), 1.81–1.70 (m, 1H), 1.42–1.33 (m, 18H), 1.29 (td, *J* = 7.1, 2.9 Hz, 6H), 1.11 (d, *J* = 6.7 Hz, 4H), 0.97 (d, *J* = 6.7 Hz, 4H), 0.93 (d, *J* = 6.8 Hz, 2H), 0.88 (d, *J* = 6.8 Hz, 2H). *Mixture of two diastereomers is reported*.

^{13}C NMR (126 MHz, $CDCl_3$) δ 172.30, 172.02, 155.69, 155.42, 141.39, 141.17, 138.03, 137.73, 137.57, 136.95, 136.92, 131.08, 131.04, 131.01, 79.68, 79.50, 62.46, 62.00, 61.80, 59.55, 58.97, 57.84, 57.33, 30.51, 30.07, 29.37, 28.43, 28.41, 28.38, 28.35, 21.20, 21.17, 21.14, 20.17, 19.99, 19.70, 19.58, 19.55, 19.48, 19.43, 19.30, 18.74, 17.49, 14.24, 14.19, 14.16, 14.11. *Mixture of two diastereomers is reported*.

R_f = 0.26 & 0.40 for two diastereomers at β-position (chloroform/ethyl acetate 20:1)

Compound **3o** (ethyl (2*R*)-3-((*tert*-butoxycarbonyl)amino)-2-(((*R*)-mesitylsulfinyl)amino)-4-phenylbutanoate)

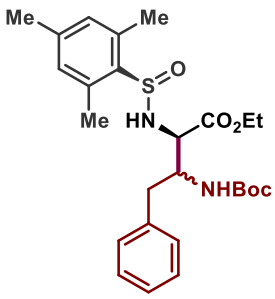

Synthesized according to the general procedure described in **Section 3** on 0.2 mmol scale and 3 h reaction time (1 h reaction time for NMR yield). The crude product was purified by column chromatography using hexane/CH_2Cl_2/ethyl acetate 6:1:1 as eluent. Two sets of fractions were combined and concentrated, resulting in pure β-diastereomer **3o-1** (20.5 mg, >95:5 α dr, >95:5 β dr) and a mixture of β-diastereomers **3o-1** and **3o-2** (78.6 mg, >95:5 α dr, 1:1 β dr). The products are pale-yellow oils (in total 99.1 mg, **>99% yield**, >95:5 α dr, 1.5:1 β dr).

^{1}H NMR for diastereomer **3o-1** (500 MHz, $CDCl_3$) δ 7.37–7.28 (m, 2H), 7.28–7.17 (m, 3H), 6.93 (s, 2H), 5.40 (d, *J* = 7.3 Hz, 1H), 4.58–4.41 (m, 2H), 4.28–4.12 (m, 2H), 4.04 (dd, *J* = 7.4, 2.3 Hz, 1H), 2.95–2.88 (m, 1H), 2.88–2.79 (m, 1H), 2.67 (s, 6H), 2.33 (s, 3H), 1.35–1.21 (m, 12H).

^{13}C NMR for diastereomer **3o-1** (126 MHz, $CDCl_3$) δ 171.83, 154.92, 141.50, 138.05, 137.11, 137.02, 131.13, 129.55, 129.43, 128.83, 128.64, 126.95, 79.73, 62.52, 58.00, 54.25, 39.12, 28.38, 28.29, 21.22, 19.64, 19.61, 14.10.

^{1}H NMR for a mixture of diastereomers **3o-1** and **3o-2** (500 MHz, $CDCl_3$) δ 7.35–7.29 (m, 2H), 7.29–7.23 (m, 4H), 7.23–7.17 (m, 2H, *diastereomer* **3o-2**), 7.14 (d, *J* = 7.5 Hz, 2H, *diastereomer* **3o-2**), 6.93 (s, 2H), 6.89 (s, 2H, *diastereomer* **3o-2**), 5.40 (d, *J* = 7.3 Hz, 1H), 5.28 (d, *J* = 8.7 Hz, 1H, *diastereomer* **3o-2**), 4.77 (d, *J* = 9.1 Hz, 1H, *diastereomer* **3o-2**), 4.57–4.42 (m, 2H), 4.36–4.30 (m, 1H, *diastereomer* **3o-2**), 4.30–4.07 (m, 7H), 4.04 (dd, *J* = 7.6, 2.2 Hz, 1H), 2.95–2.88 (m, 1H), 2.88–2.79 (m, 1H), 2.67 (s, 6H), 2.61 (s, 6H, *diastereomer* **3o-2**), 2.32 (s, 3H), 2.30 (s, 3H, *diastereomer* **3o-2**), 1.38 (s, 9H, *diastereomer* **3o-2**), 1.32–1.21 (m, 15H).

^{13}C NMR for a mixture of diastereomers **3o-1** and **3o-2** (126 MHz, $CDCl_3$) δ 171.82, 171.44, 155.06, 154.91, 141.49, 141.27, 138.04, 137.65, 137.10, 137.00, 136.90, 131.12, 131.08, 130.92, 129.54, 129.48, 129.42, 129.39, 128.82, 128.71, 128.63, 128.59, 128.52, 126.94, 126.84, 126.73, 79.89, 79.72, 62.51, 62.22, 62.06, 59.65, 57.99, 54.24, 53.68, 39.10, 36.36, 31.72, 28.42, 28.28, 23.20, 22.79, 21.20, 21.18, 19.63, 19.60, 19.58, 19.52, 14.25, 14.22, 14.09.

***R*$_f$** = 0.23 & 0.19 for diastereomers **3o-1** & **3o-2**, respectively (hexane/CH_2Cl_2/ /ethyl acetate 6:1:1)

Compound **3p** (ethyl (*R*)-2-(((*R*)-mesitylsulfinyl)amino)-2-((*R*)-tetrahydrofuran-2-yl)acetate)

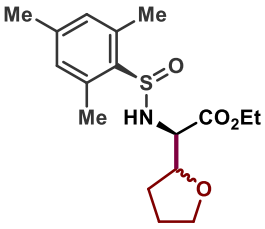

Synthesized according to the general procedure described in **Section 3** on 2 mmol scale and 3 h reaction time (2 h reaction time for NMR yield). The crude product was purified by column chromatography using hexane/CH_2Cl_2/ethyl acetate 5:2:2 as eluent. The product is a pale-yellow oil (30.4 mg, **45% yield**, >95:5 α dr, 1.3:1 β dr).

^{1}H NMR (500 MHz, $CDCl_3$) δ 6.86 (s, 4H), 5.20 (d, *J* = 9.0 Hz, 1H), 5.14 (d, *J* = 8.6 Hz, 1H, *minor diastereomer*), 4.33–4.26 (m, 1H), 4.26–4.18 (m, 4H), 4.18–4.11 (m, 1H), 4.11–4.01 (m, 1H), 4.00–3.90 (m, 1H), 3.89–3.80 (m, 1H), 3.80–3.71 (m, 2H), 3.71–3.63 (m, 1H), 2.64–2.54 (m, 12H), 2.28 (s, 6H), 2.05–1.96 (m, 1H), 1.96–1.88 (m, 2H), 1.88–1.75 (m, 5H), 1.33–1.23 (m, 6H). *Mixture of two diastereomers is reported*.

^{13}C NMR (126 MHz, $CDCl_3$) δ 171.66, 171.59, 141.03, 141.00, 140.97, 138.14, 137.89, 137.35, 137.30, 136.93, 136.86, 131.04, 130.99, 130.94, 130.93, 80.11, 79.44, 69.40, 69.04, 68.93, 62.00, 61.96, 61.82, 61.62, 60.56, 60.03, 60.01, 59.89, 28.30, 28.26, 28.04, 27.70, 26.22, 26.12, 25.75, 25.46, 21.16, 19.57, 19.53, 19.39, 14.29, 14.27, 14.25, 14.22. *Mixture of two diastereomers is reported*.

R_f = 0.27 (hexane/CH_2Cl_2/ethyl acetate 5:2:2)

Compound **3q** (ethyl (2*R*,3*S*)-2-(((*R*)-mesitylsulfinyl)amino)-3-methoxy-3-phenylpropanoate)

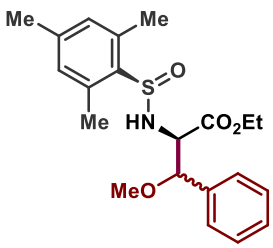

Synthesized according to the general procedure described in **Section 3** on 0.15 mmol scale and 3 h reaction time (2 h reaction time for NMR yield). The crude product was purified by preparative TLC using chloroform/ethyl acetate 5:1 as eluent. The product is a colorless oil (35.1 mg, **60% yield**, >95:5 α dr, 1.4:1 β dr).

^{1}H NMR (500 MHz, $CDCl_3$) δ 7.39–7.24 (m, 4H), 7.24–7.18 (m, 1H), 6.80 (s, 2H), 5.26 (d, *J* = 8.8 Hz, 1H, *minor diastereomer*), 4.95 (d, *J* = 9.4 Hz, 1H), 4.72 (d, *J* = 3.4 Hz, 1H, *minor diastereomer*), 4.37 (d, *J* = 6.8 Hz, 1H), 4.34–4.26 (m, 1H, *minor diastereomer*), 4.26–4.16 (m, 2H), 4.16–4.08 (m, 1H), 3.24 (s, 3H), 3.23 (s, 3H, *minor diastereomer*), 2.36 (s, 3H), 2.33 (s, 3H), 2.26 (s, 3H), 1.28 (t, *J* = 7.1 Hz, 3H, *minor diastereomer*), 1.25 (t, *J* = 7.1 Hz, 3H). *Mixture of two diastereomers is reported*.

^{13}C NMR (126 MHz, $CDCl_3$) δ 171.62, 171.03, 140.84, 140.79, 138.19, 137.90, 137.50, 137.43, 137.34, 136.87, 136.82, 131.02, 130.97, 130.92, 130.77, 130.68, 128.48, 128.42, 128.39, 128.37, 128.20, 128.13, 127.75, 127.38, 127.25, 127.09, 84.77, 84.03, 63.40, 62.62, 62.04, 61.83, 57.74, 57.29, 21.14, 19.40, 19.19, 19.15, 14.28, 14.17. *Mixture of two diastereomers is reported*.

R_f = 0.45 & 0.61 for two diastereomers at β-position (chloroform/ethyl acetate 5:1)

8. *NMR spectra*

^{1}H NMR (500 MHz, $CDCl_3$) of compound **1**

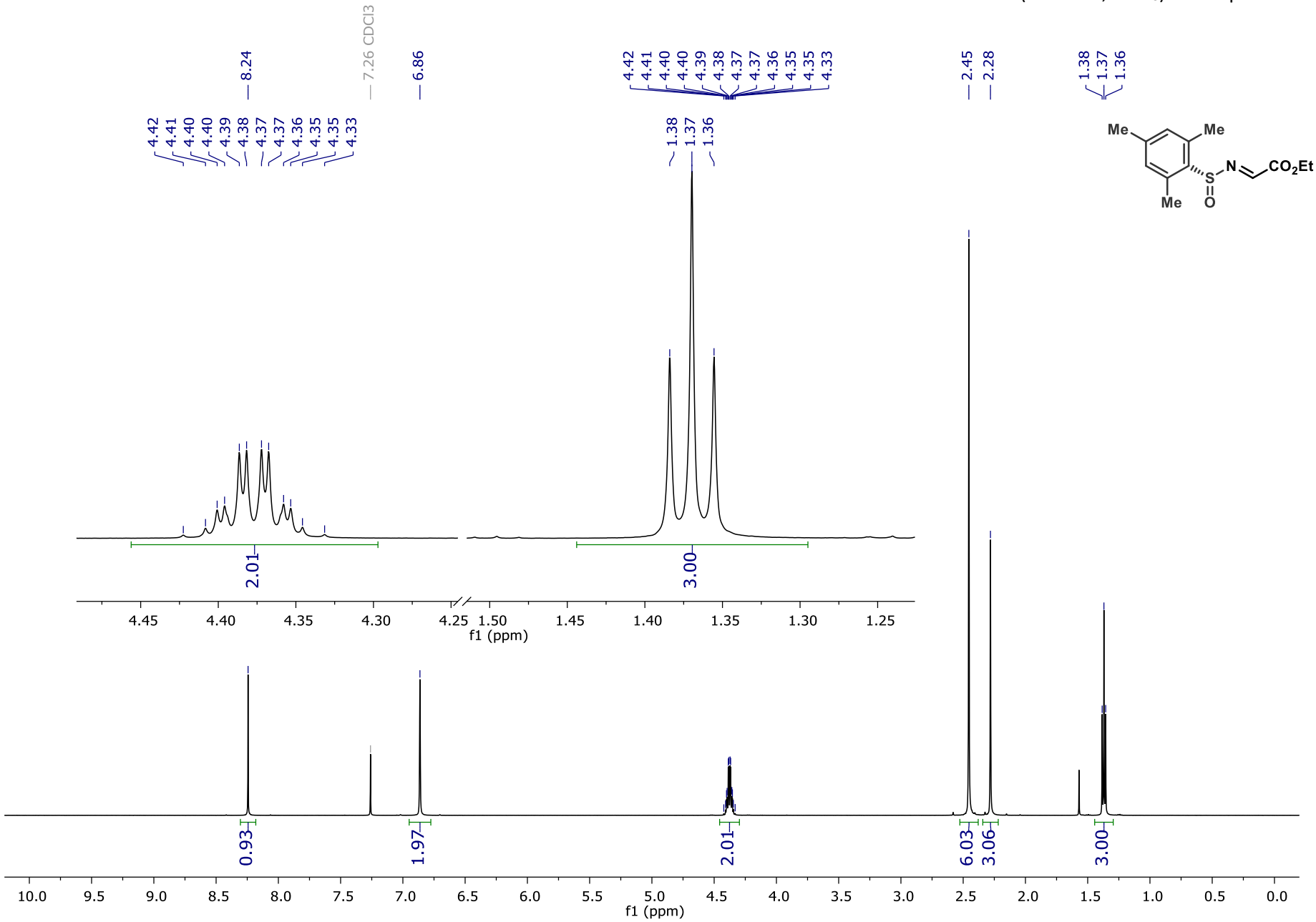

^{13}C NMR (126 MHz, $CDCl_3$) of compound **1**

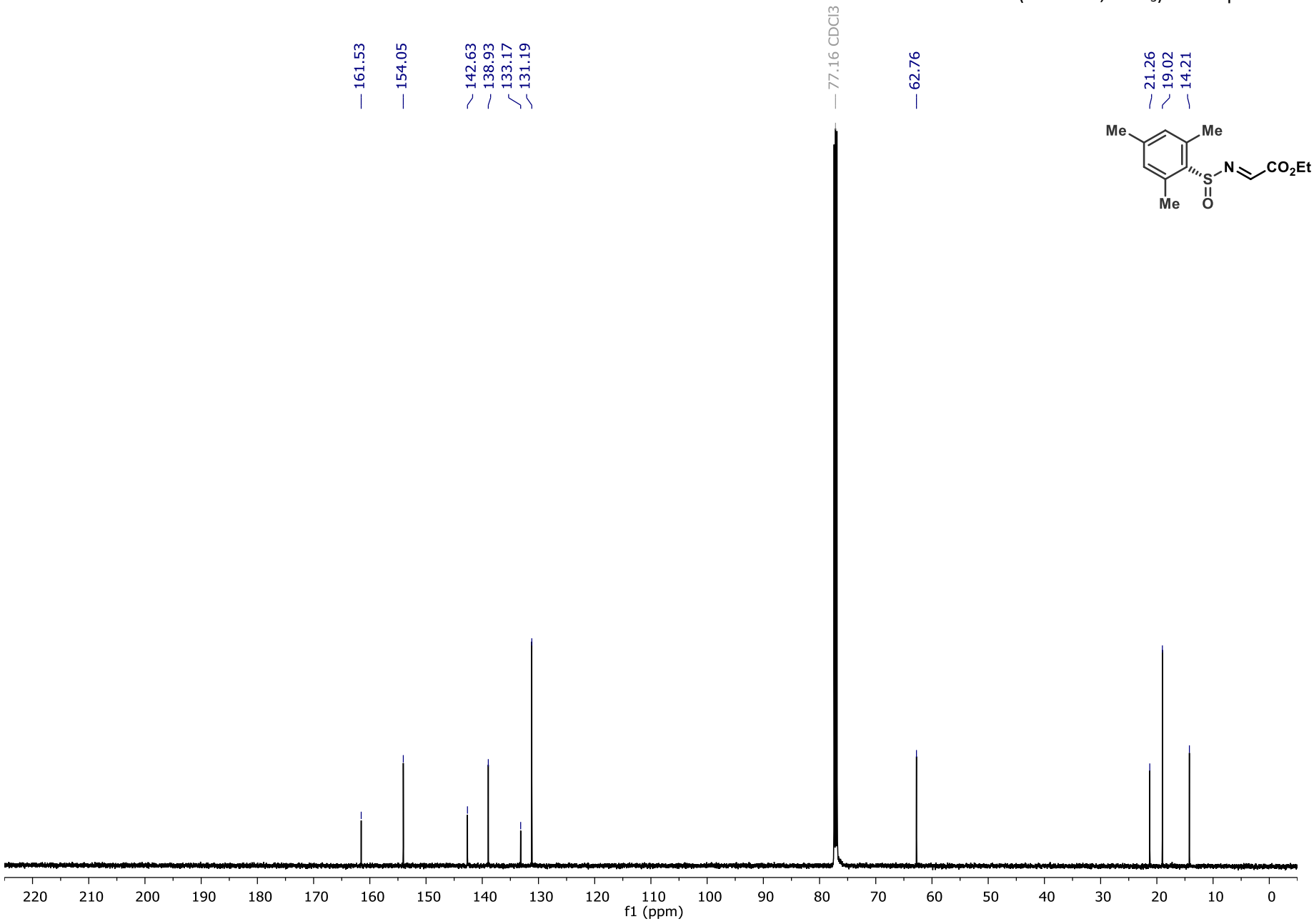

^{1}H NMR (400 MHz, $CDCl_3$) of compound **4**

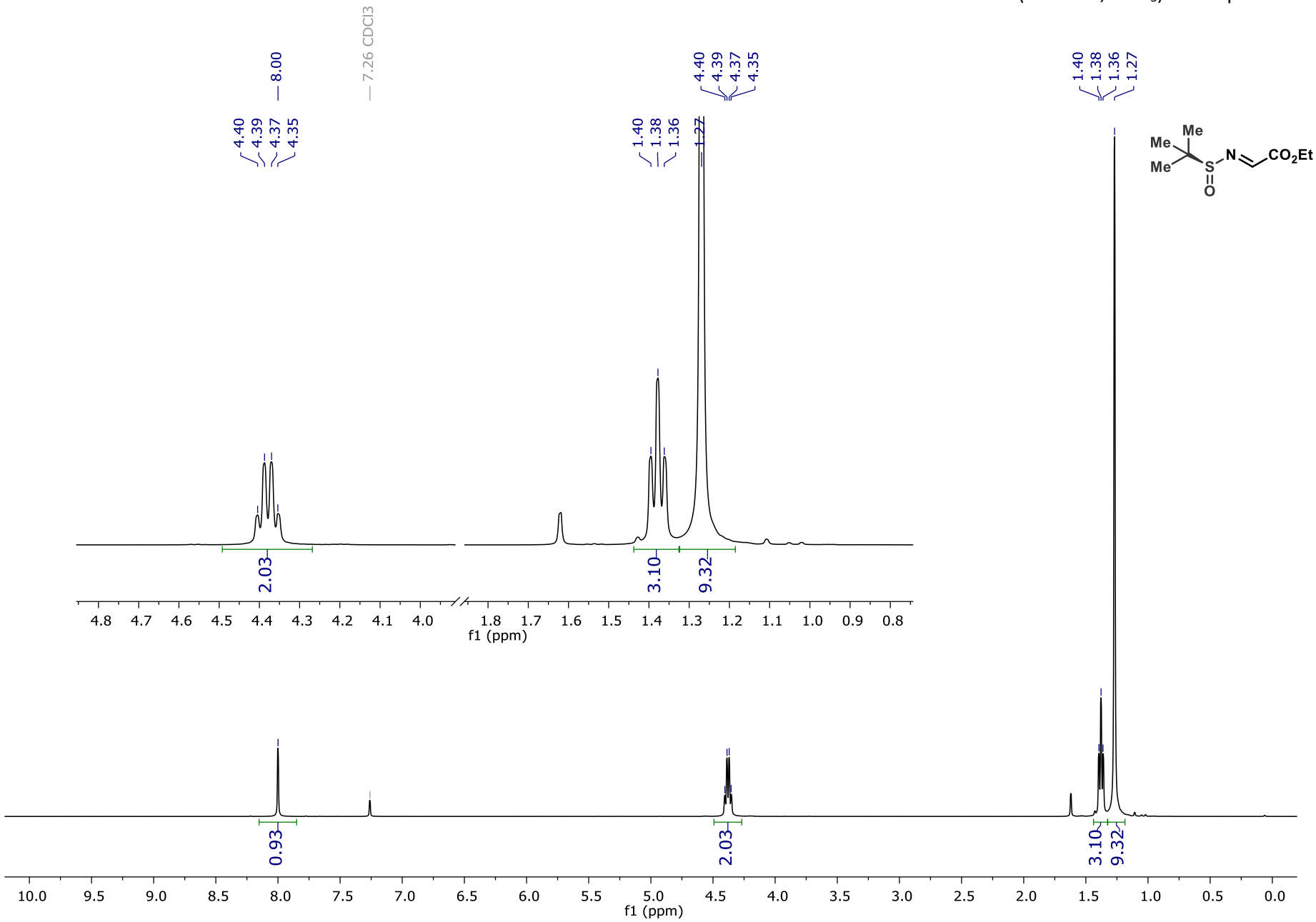

^{13}C NMR (101 MHz, $CDCl_3$) of compound **4**

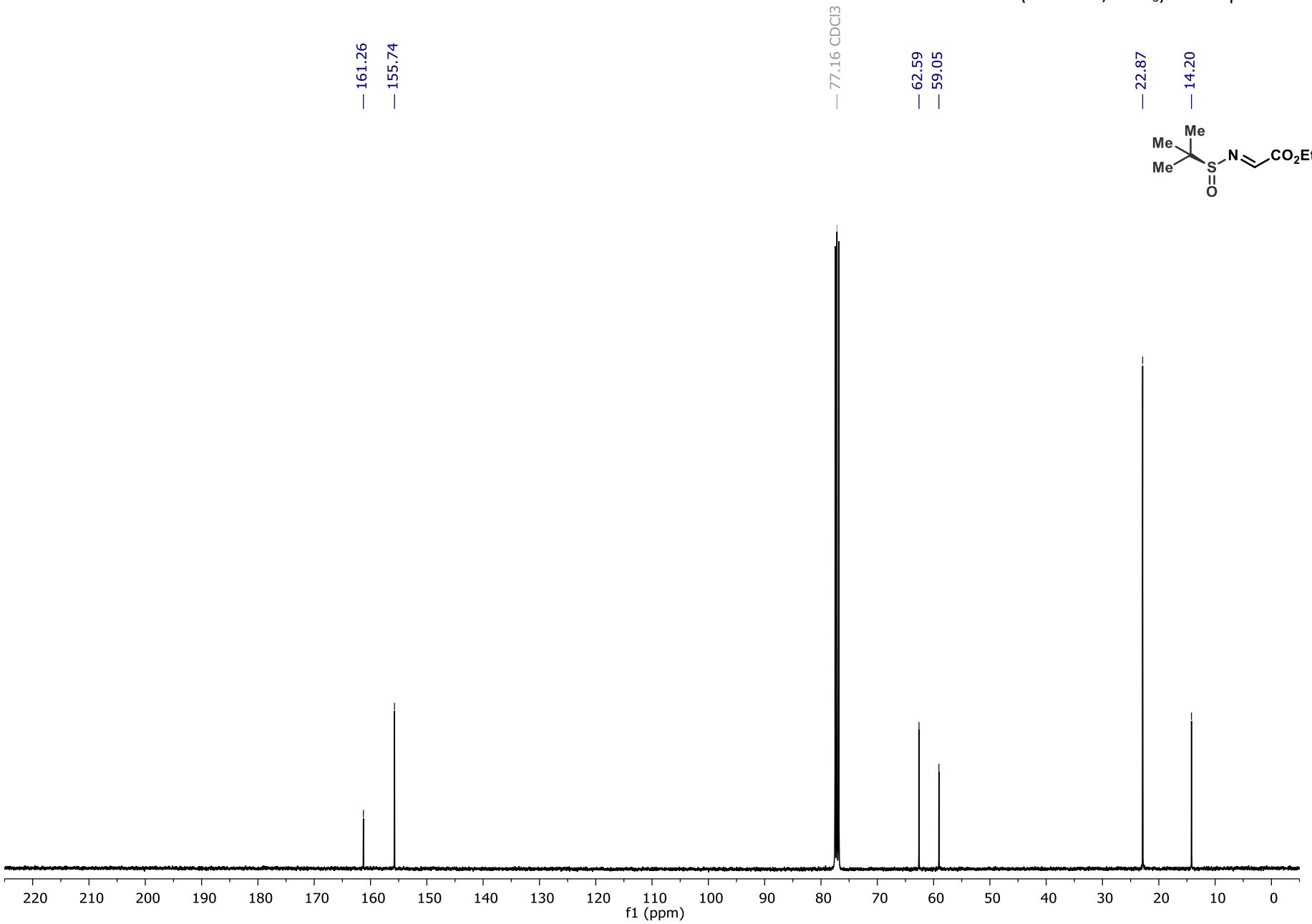

^{1}H NMR (400 MHz, $CDCl_3$) of compound **5**

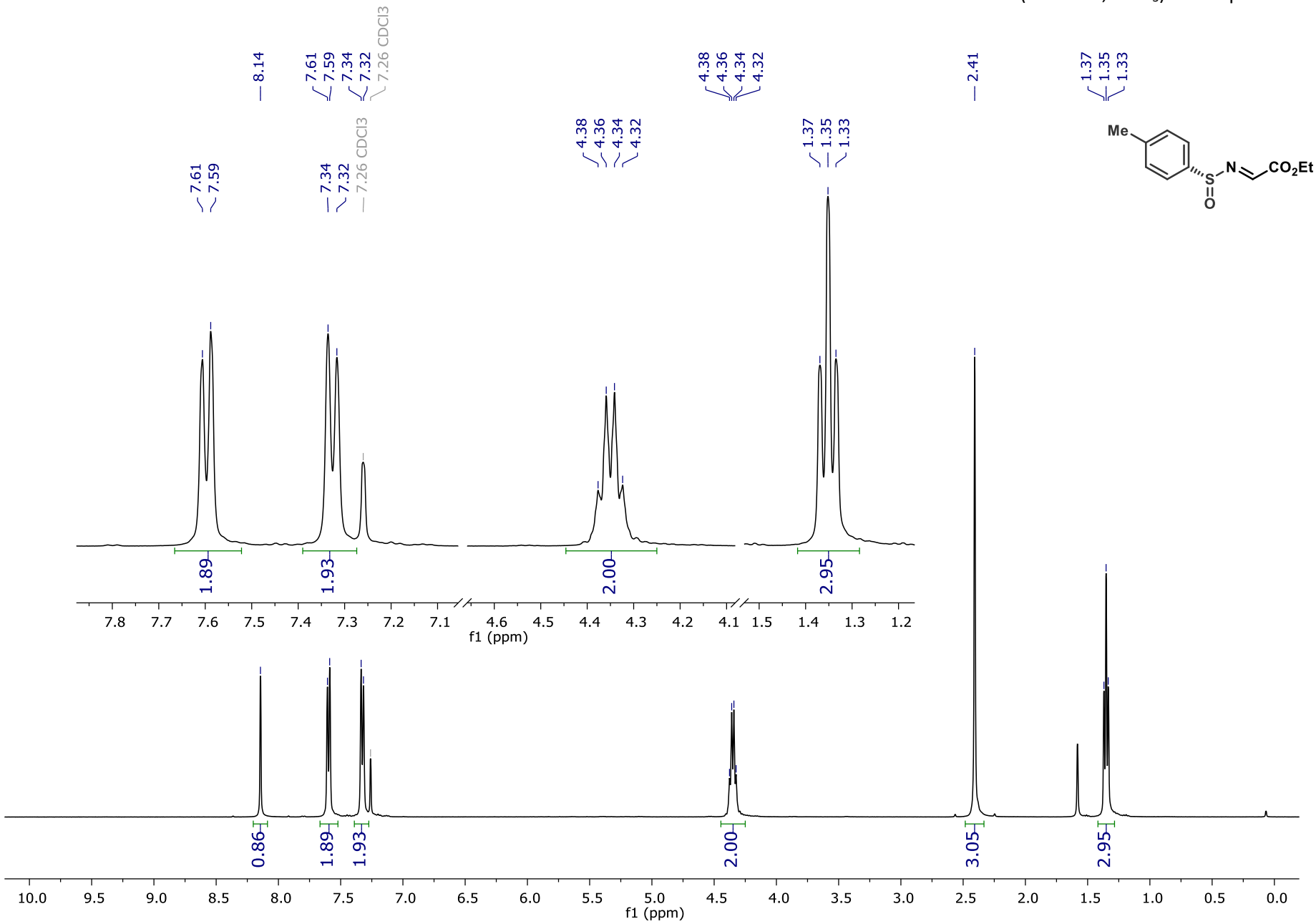

^{13}C NMR (101 MHz, $CDCl_3$) of compound **5**

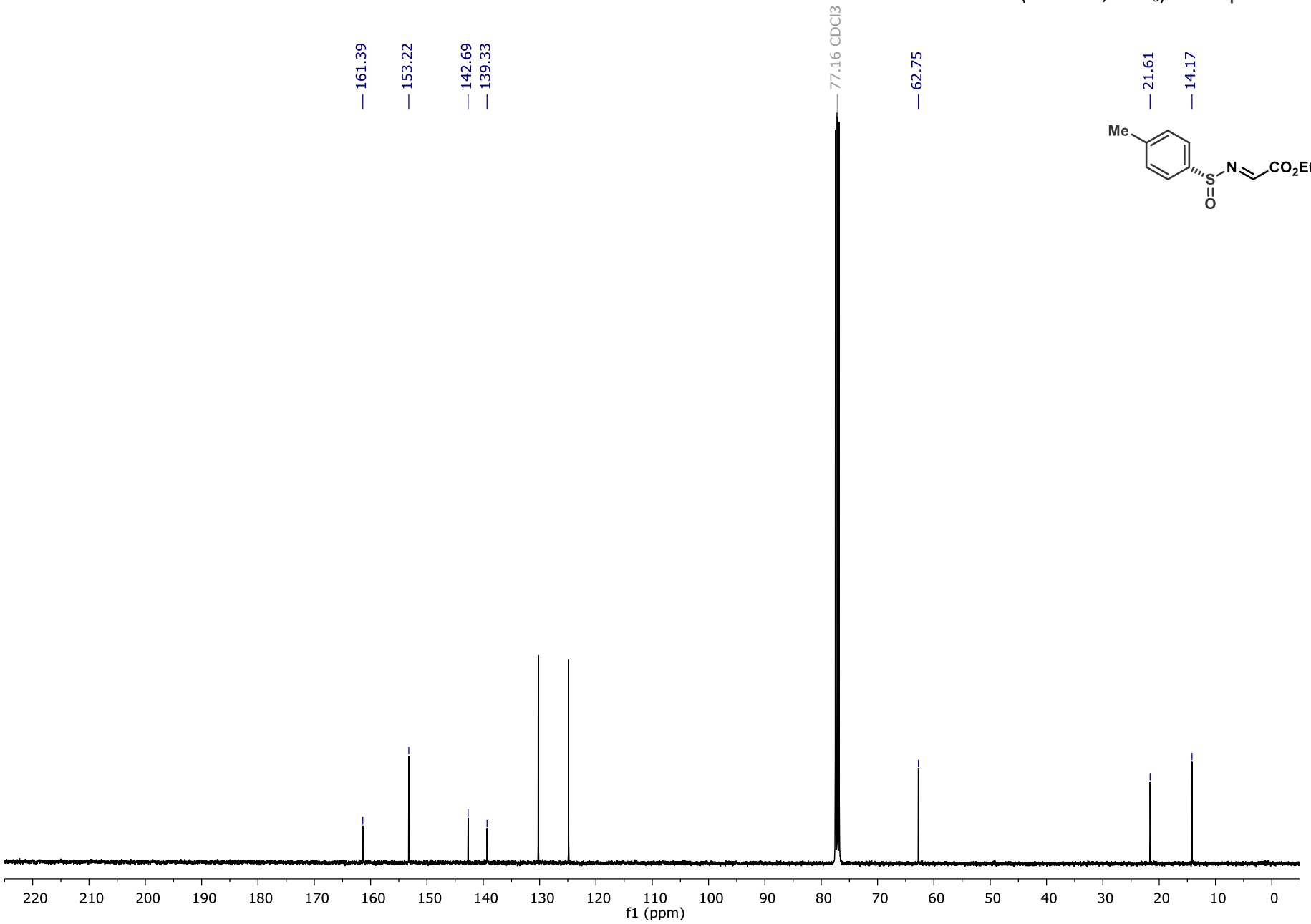

^{1}H NMR (500 MHz, $CDCl_3$) of compound **3a**

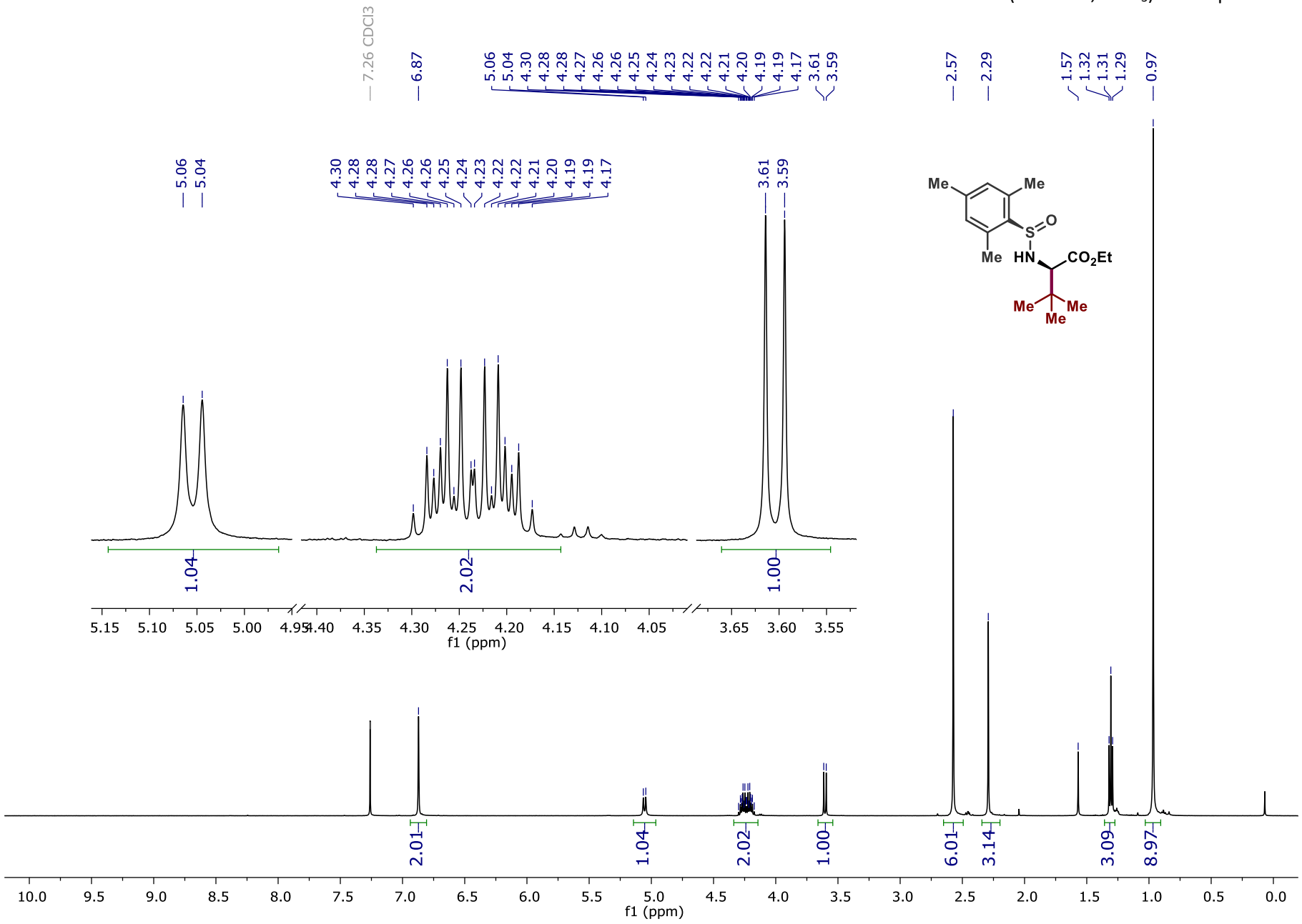

^{13}C NMR (126 MHz, $CDCl_3$) of compound **3a**

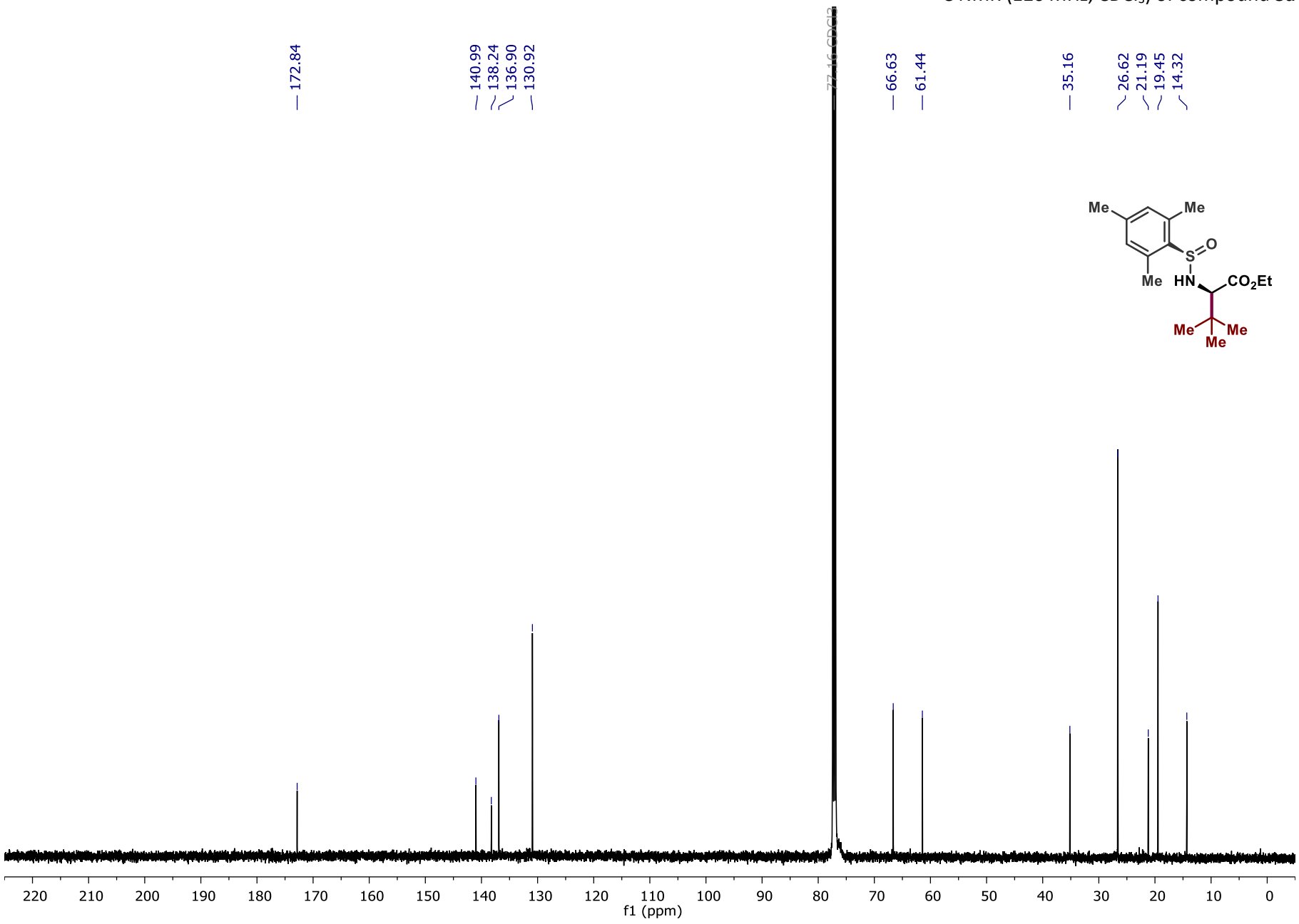

^{1}H NMR (500 MHz, $CDCl_3$) of compound **3b**

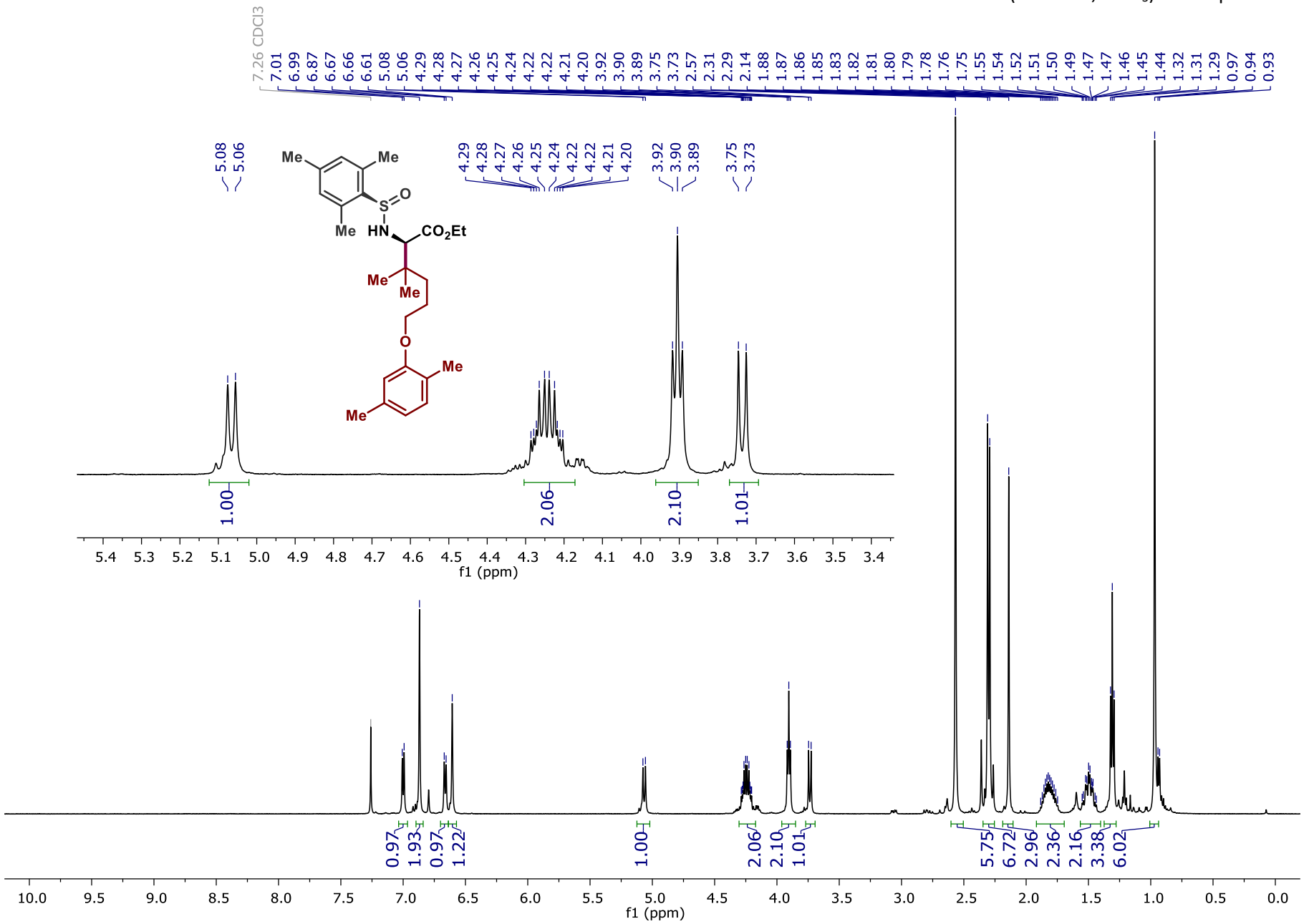

^{13}C NMR (126 MHz, $CDCl_3$) of compound **3b**

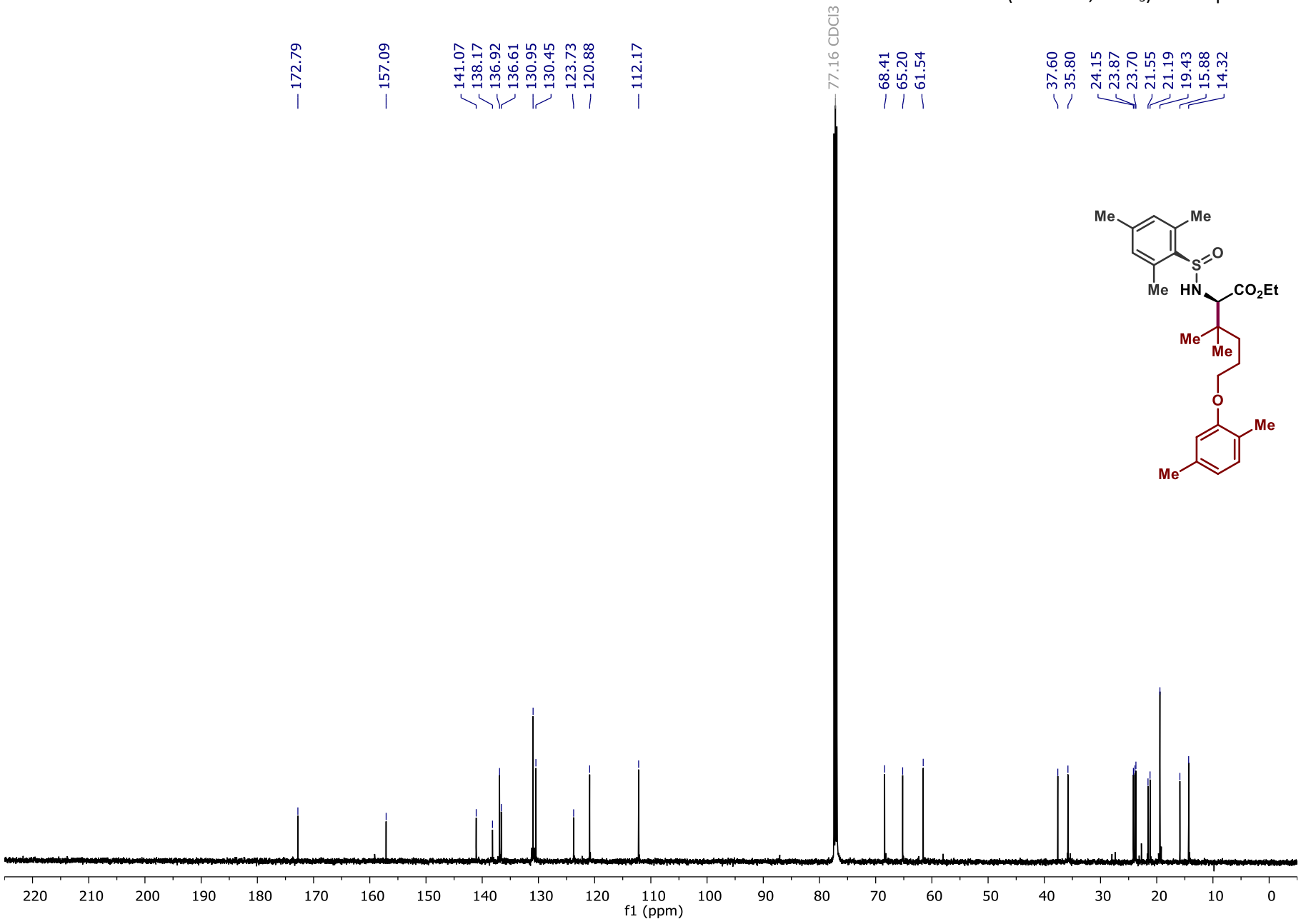

^{1}H NMR (500 MHz, $CDCl_3$) of compound **3c**

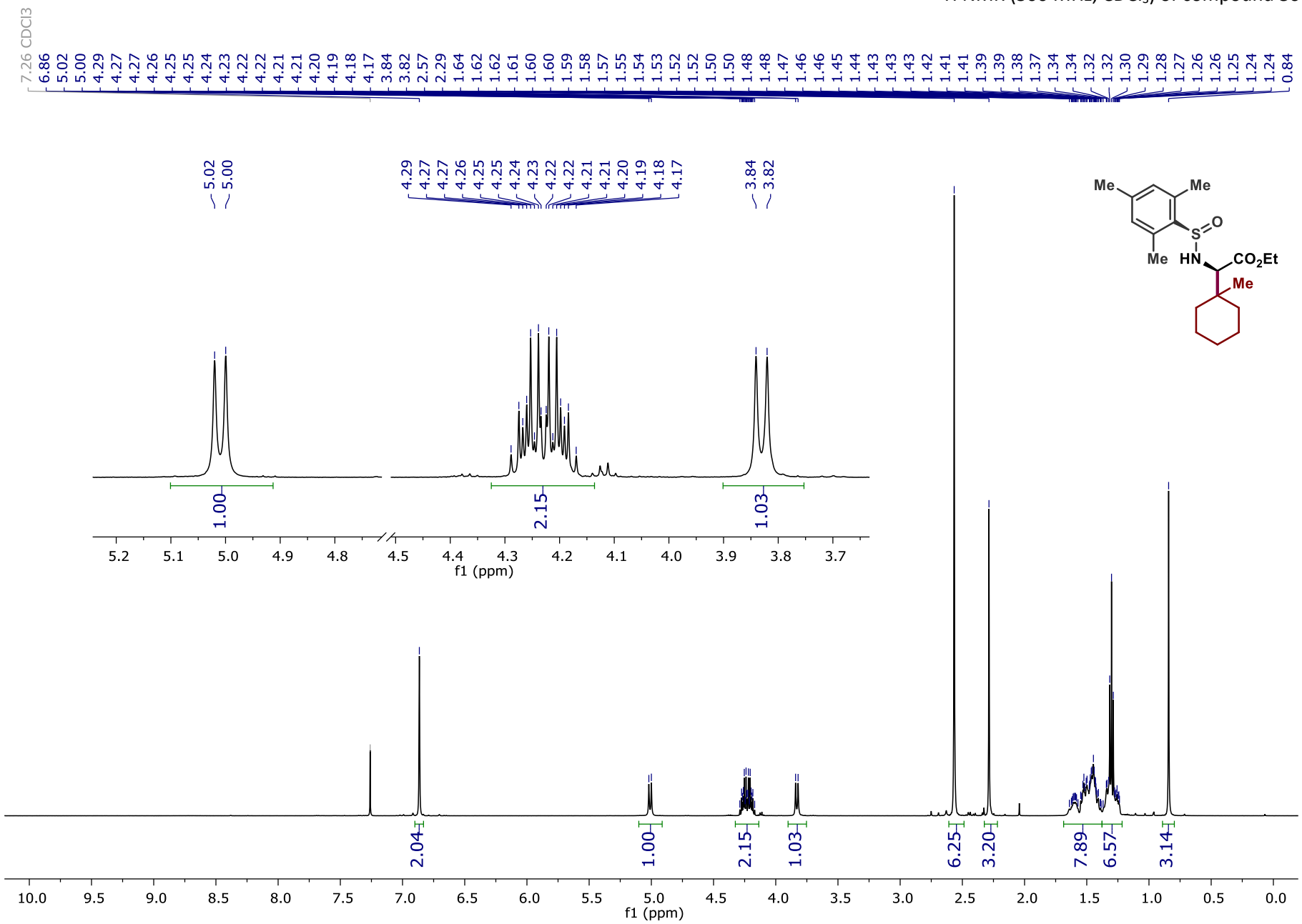

^{13}C NMR (126 MHz, $CDCl_3$) of compound **3c**

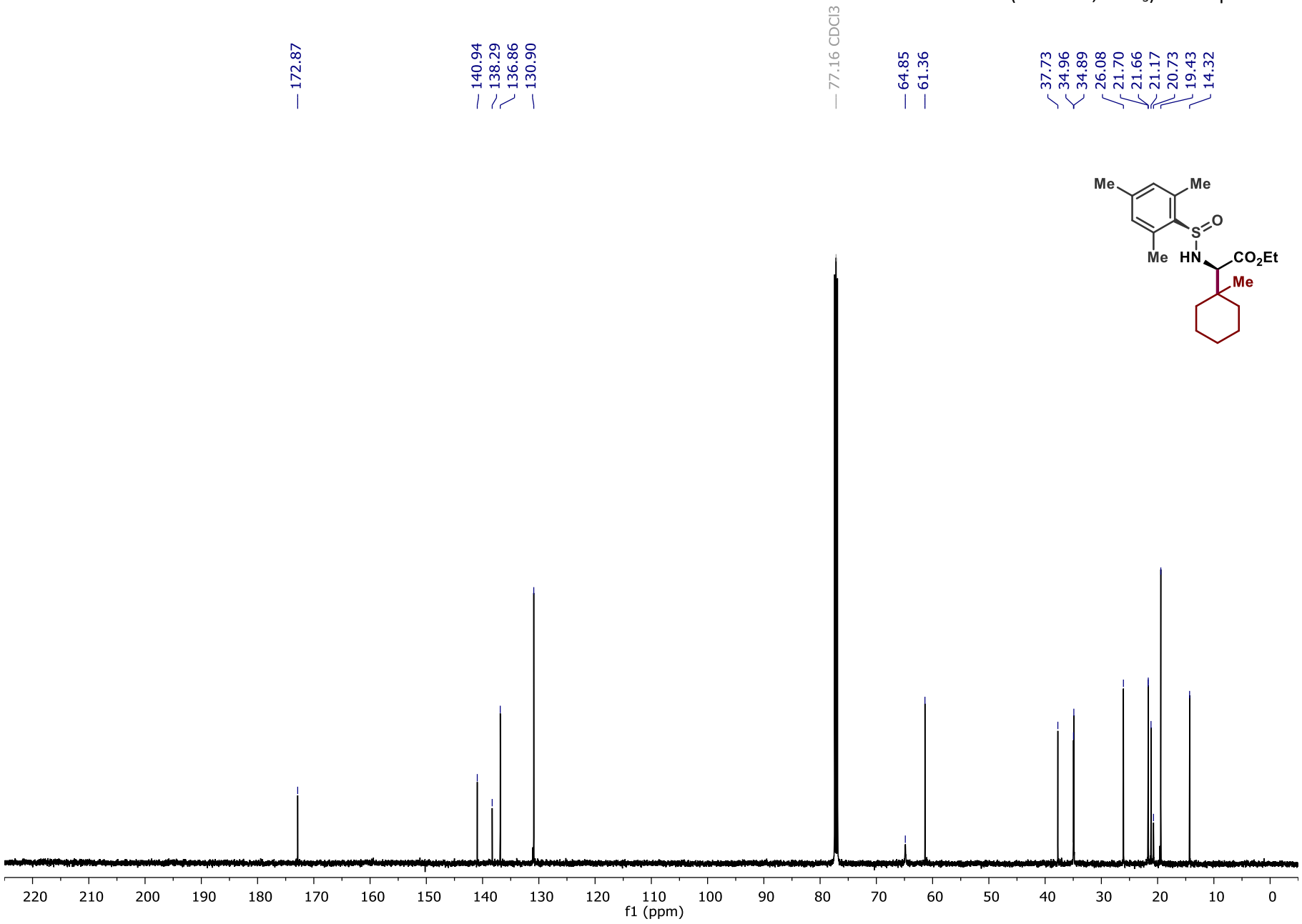

^{1}H NMR (500 MHz, $CDCl_3$) of compound **3d**

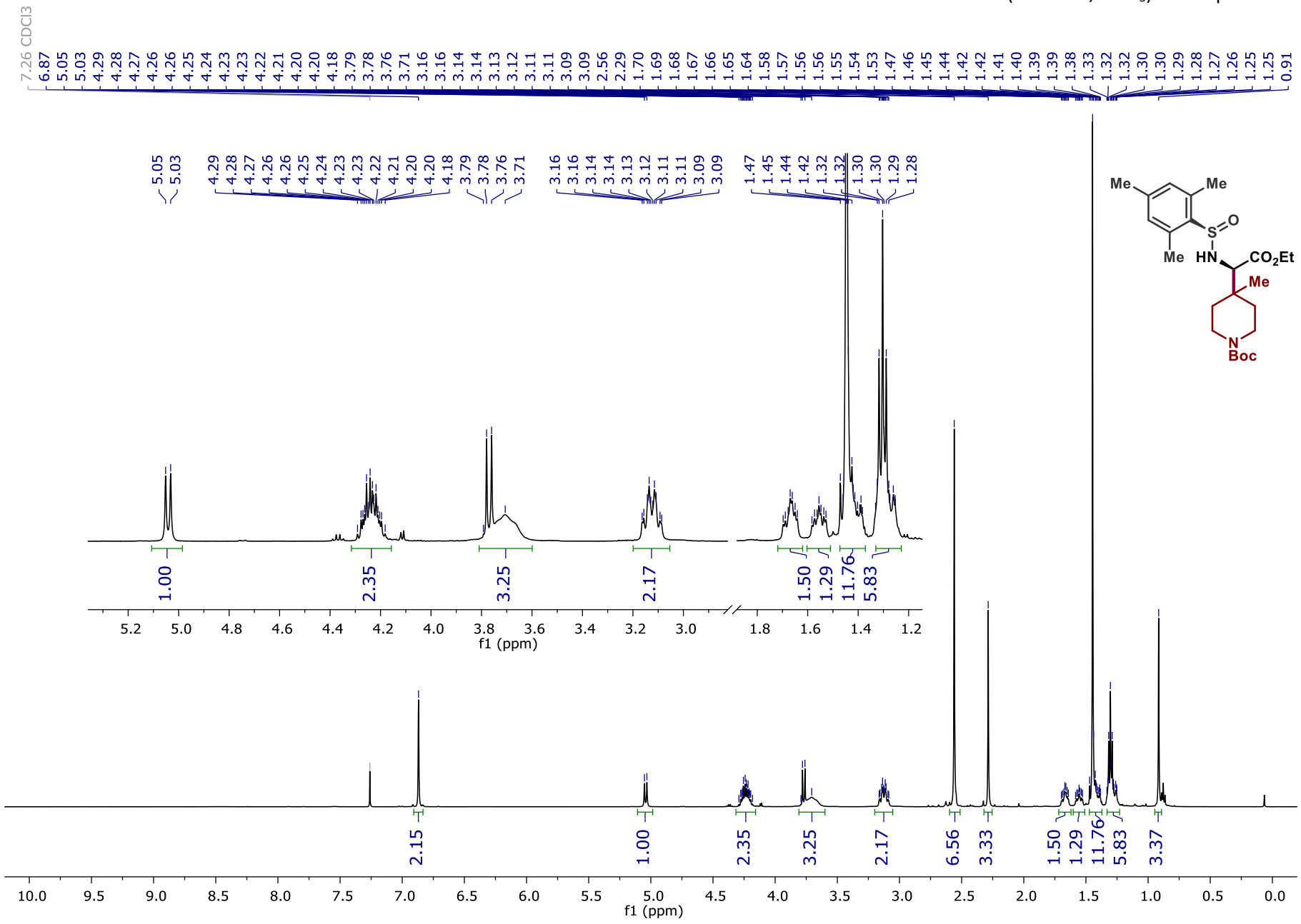

^{13}C NMR (126 MHz, $CDCl_3$) of compound **3d**

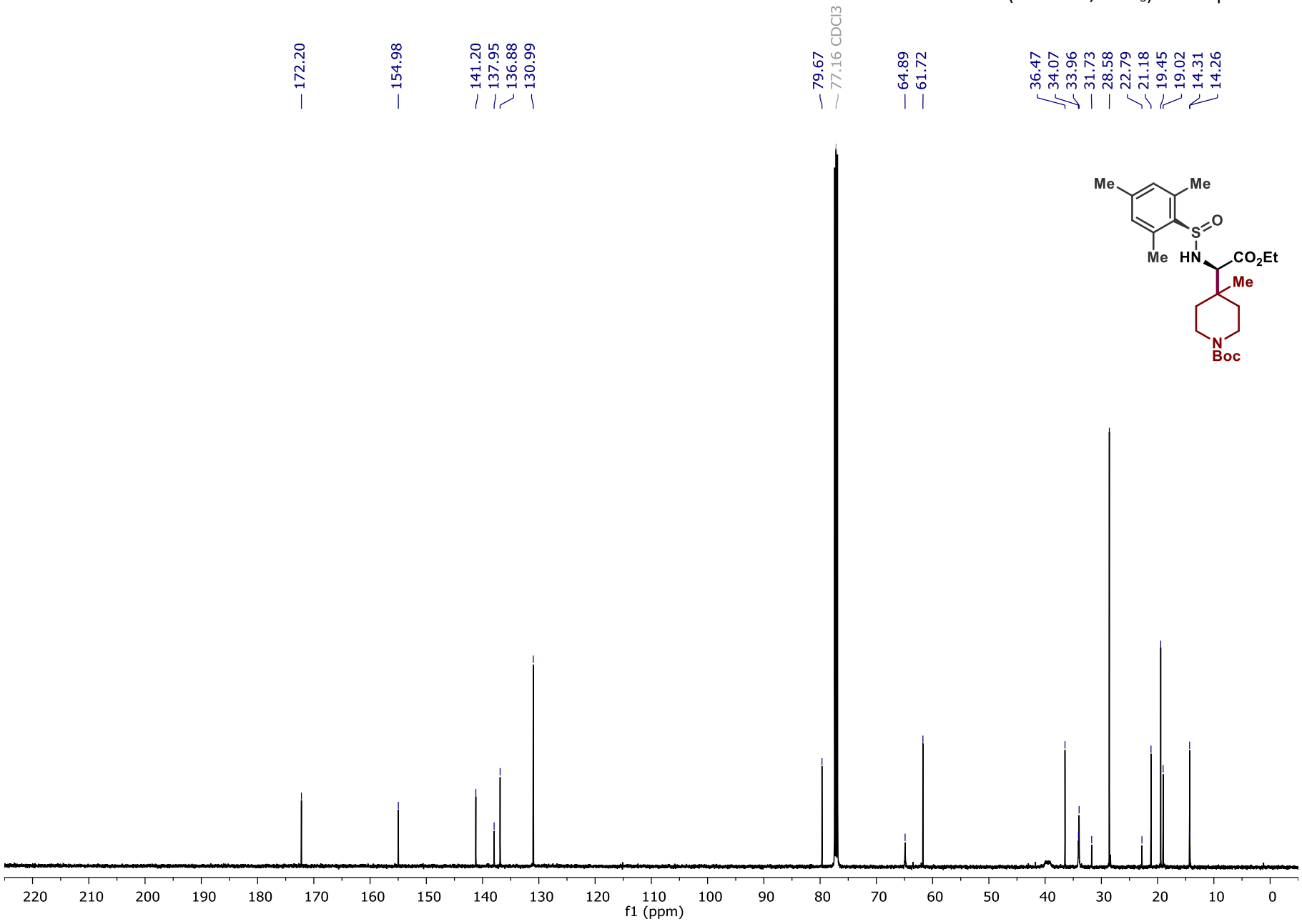

^{1}H NMR (500 MHz, $CDCl_3$) of compound **3e**

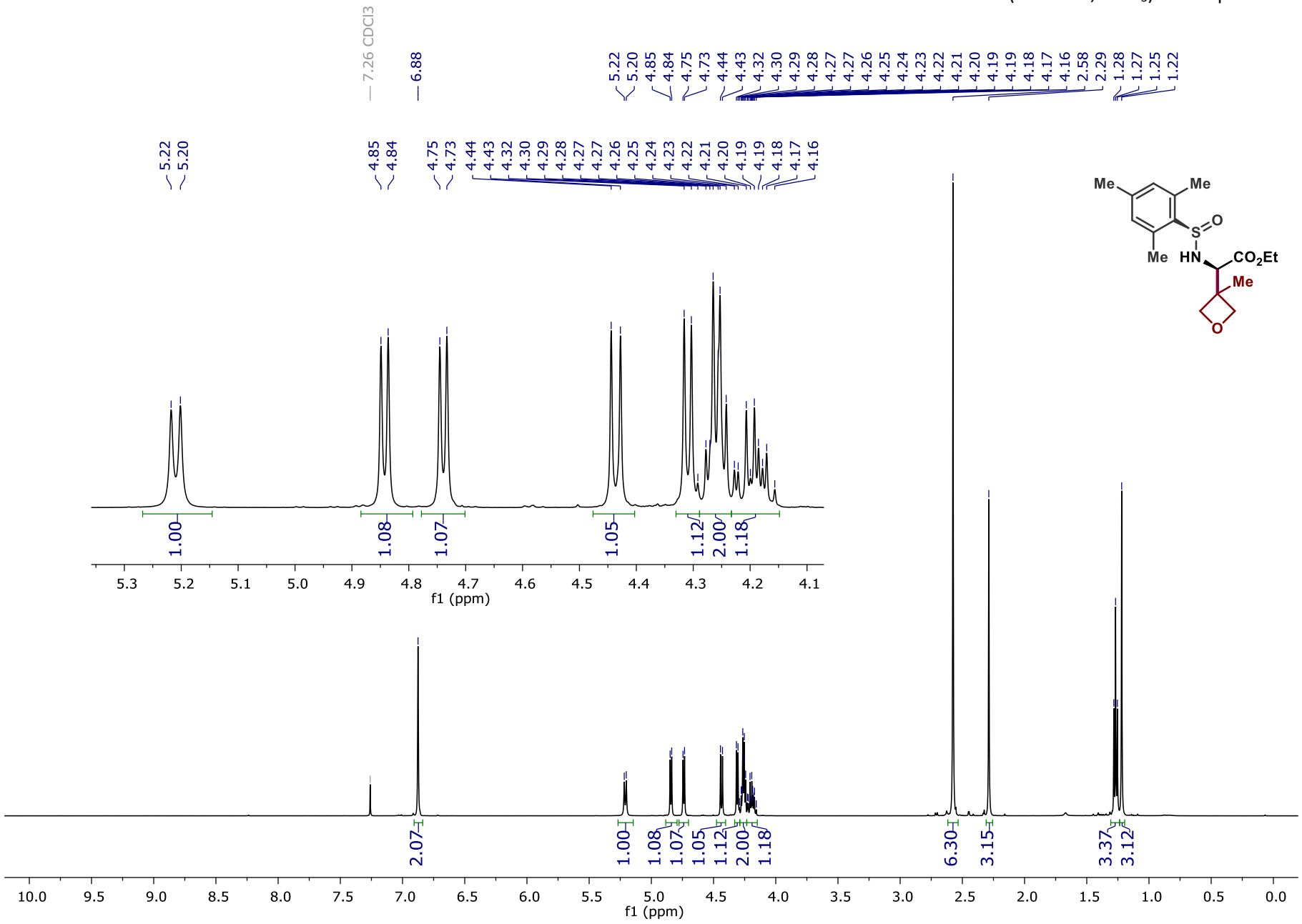

^{13}C NMR (126 MHz, $CDCl_3$) of compound **3e**

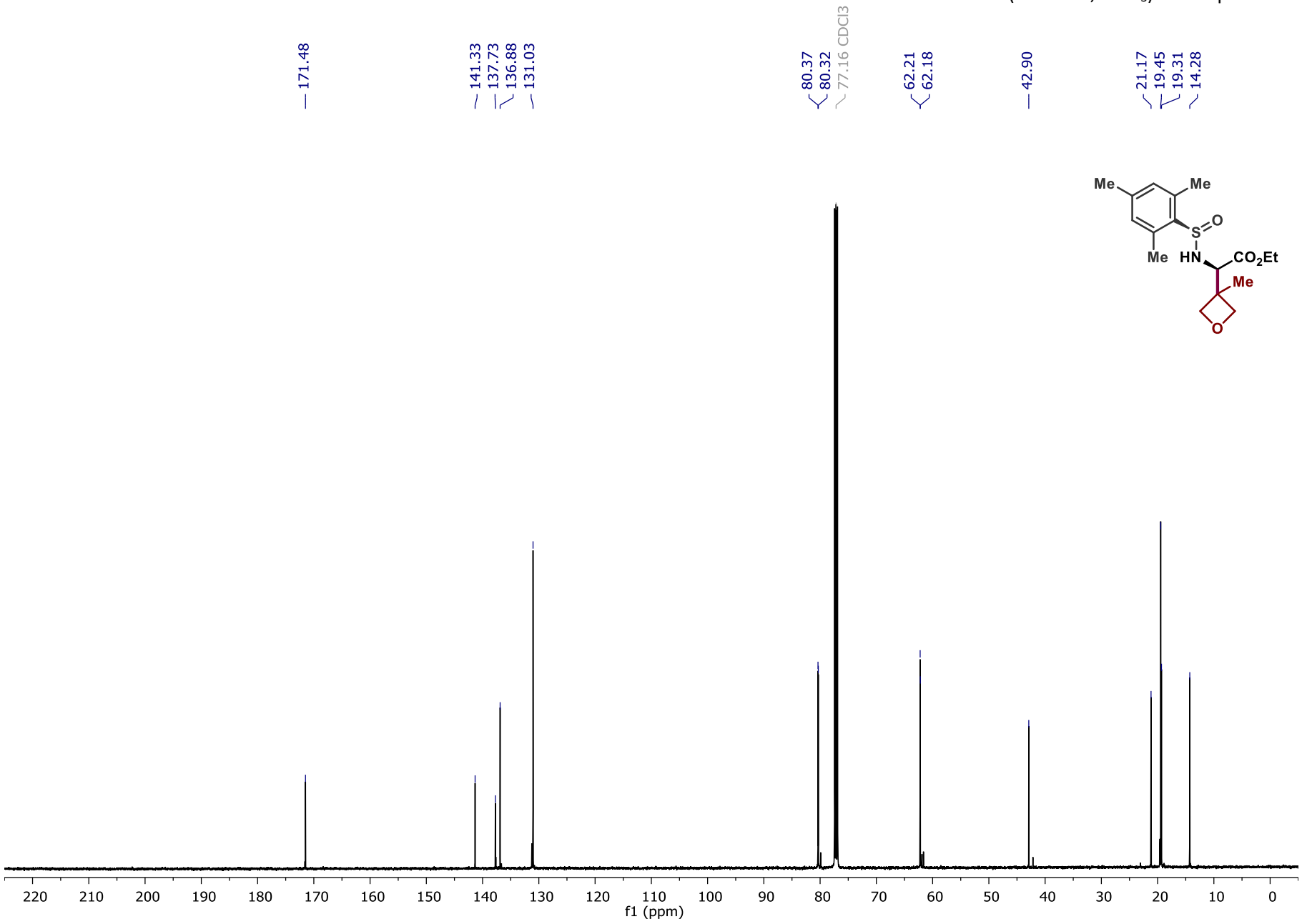

^{1}H NMR (500 MHz, $CDCl_3$) of compound **3f**

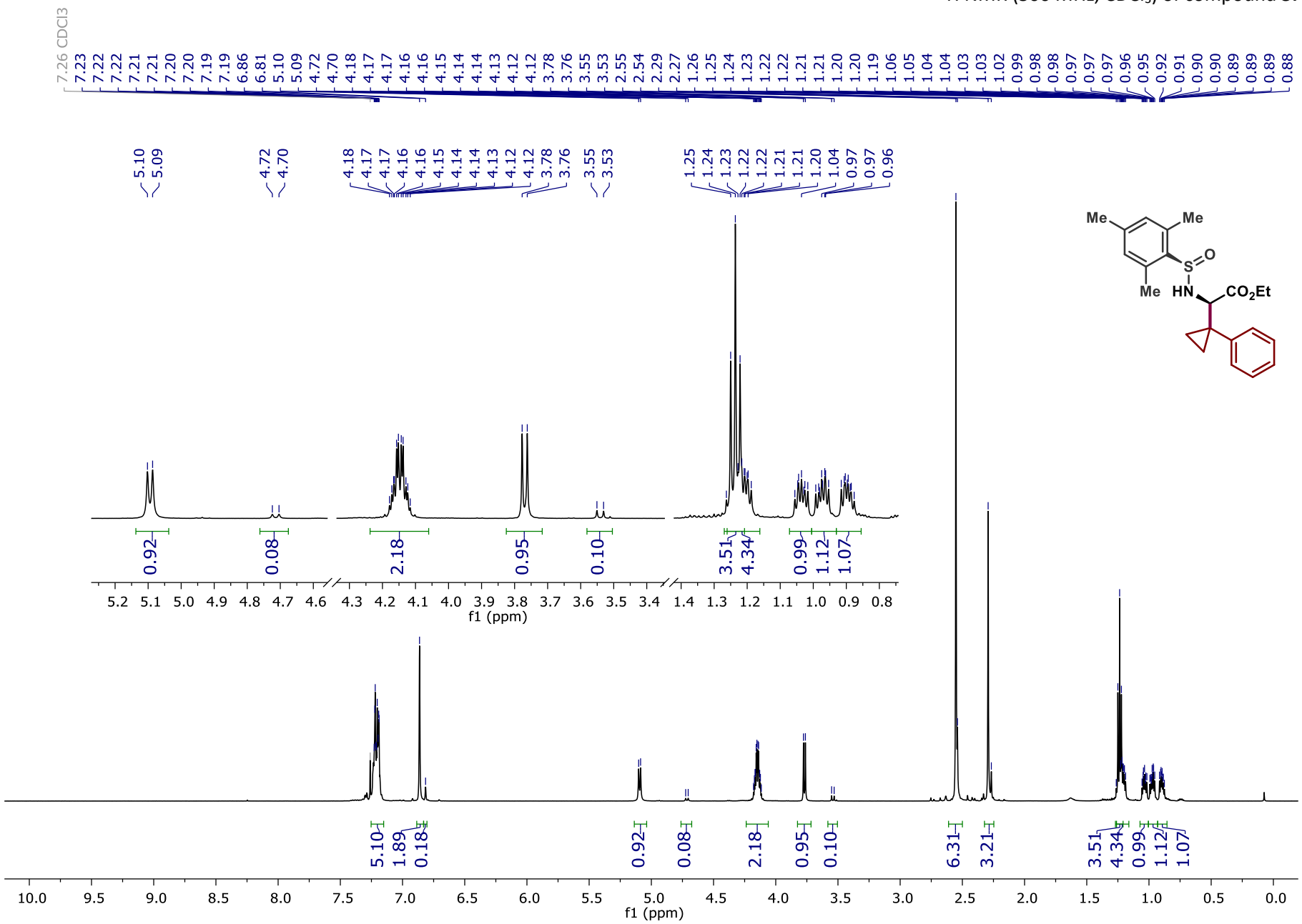

^{1}H NMR (126 MHz, $CDCl_3$) of compound **3f**

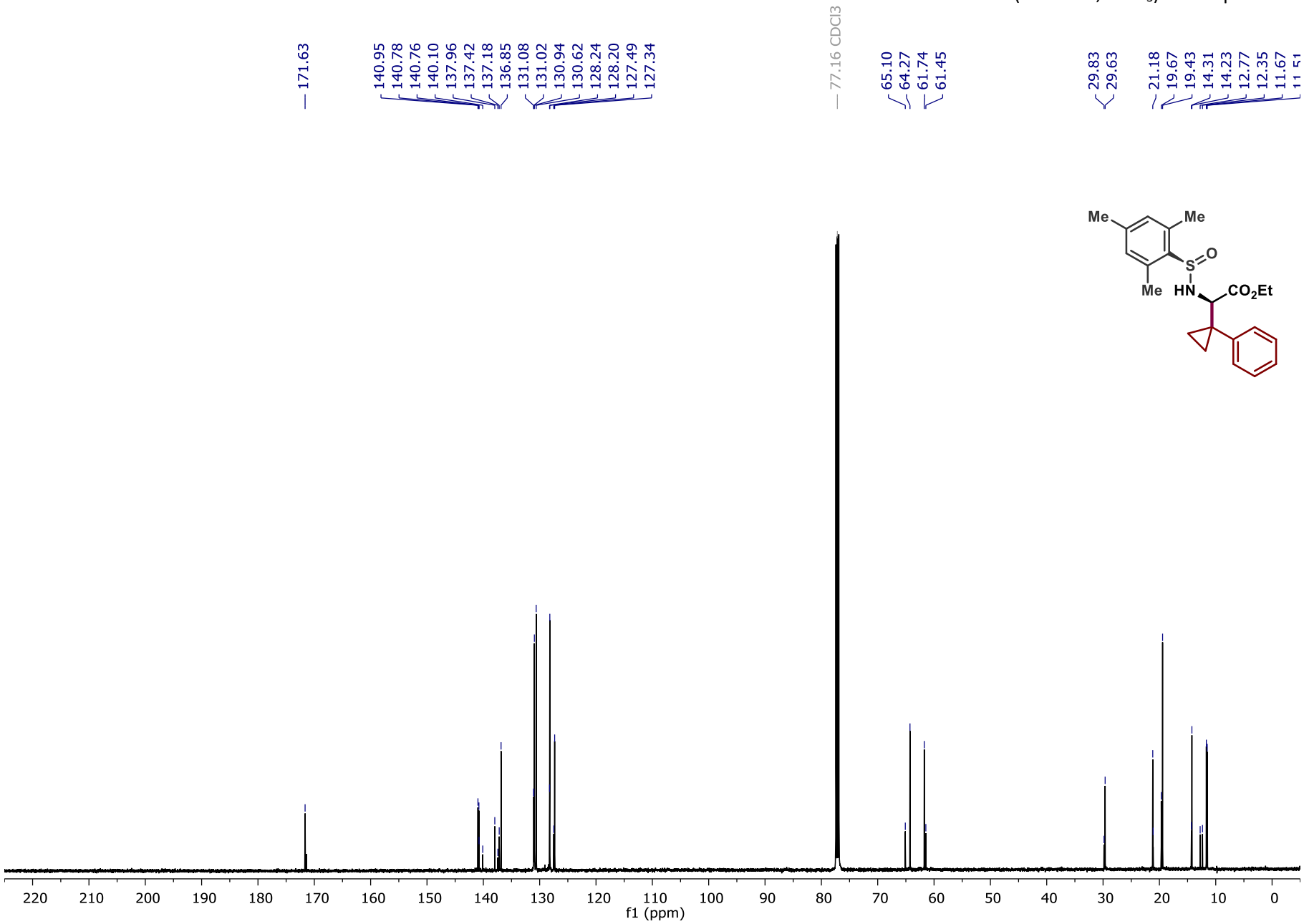

^{1}H NMR (500 MHz, $CDCl_3$) of compound **3g**

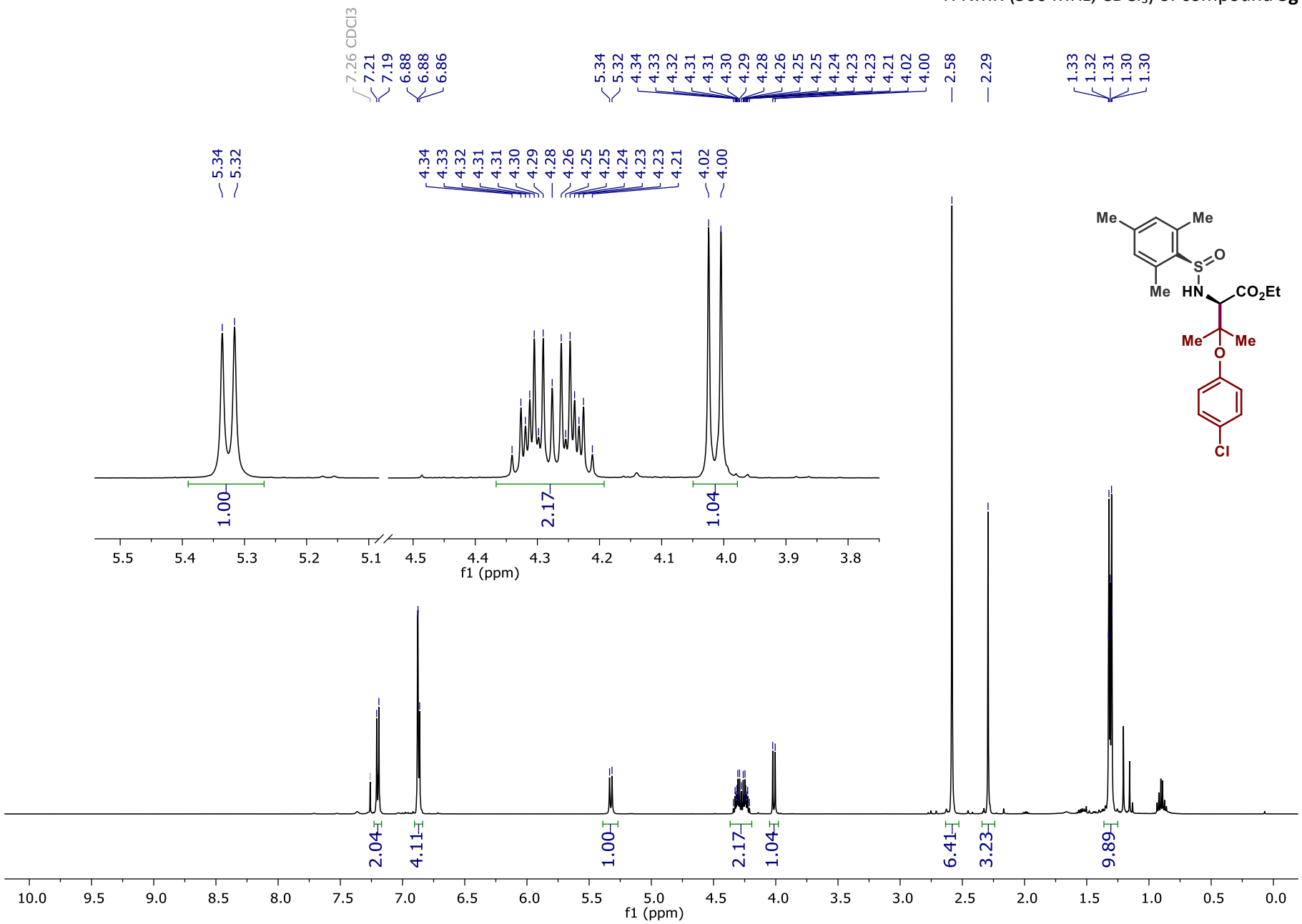

^{13}C NMR (126 MHz, $CDCl_3$) of compound **3g**

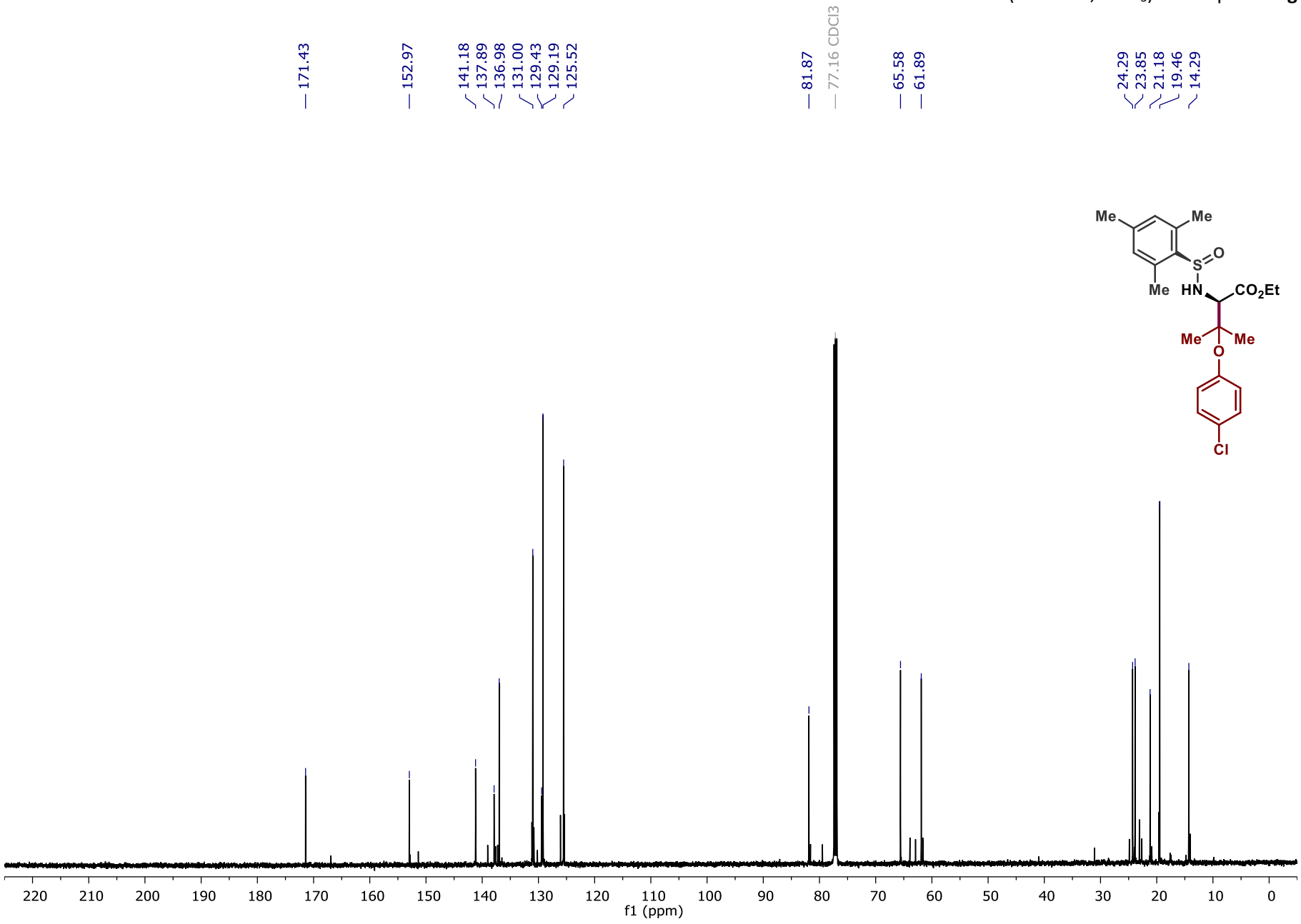

^{1}H NMR (500 MHz, $CDCl_3$) of compound **3h**

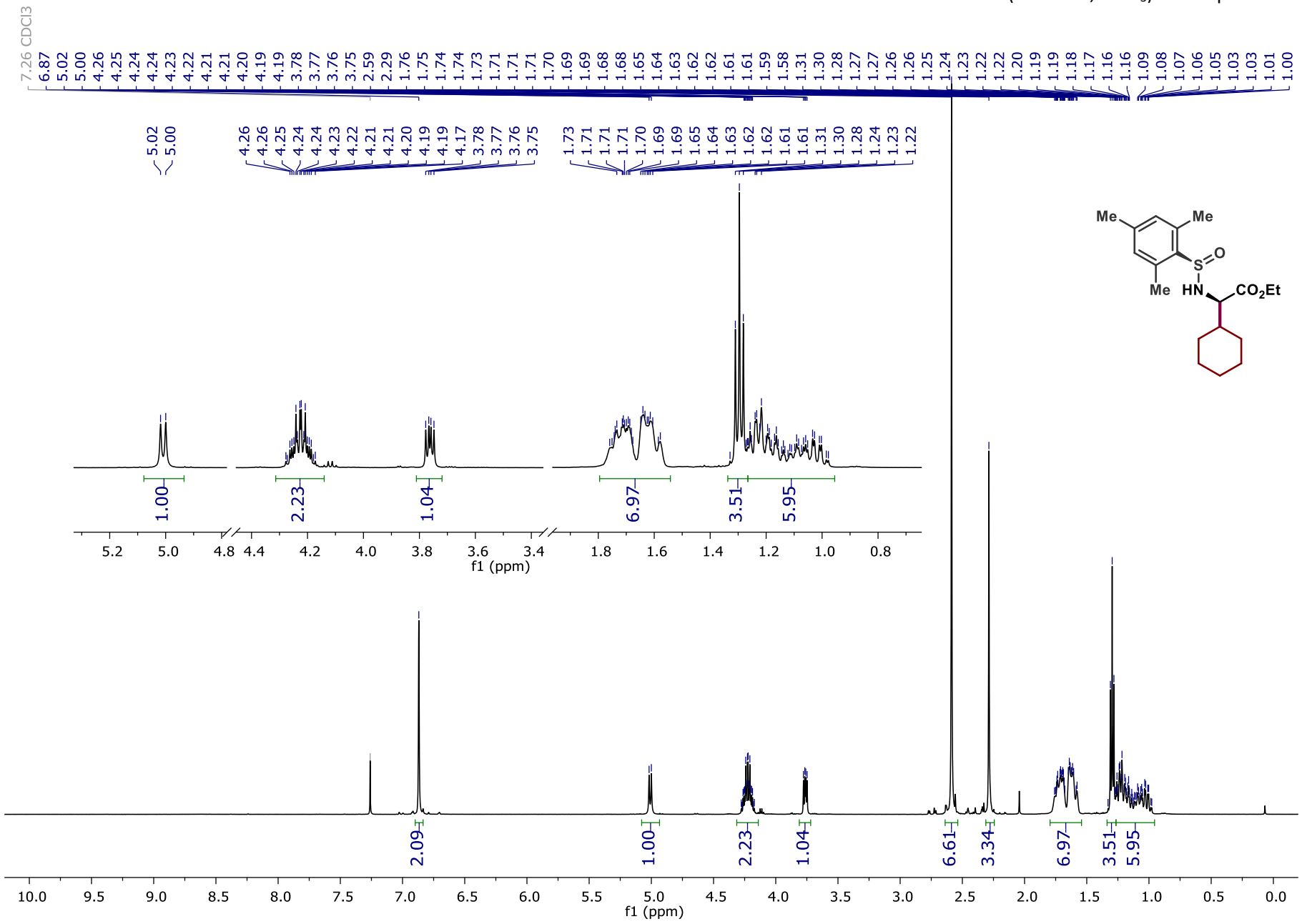

^{13}C NMR (126 MHz, $CDCl_3$) of compound **3h**

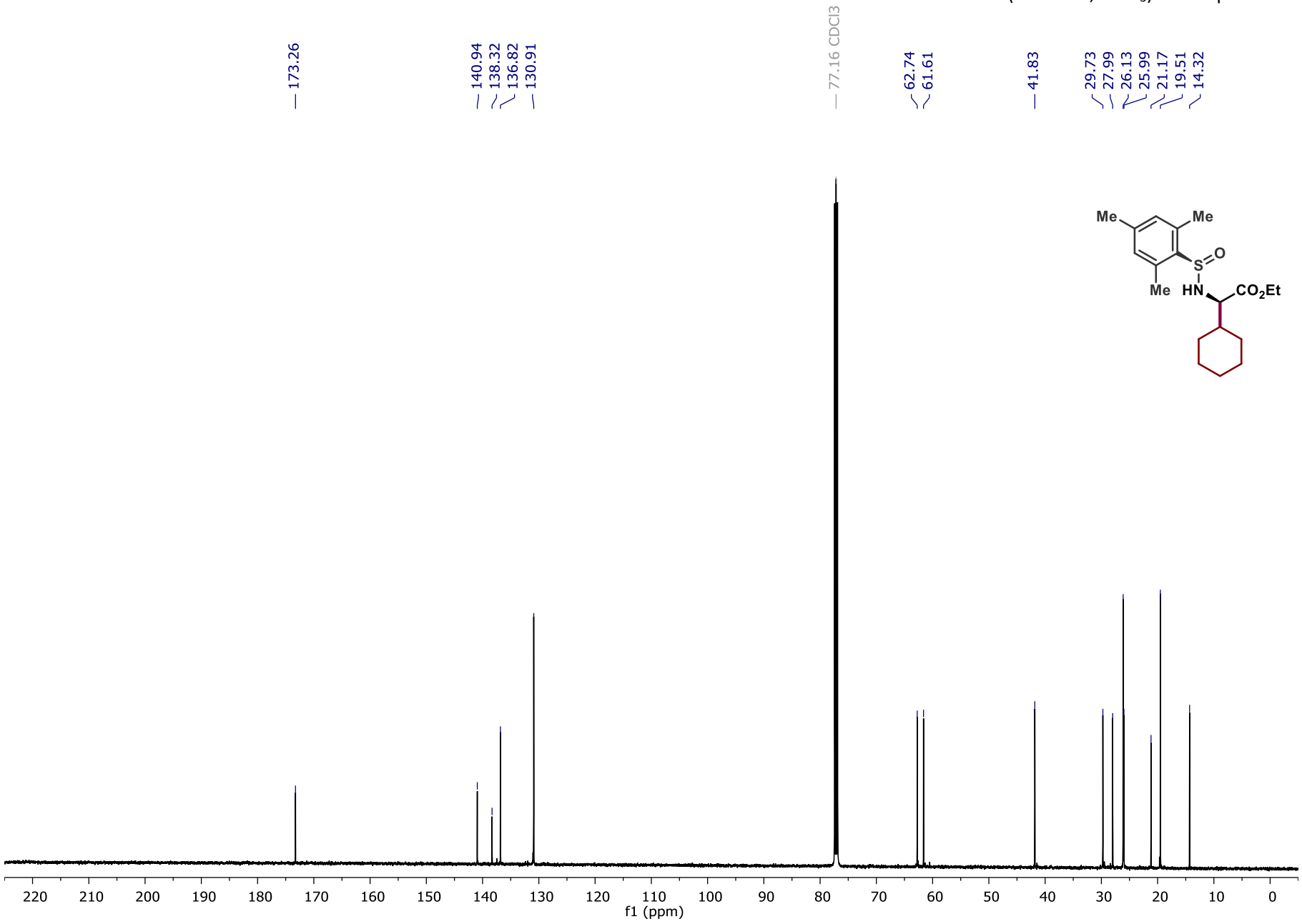

^{1}H NMR (500 MHz, $CDCl_3$) of compound **3i**

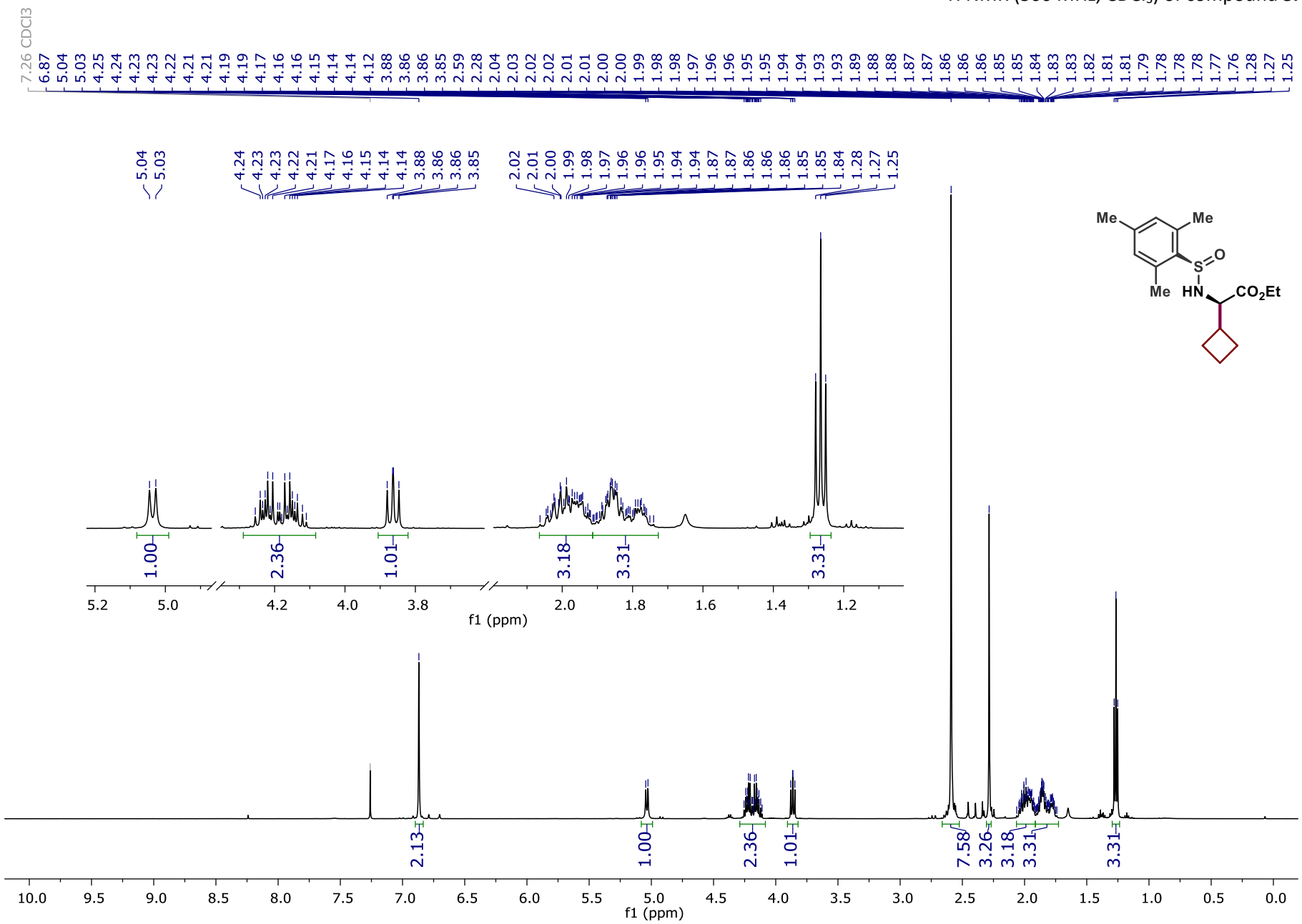

^{13}C NMR (126 MHz, $CDCl_3$) of compound **3i**

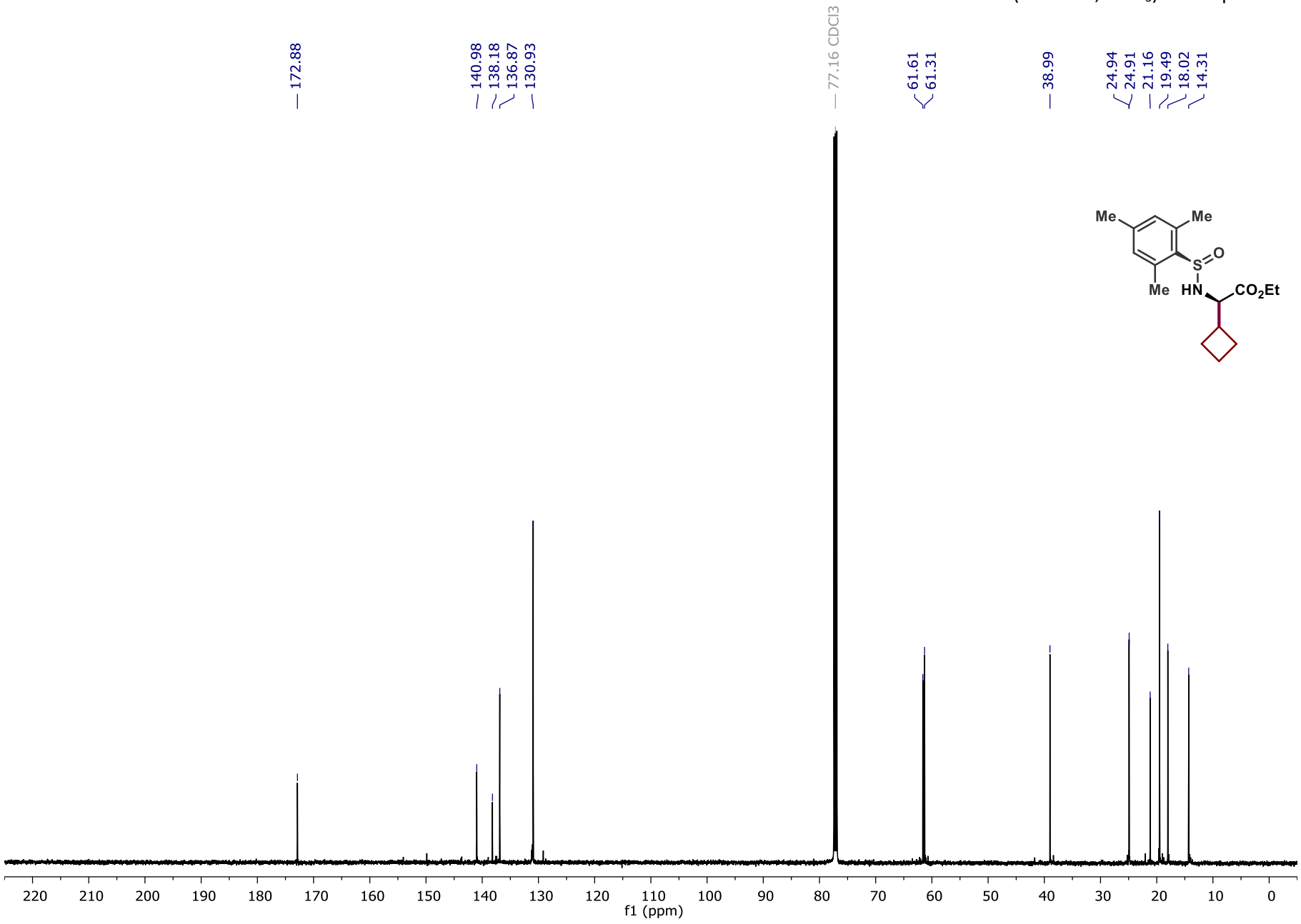

^{1}H NMR (500 MHz, $CDCl_3$) of compound **3j**

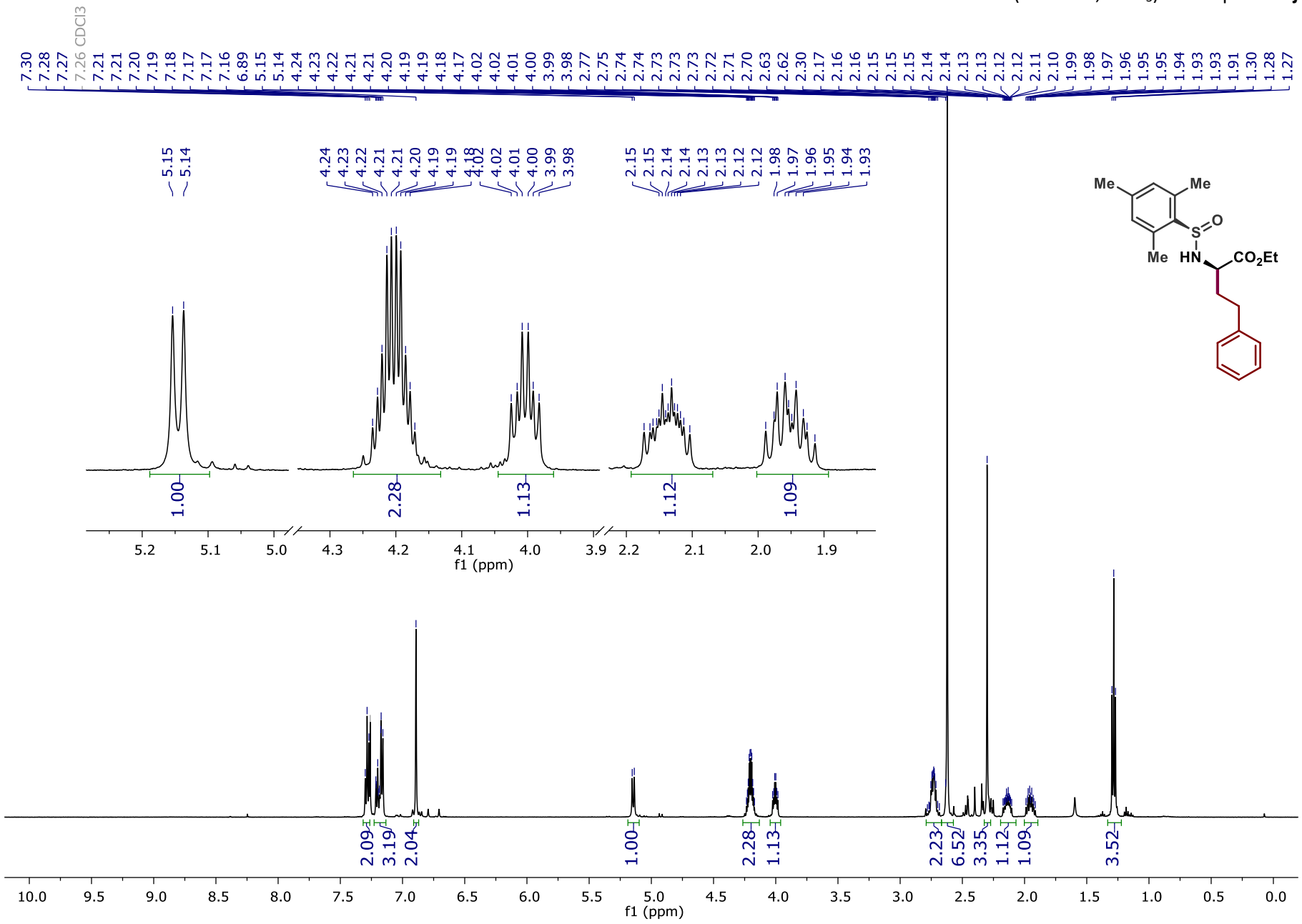

^{13}C NMR (126 MHz, $CDCl_3$) of compound **3j**

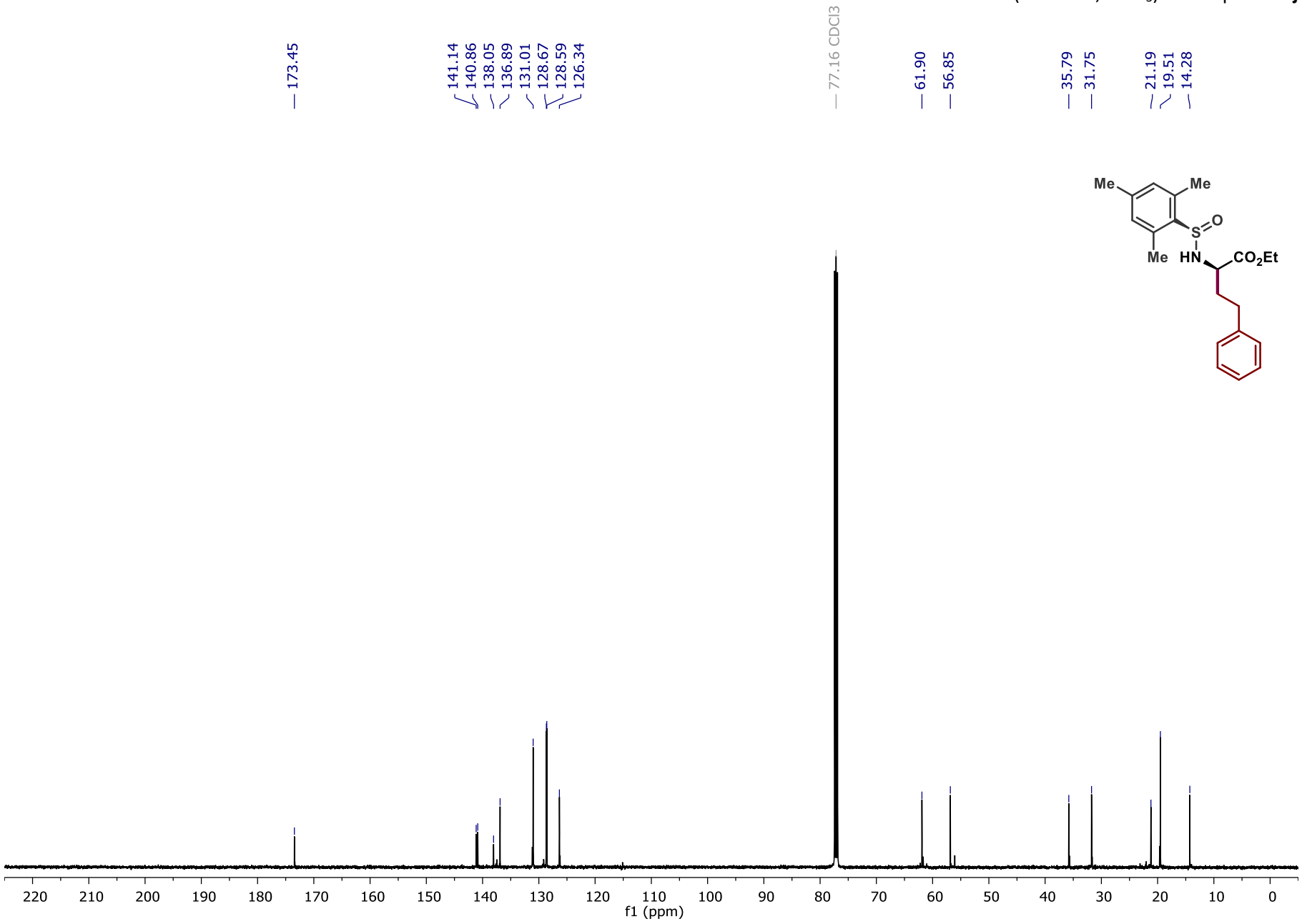

^{1}H NMR (500 MHz, $CDCl_3$) of compound **3k**

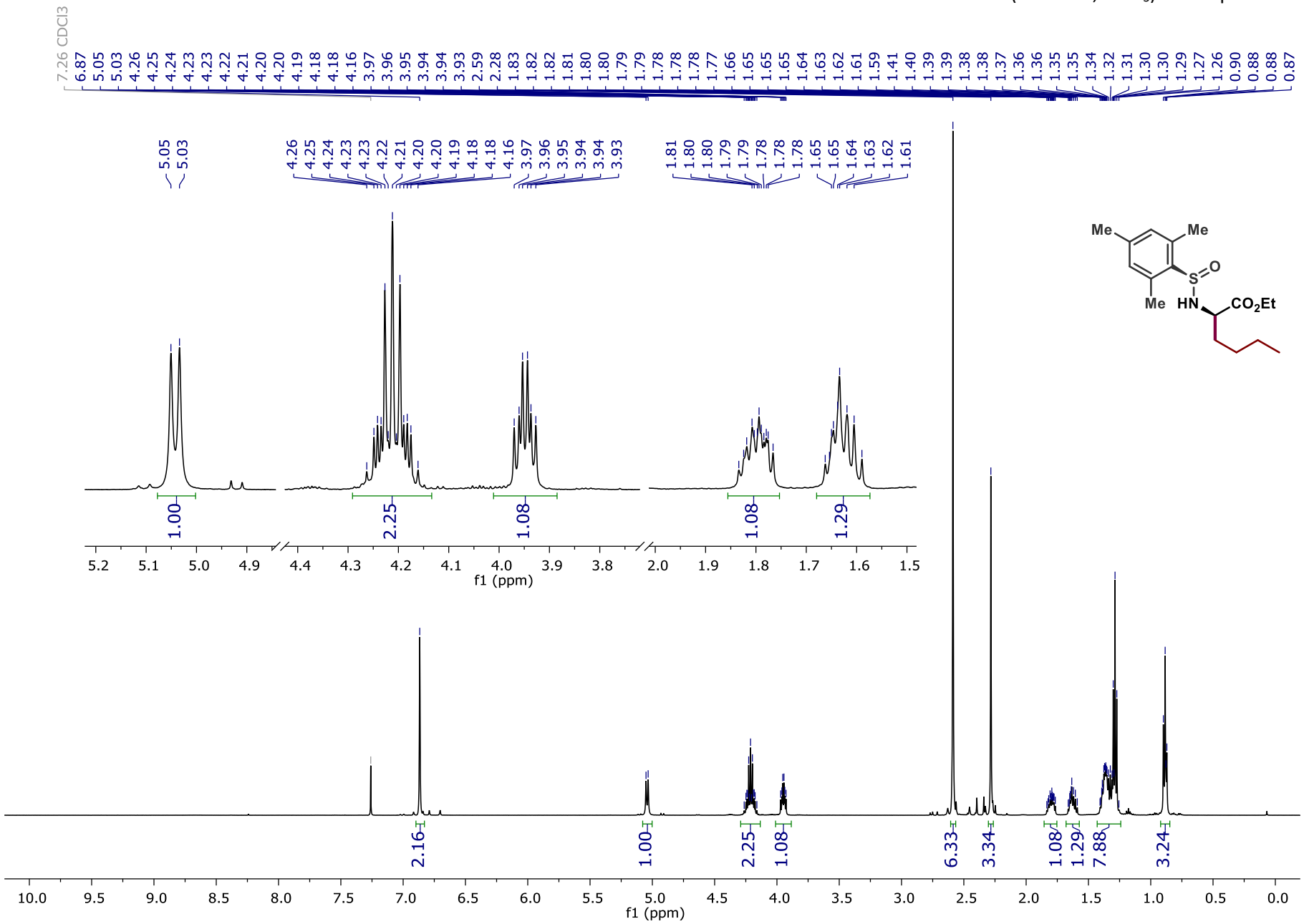

^{13}C NMR (126 MHz, $CDCl_3$) of compound **3k**

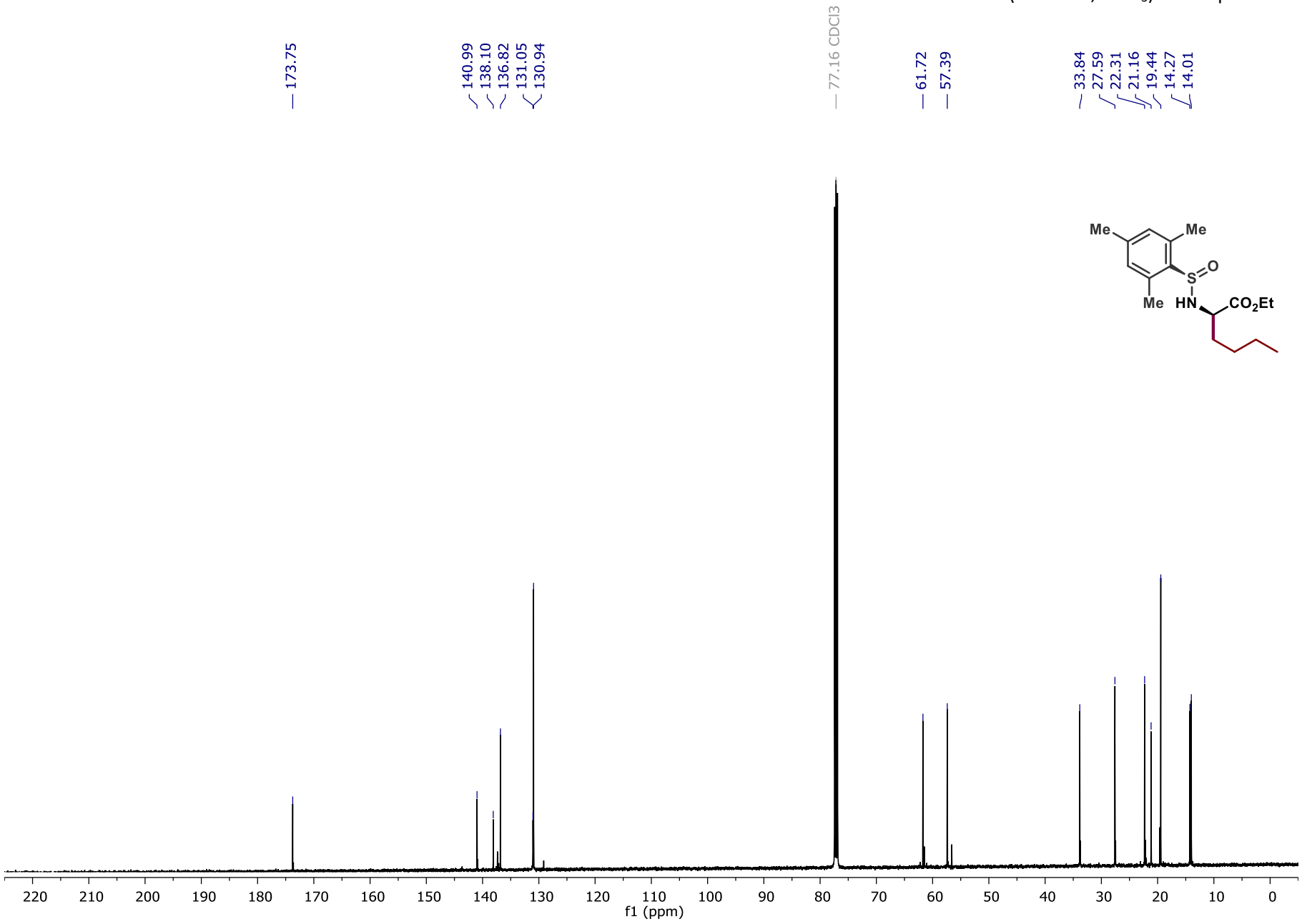

^{1}H NMR (500 MHz, $CDCl_3$) of compound **3l**

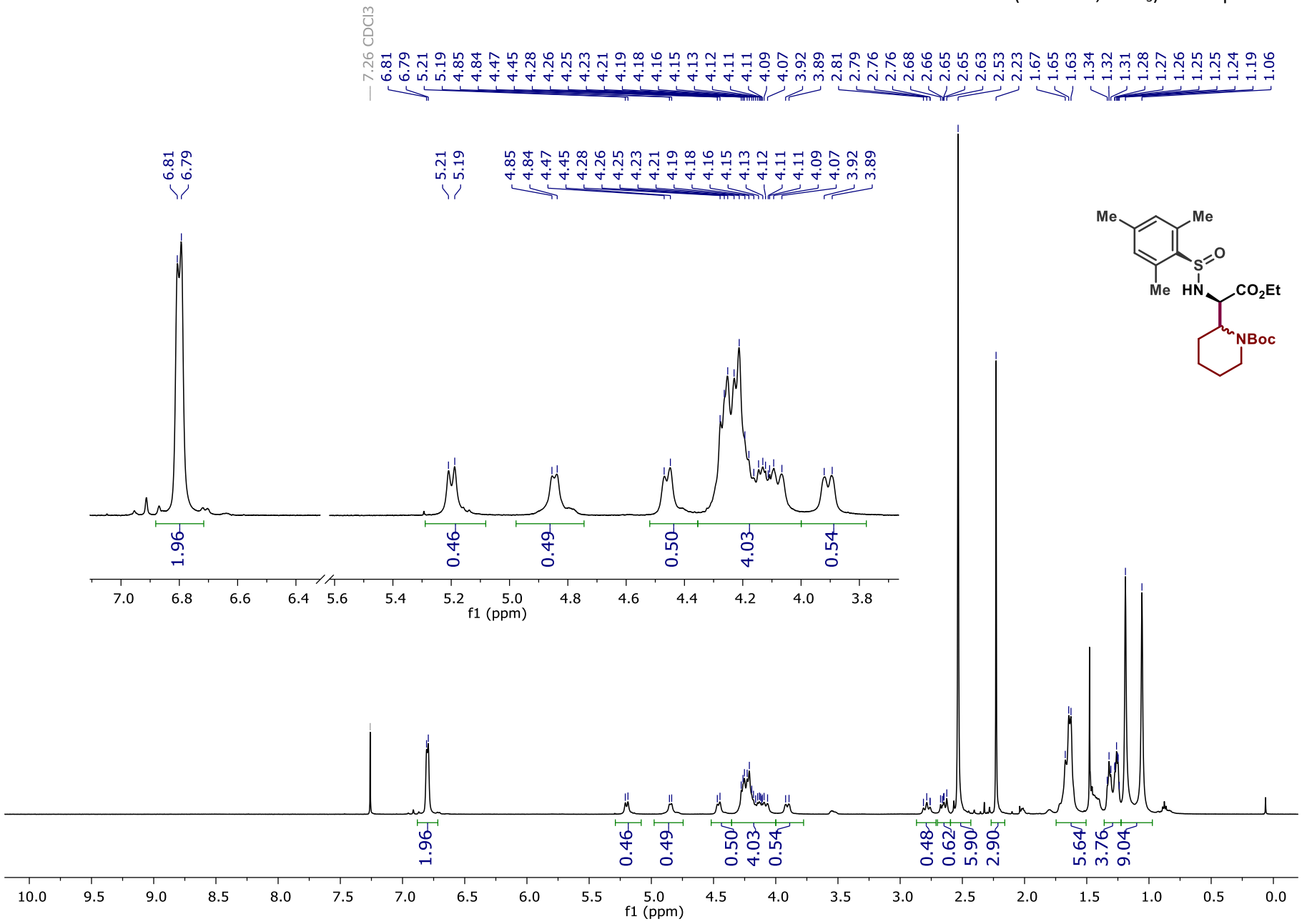

^{13}C NMR (126 MHz, $CDCl_3$) of compound **3l**

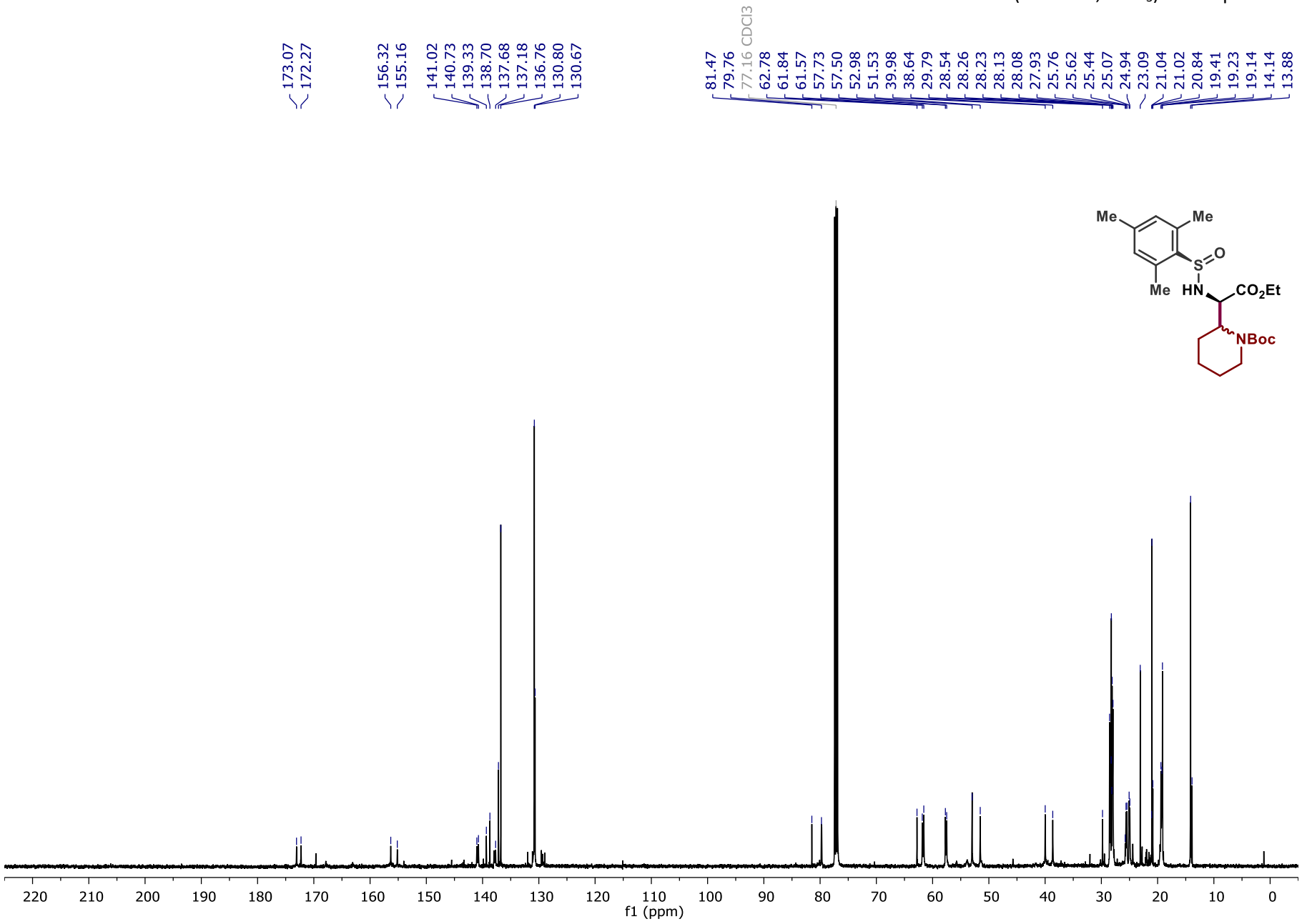

^{1}H NMR (500 MHz, $CDCl_3$) of compound **3m**

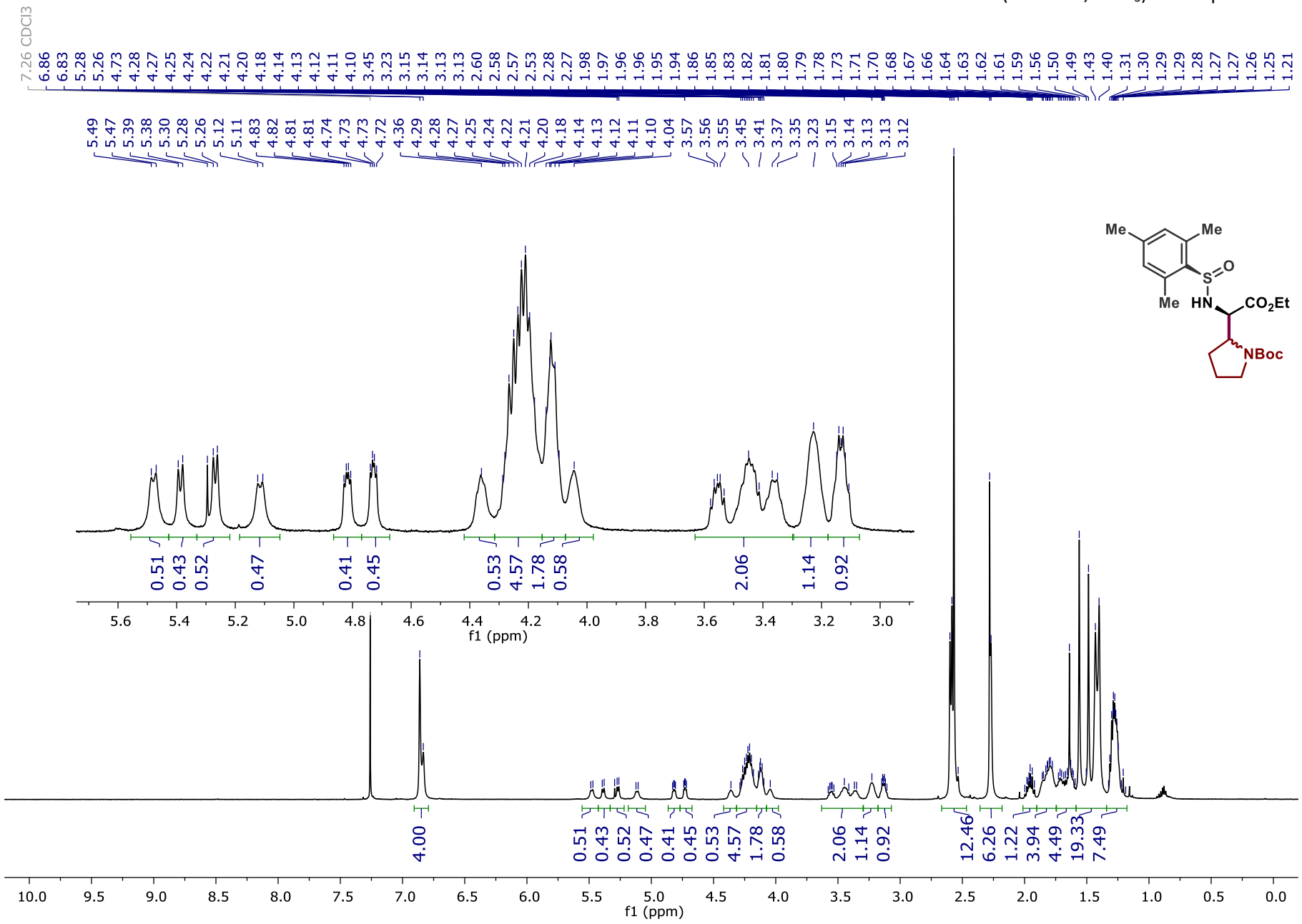

^{13}C NMR (126 MHz, $CDCl_3$) of compound **3m**

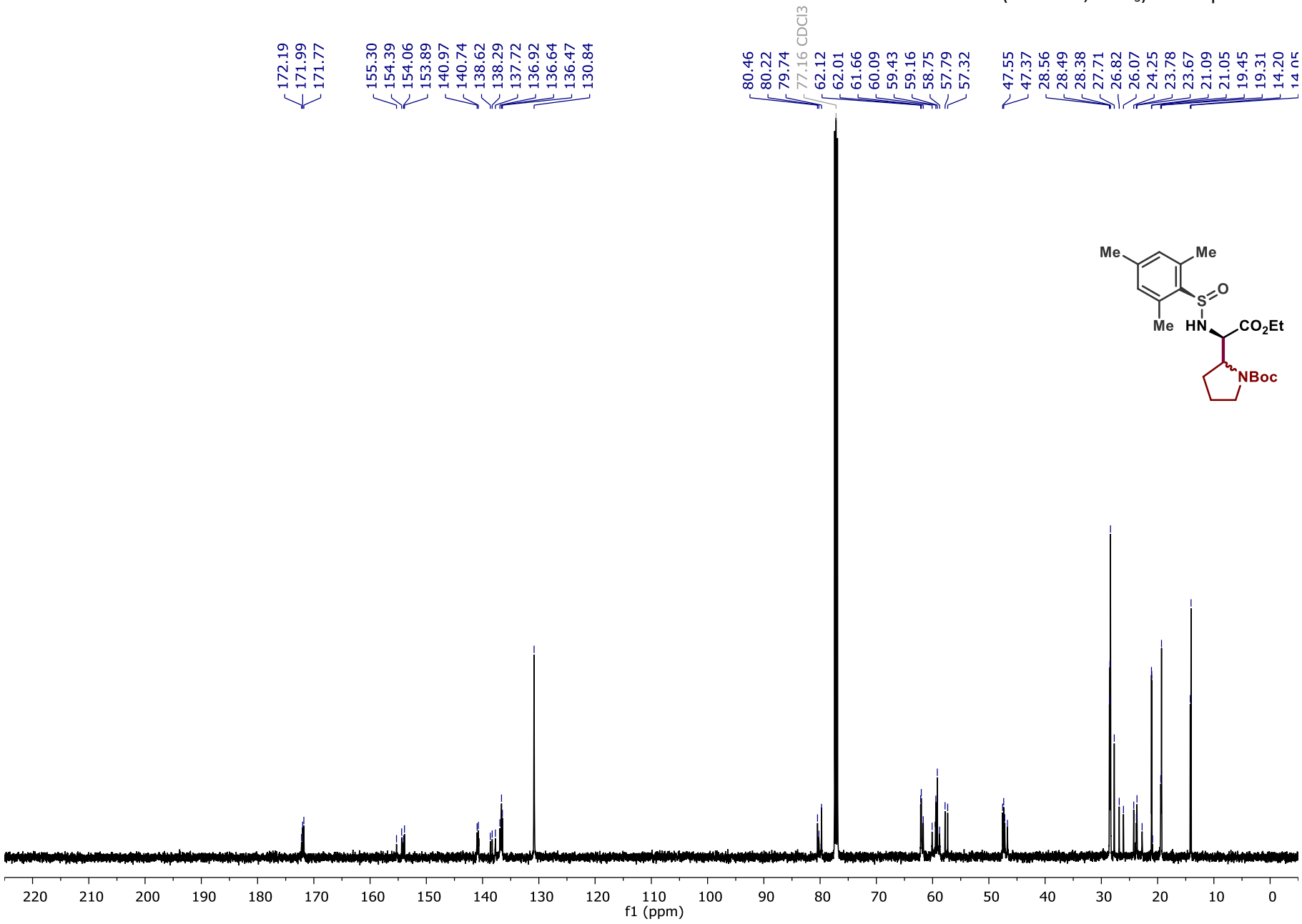

^{1}H NMR (500 MHz, $CDCl_3$) of compound **3n**

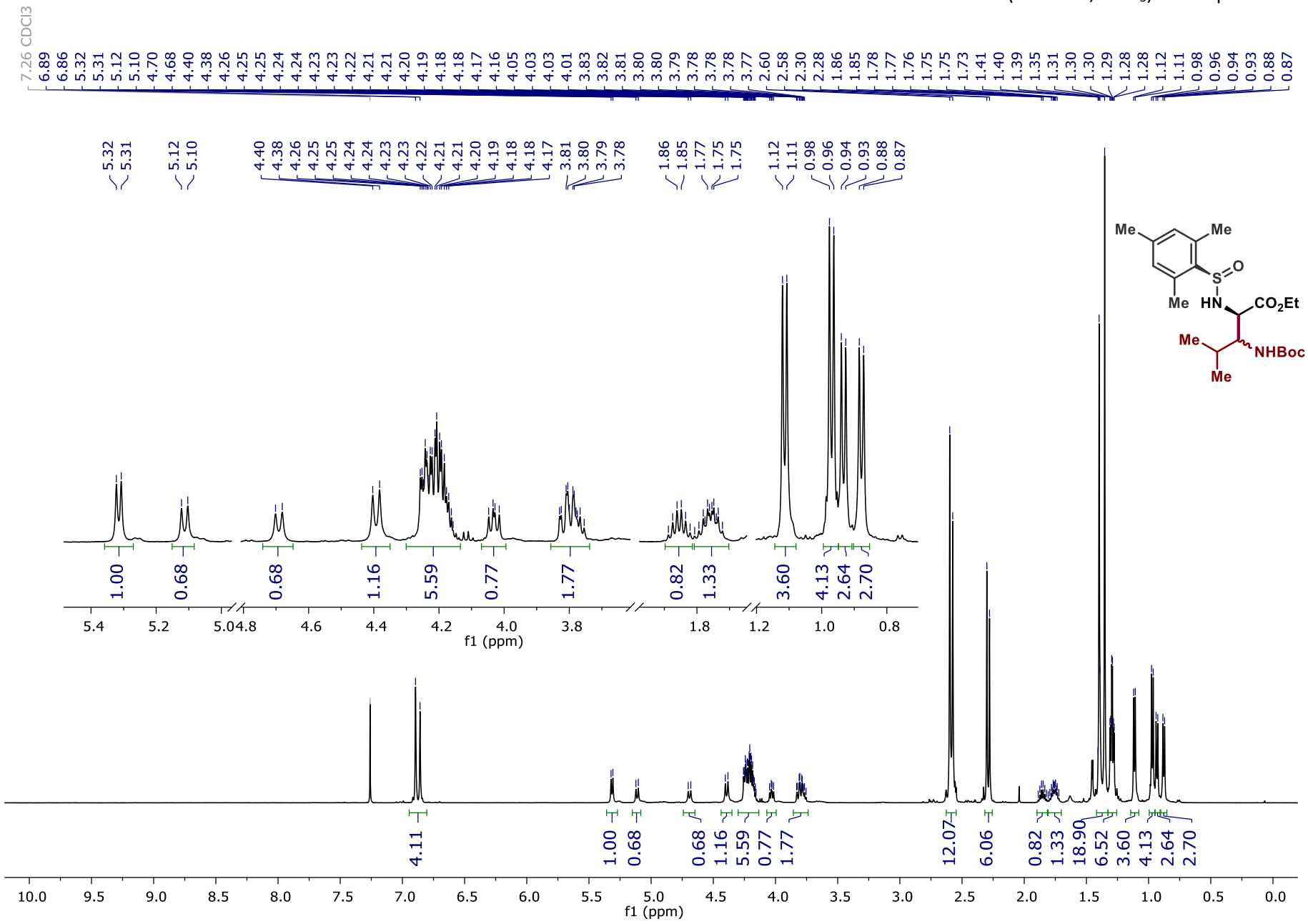

^{13}C NMR (126 MHz, $CDCl_3$) of compound **3n**

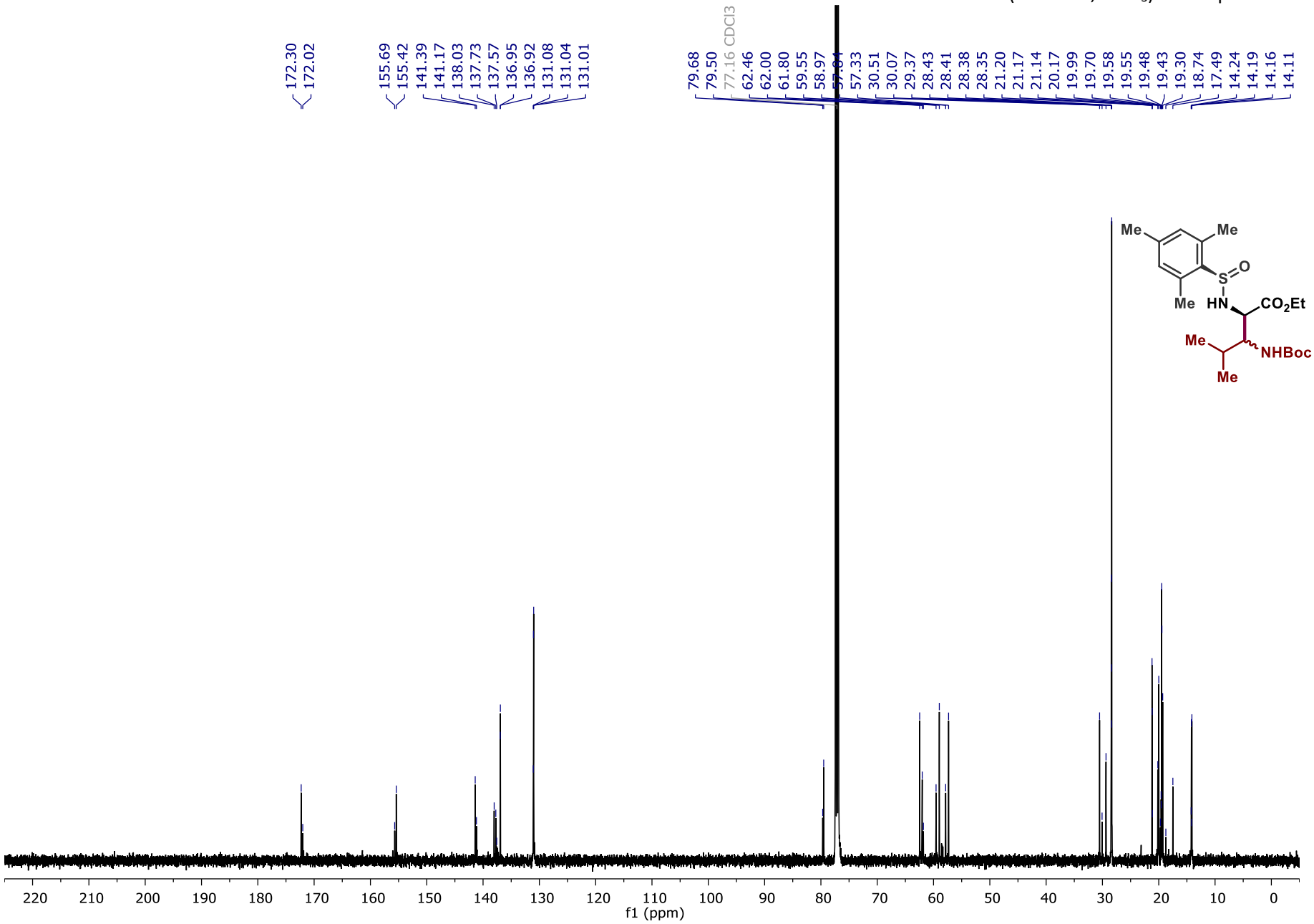

^{1}H NMR (500 MHz, $CDCl_3$) of compound **3o** (diastereomer **3o-1**)

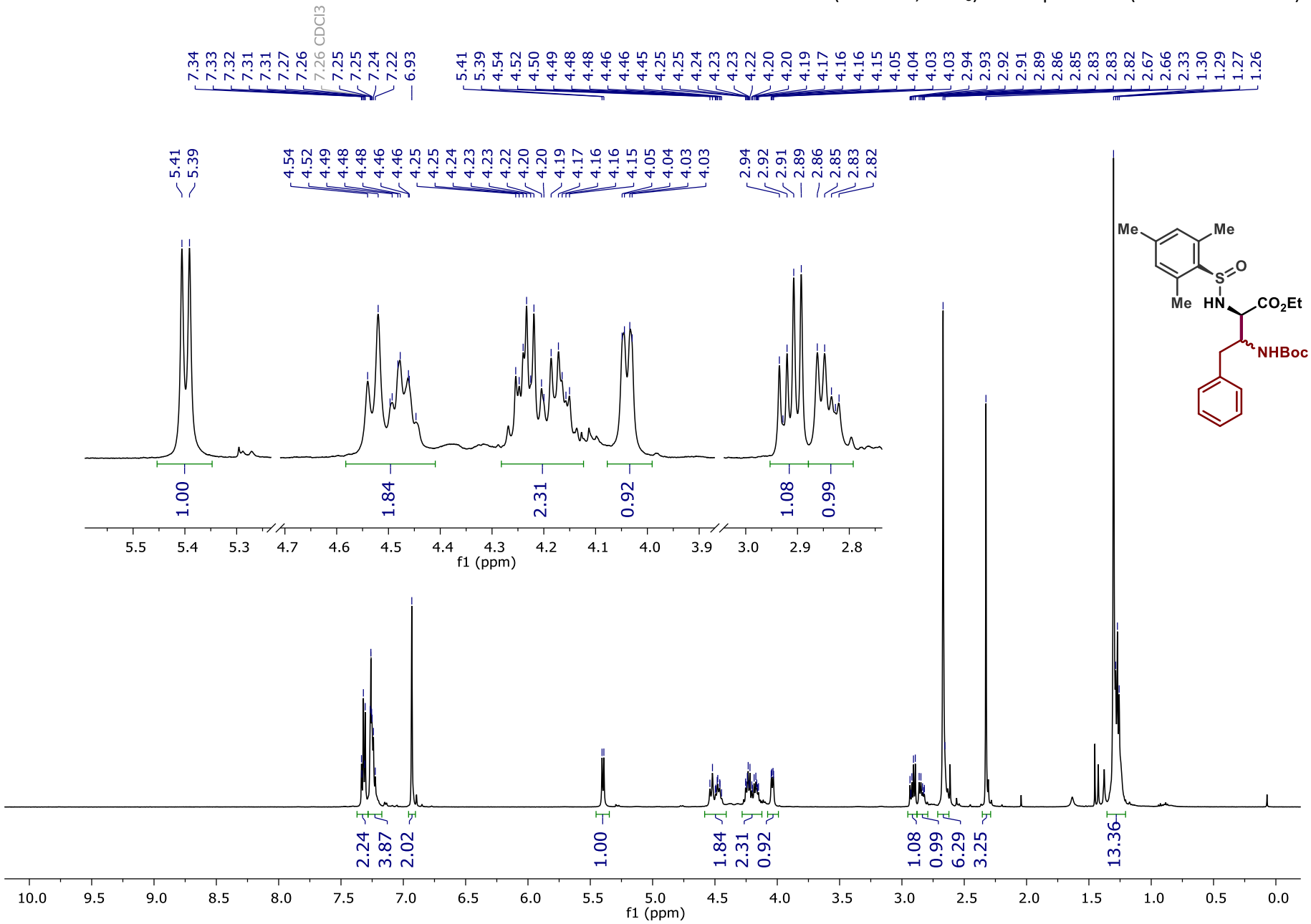

^{13}C NMR (126 MHz, $CDCl_3$) of compound **3o** (diastereomer **3o-1**)

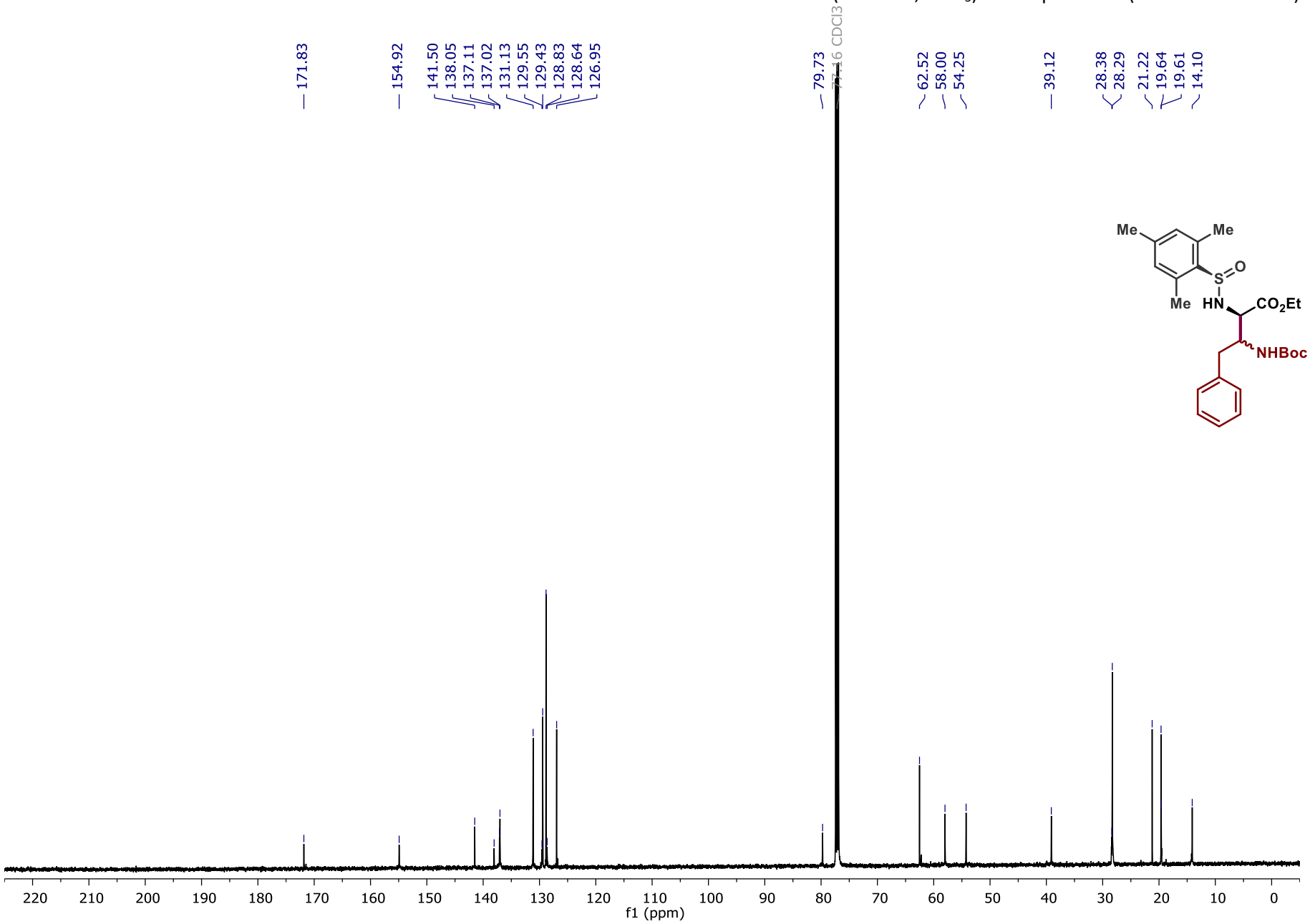

^{1}H NMR (500 MHz, $CDCl_3$) of compound **3o** (diastereomers **3o-1**/**3o-2** 1:1)

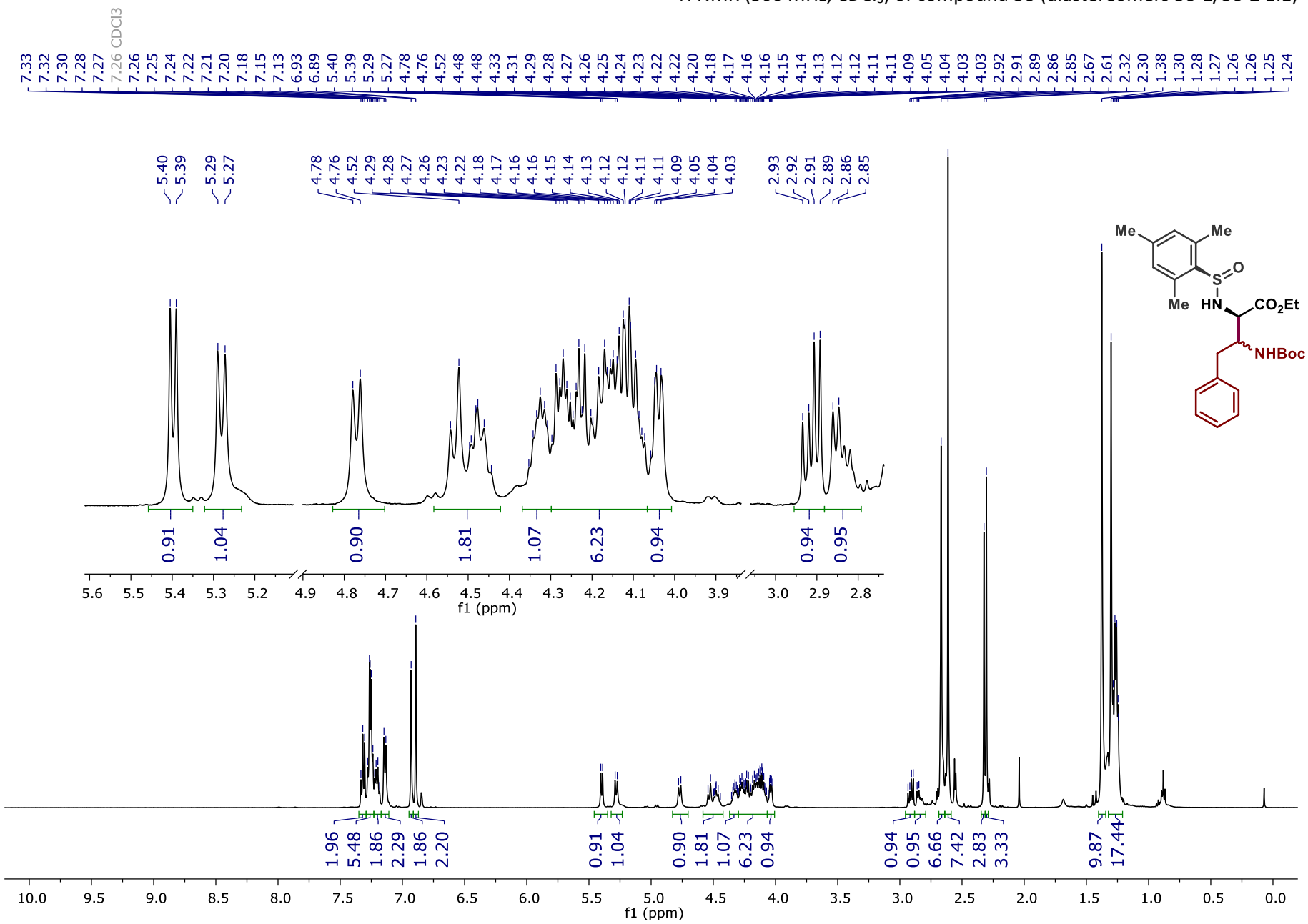

^{13}C NMR (126 MHz, $CDCl_3$) of compound **3o** (diastereomers **3o-1**/**3o-2** 1:1)

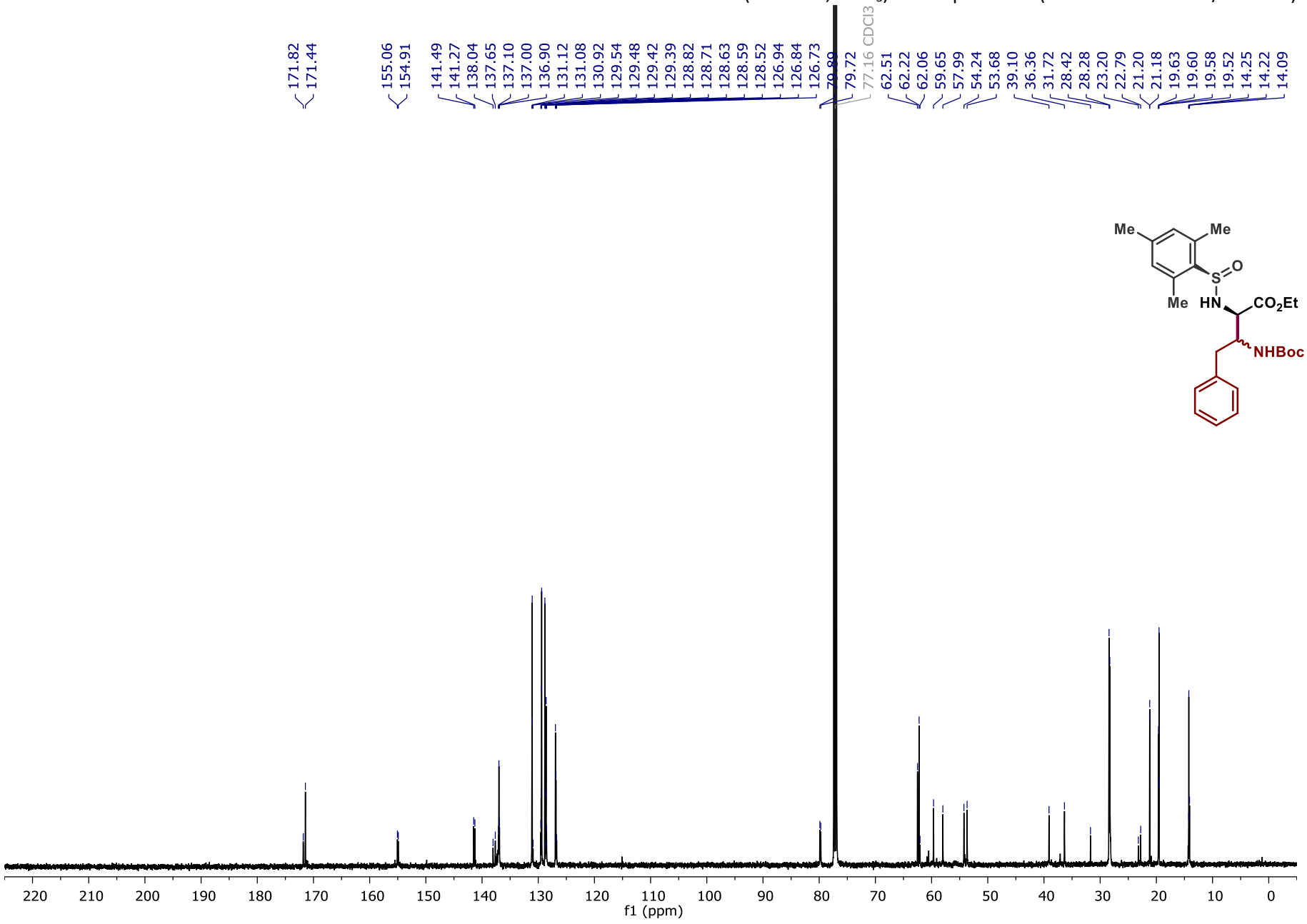

^{1}H NMR (500 MHz, $CDCl_3$) of compound **3p**

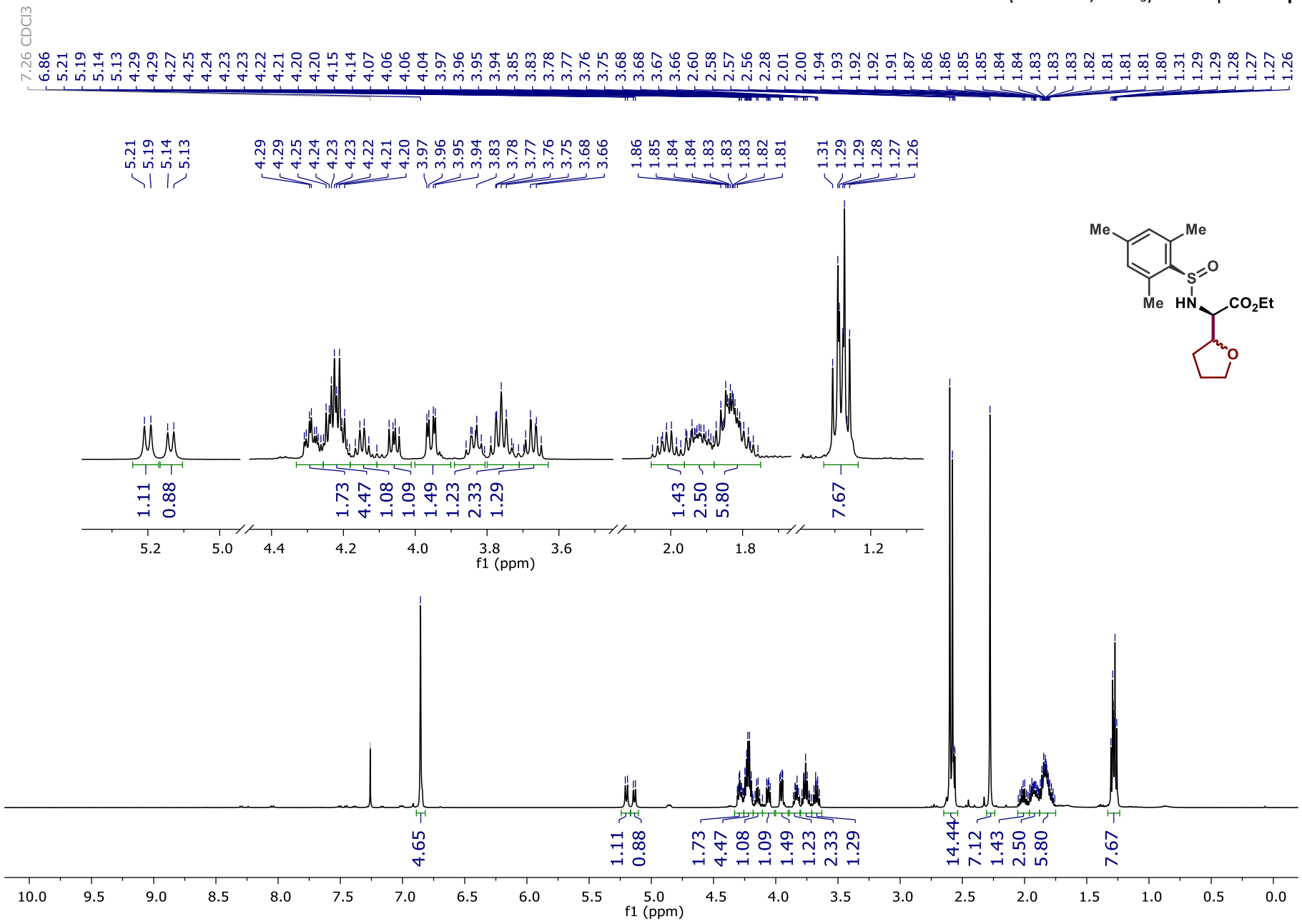

^{13}C NMR (126 MHz, $CDCl_3$) of compound **3p**

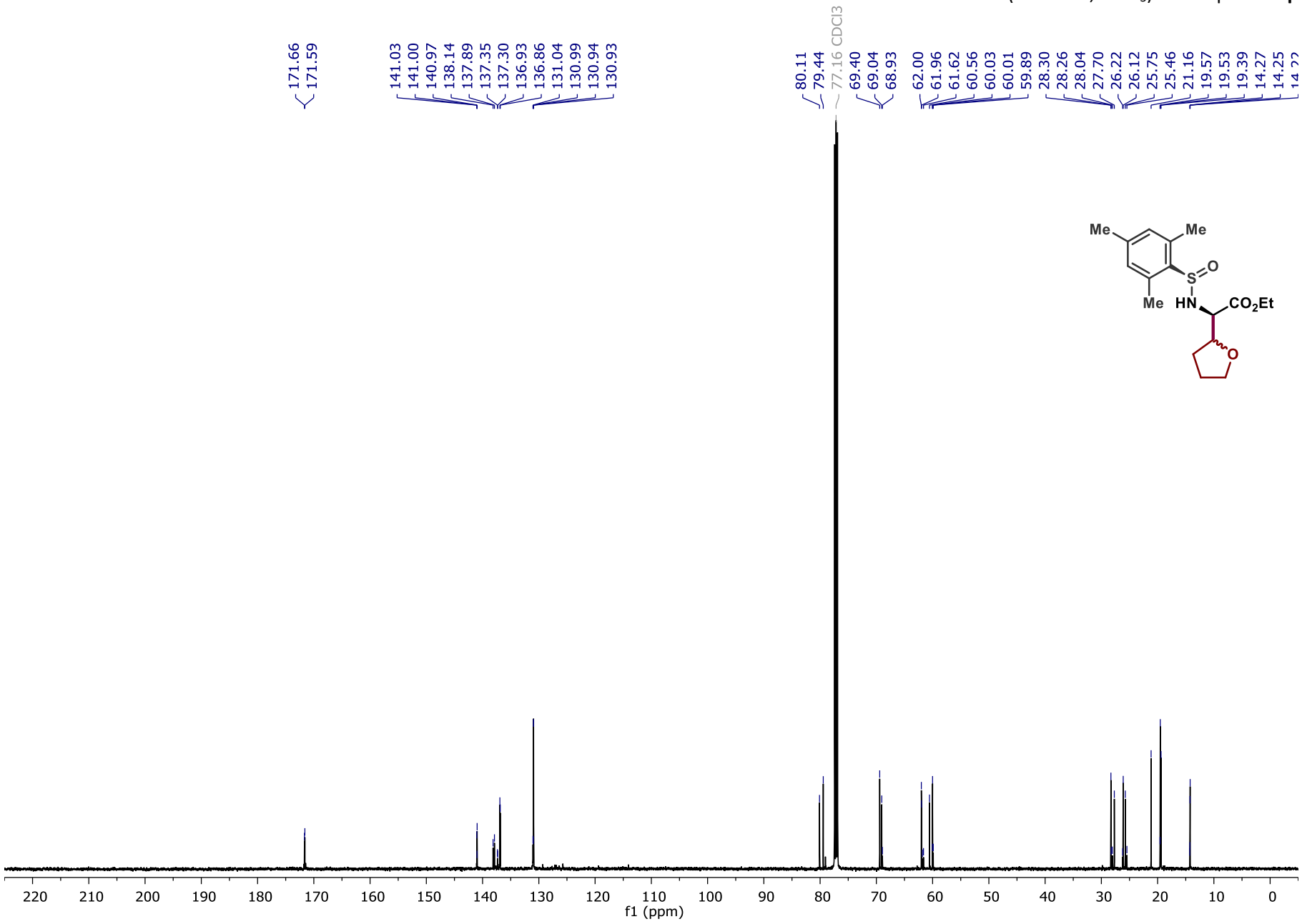

^{1}H NMR (500 MHz, $CDCl_3$) of compound **3q**

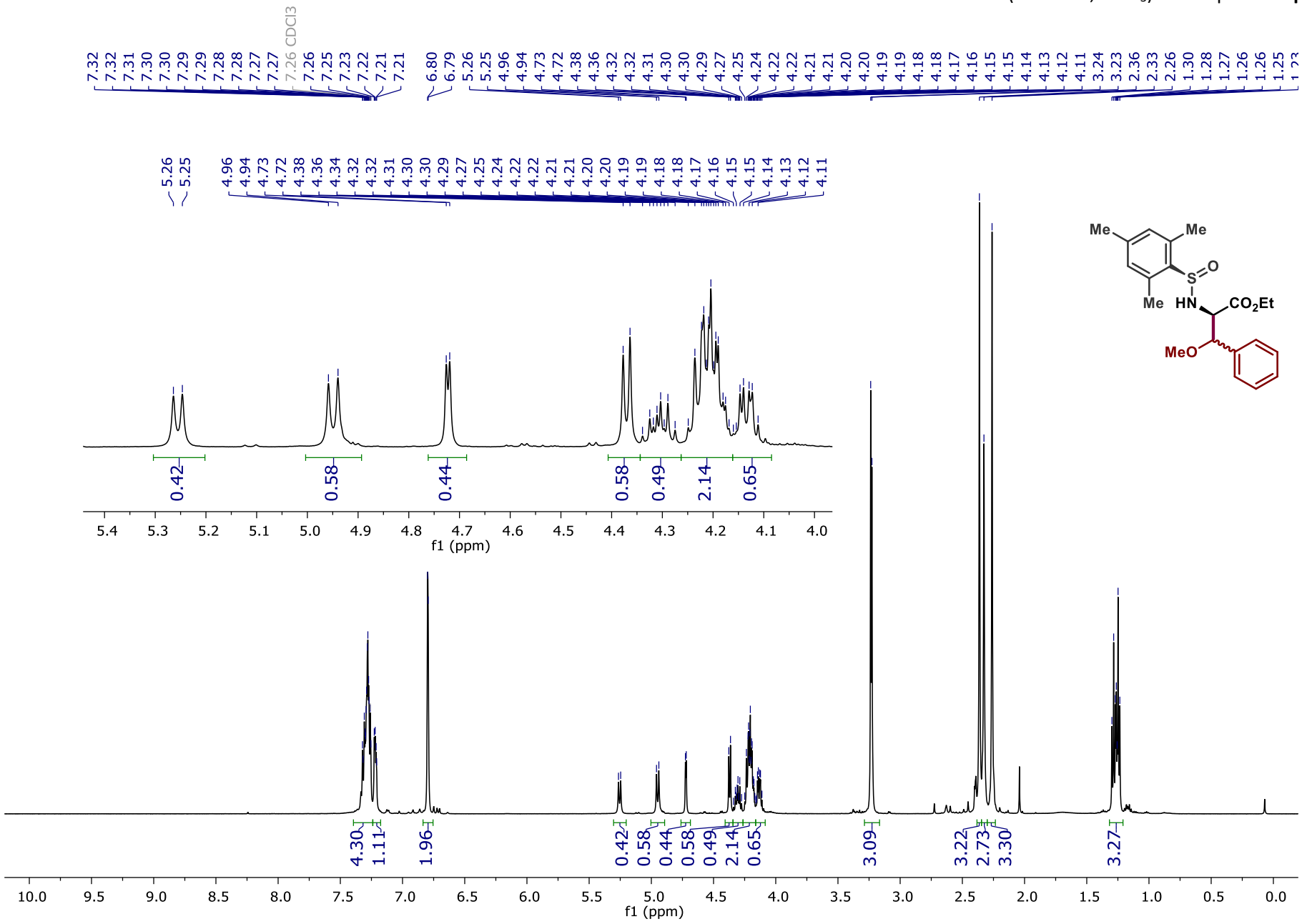

^{13}C NMR (126 MHz, $CDCl_3$) of compound **3q**

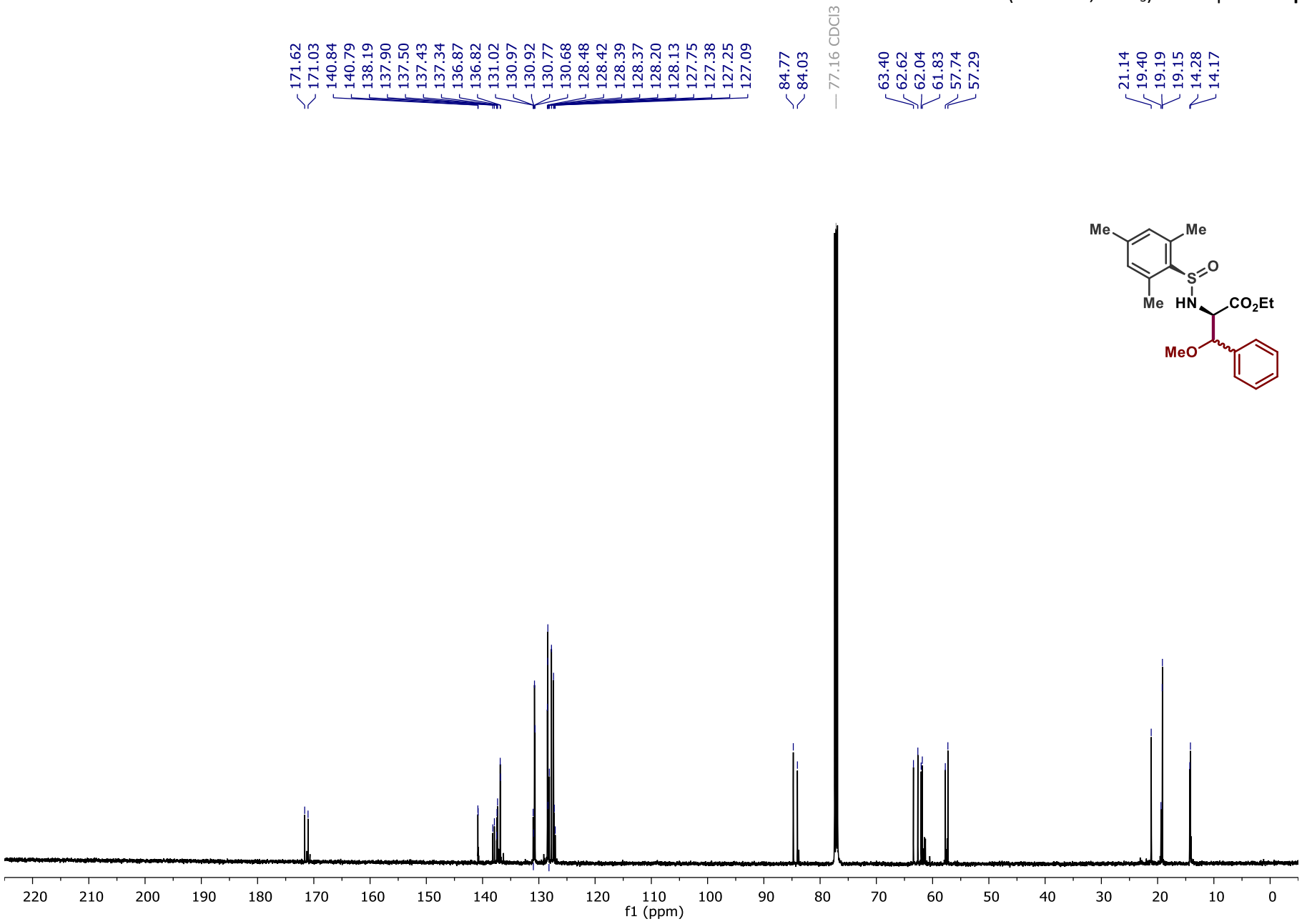

9. *Cartesian coordinates and energies*

The electronic energies (*E*) and the thermal correction to Gibbs free energy (ΔG_{corr}) were calculated at the M062X-D3/6-311+G(d,p)/SMD(chlorobenzene) level of theory. For *re*-TS and *si*-TS the single point electronic energies were also recalculated using the B3LYP-D3 functional (EB3LYP-D3) and the wB97XD (EwB97XD) level of theory including SMD solvation (chlorobenzene). The standard Gibbs free energy ($\Delta G°$) is obtained by the following $\Delta G° = E + \Delta G_{corr} + 0.0003027843$, where 0.003027843 is an entropic term to account for the change in standard state (1 atm → 1 M). All energies are given in Hartree.

Tert-butyl radical

Charge: 0

Multiplicity: 2

$E = -157.749516456$

$\Delta G_{corr} = 0.088724$

$\Delta G° = -157.6577646$

Cartesian coordinates:

C	0.0000000000	0.0000000000	-0.2013590000
C	0.0000000000	1.4774920000	0.0205060000
H	0.0000000000	1.7165170000	1.0971560000
H	0.8874690000	1.9509610000	-0.4087350000
H	-0.8874690000	1.9509610000	-0.4087350000
C	-1.2795450000	-0.7387460000	0.0205060000
H	-2.1333170000	-0.2069090000	-0.4087350000
H	-1.2458470000	-1.7440520000	-0.4087350000
H	-1.4865470000	-0.8582580000	1.0971560000
C	1.2795450000	-0.7387460000	0.0205060000
H	1.2458470000	-1.7440520000	-0.4087350000
H	2.1333170000	-0.2069090000	-0.4087350000
H	1.4865470000	-0.8582580000	1.0971560000

There are no imaginary frequencies

s-cis N-sulfinyl imine

Charge: 0

Multiplicity: 1

E = −1184.08398538

ΔG_{corr} = 0.232274

$\Delta G°$ = −1183.848684

Cartesian coordinates

C	-2.1624280000	0.4487600000	1.2067980000
C	-3.1403390000	1.2882390000	0.6775820000
C	-3.5058870000	1.2296320000	-0.6657980000
C	-2.8525560000	0.3197290000	-1.4950850000
C	-1.8609550000	-0.5413120000	-1.0241760000
C	-1.5445580000	-0.4641320000	0.3398570000
H	-3.6242070000	2.0054480000	1.3332360000
H	-3.1130850000	0.2793320000	-2.5484920000
C	-1.7826680000	0.5675390000	2.6626210000
H	-1.9671630000	-0.3632410000	3.2048550000
H	-0.7243590000	0.8151750000	2.7797170000
H	-2.3682610000	1.3559950000	3.1353330000
H	-1.5151010000	-1.2455580000	-3.0079390000
H	-0.0977380000	-1.3741910000	-1.9586200000
H	-1.4135220000	-2.5163230000	-1.7694390000
C	-1.1843370000	-1.4745950000	-1.9945570000
C	-4.5941670000	2.1163370000	-1.2066300000
H	-4.4314810000	2.3396350000	-2.2622490000
H	-5.5654330000	1.6205480000	-1.1173480000
H	-4.6489580000	3.0554520000	-0.6537810000
S	-0.3304240000	-1.5639840000	1.1082310000
O	-0.2899470000	-2.8681730000	0.3761870000
N	1.0330460000	-0.5817560000	0.6538180000
C	1.9134400000	-1.1667450000	-0.0376430000

H	1.8337190000	-2.2039050000	-0.3749060000
C	3.1589300000	-0.4432200000	-0.4766270000
O	3.9528110000	-0.9673000000	-1.2157720000
H	5.3222680000	0.9588800000	-0.0668240000
H	4.4415610000	1.6141440000	-1.4576050000
O	3.2640330000	0.7748850000	0.0205100000
C	4.4382480000	1.5232970000	-0.3697830000
C	4.3612390000	2.8667060000	0.3118220000
H	5.2351970000	3.4605790000	0.0371670000
H	3.4643670000	3.4069120000	0.0039150000
H	4.3487030000	2.7504350000	1.3968860000

There are no imaginary frequencies

s-trans N-sulfinyl imine

Charge: 0

Multiplicity: 1

E = −1184.07751

ΔG_{corr} = 0.231867

$\Delta G°$ = −1183.842615

Cartesian coordinates:

C	-2.2975130000	0.2486640000	-1.1277980000
C	-3.2860240000	-0.7122190000	-0.9061460000
C	-3.4953520000	-1.2675770000	0.3525860000
C	-2.6846620000	-0.8534980000	1.4122610000
C	-1.6845250000	0.1005550000	1.2512830000
C	-1.5121520000	0.6395760000	-0.0357530000
H	-3.9025450000	-1.0313800000	-1.7404910000
H	-2.8349530000	-1.2888420000	2.3960280000
C	-2.1043890000	0.8129290000	-2.5151800000
H	-2.2782290000	1.8915090000	-2.5377710000
H	-1.0932110000	0.6349910000	-2.8903090000

H	-2.8048860000	0.3442540000	-3.2061990000
H	-0.9746170000	-0.2202520000	3.2401920000
H	0.2125040000	0.5727830000	2.1888280000
H	-1.1474010000	1.4914850000	2.7982310000
C	-0.8482140000	0.5061110000	2.4367180000
C	-4.5696450000	-2.2952730000	0.5815800000
H	-4.1479020000	-3.2050680000	1.0157220000
H	-5.3190470000	-1.9161830000	1.2814250000
H	-5.0720070000	-2.5570000000	-0.3501770000
S	-0.2779050000	1.9145510000	-0.3460810000
O	-0.2760750000	2.8675760000	0.8028920000
N	1.1901250000	0.9778140000	-0.1616170000
C	1.2469590000	-0.1745110000	-0.6727210000
H	0.4184210000	-0.6959940000	-1.1616690000
C	2.5243860000	-0.9758450000	-0.6350610000
O	2.5786710000	-2.0710070000	-1.1347060000
H	4.5878660000	-2.0321770000	0.5676050000
H	5.0951750000	-1.3039640000	-0.9662830000
O	3.5156960000	-0.3638570000	-0.0186210000
C	4.7666990000	-1.0868180000	0.0519270000
C	5.7488440000	-0.2128590000	0.7912020000
H	6.7076940000	-0.7299430000	0.8628980000
H	5.9019020000	0.7302170000	0.2638560000
H	5.3940410000	0.0009370000	1.8008090000

There are no imaginary frequencies

s-cis N-sulfinyl imidoyl flouride

Charge: 0

Multiplicity: 1

E = −1283.321846

ΔG_{corr} = 0.221763

$\Delta G°$ = −1283.097055

Cartesian coordinates:

C	-2.2426380000	0.4898420000	1.2051090000
C	-3.2410640000	1.2967790000	0.6618580000
C	-3.6095850000	1.2020790000	-0.6785580000
C	-2.9413600000	0.2878940000	-1.4922640000
C	-1.9333680000	-0.5435740000	-1.0055830000
C	-1.6132650000	-0.4277900000	0.3542420000
H	-3.7374750000	2.0178230000	1.3038270000
H	-3.2043010000	0.2212570000	-2.5438040000
C	-1.8577790000	0.6458770000	2.6558690000
H	-2.0300360000	-0.2742880000	3.2199110000
H	-0.8017510000	0.9071800000	2.7623990000
H	-2.4501450000	1.4379480000	3.1136700000
H	-1.5089410000	-1.2425840000	-2.9771630000
H	-0.1576260000	-1.4478630000	-1.8545110000
H	-1.5339430000	-2.5259510000	-1.7487630000
C	-1.2440730000	-1.4938240000	-1.9497710000
C	-4.7165900000	2.0549350000	-1.2358180000
H	-4.5365400000	2.2963930000	-2.2847280000
H	-5.6704790000	1.5222570000	-1.1772030000
H	-4.8195110000	2.9847270000	-0.6744470000
S	-0.3805400000	-1.5055690000	1.1230570000
O	-0.4600090000	-2.8501540000	0.4876570000
N	0.9542270000	-0.5527240000	0.5747190000
C	1.9645650000	-1.0006760000	-0.0050260000
C	3.1627160000	-0.1436830000	-0.3795620000
O	4.1059400000	-0.6016150000	-0.9614910000
H	5.0020230000	1.6234840000	0.1707900000
H	4.2413270000	2.0011960000	-1.3864020000
O	3.0071290000	1.1020630000	0.0089830000
C	4.0968150000	2.0054670000	-0.3046140000
C	3.7106470000	3.3674920000	0.2140060000
H	4.5127010000	4.0746560000	-0.0057750000

H	2.7963050000	3.7200200000	-0.2660120000
H	3.5572640000	3.3424950000	1.2941190000
F	2.1461760000	-2.2608690000	-0.3842660000

There are no imaginary frequencies

s-trans N-sulfinyl imidoyl flouride

Charge: 0

Multiplicity: 1

E = −1283.324329

ΔG_{corr} = 0.223275

$\Delta G°$= −1283.098026

Cartesian coordinates:

C	-2.4220750000	0.8177370000	-0.5396040000
C	-3.3395300000	-0.0973460000	-1.0601150000
C	-3.4151280000	-1.4048340000	-0.5911640000
C	-2.5522350000	-1.8012560000	0.4335140000
C	-1.6172790000	-0.9355020000	0.9920220000
C	-1.5616090000	0.3694290000	0.4707480000
H	-4.0102450000	0.2278040000	-1.8489680000
H	-2.6109620000	-2.8175330000	0.8124440000
C	-2.4047500000	2.2317800000	-1.0676150000
H	-2.6174250000	2.9547270000	-0.2760250000
H	-1.4399020000	2.4933700000	-1.5060720000
H	-3.1673000000	2.3456180000	-1.8379380000
H	-0.8219090000	-2.5034410000	2.2046560000
H	0.3034320000	-1.1528880000	1.9753180000
H	-1.0579820000	-0.9688070000	3.0641860000
C	-0.7438920000	-1.4192640000	2.1207090000
C	-4.4098910000	-2.3797250000	-1.1591140000
H	-3.9048350000	-3.2765700000	-1.5261960000
H	-5.1193210000	-2.6959670000	-0.3898660000

H	-4.9709860000	-1.9373640000	-1.9827580000
S	-0.4108980000	1.5872510000	1.1372760000
O	-0.4258390000	1.5048040000	2.6226100000
N	1.0619980000	0.7502600000	0.6674210000
C	1.3984840000	0.7508830000	-0.5329990000
C	2.6774140000	0.1401740000	-1.0748850000
O	2.9466230000	0.1768860000	-2.2425940000
H	4.4080330000	-1.8020510000	-1.2488090000
H	5.2513000000	-0.2594880000	-1.0102530000
O	3.3913640000	-0.4020870000	-0.1156250000
C	4.6389470000	-1.0202890000	-0.5230870000
C	5.2916970000	-1.5692750000	0.7200170000
H	6.2362020000	-2.0441450000	0.4478090000
H	5.4981630000	-0.7709840000	1.4346860000
H	4.6534850000	-2.3153330000	1.1962820000
F	0.6636140000	1.2825900000	-1.5136160000

There are no imaginary frequencies

re-TS

Charge: 0

Multiplicity: 2

E = −1341.84503847

EB3LYP-D3: −1342.351768

EwB97XD: −1341.967714

ΔG_{corr} = 0.345723

ΔG° = −1341.496288

Cartesian coordinates:

C	-3.0526770000	-0.7656440000	0.9979450000
C	-4.2429540000	-0.0362660000	0.9545970000
C	-4.4986750000	0.8874680000	-0.0536800000

C	-3.5283870000	1.0871730000	-1.0372640000
C	-2.3208570000	0.3946730000	-1.0391360000
C	-2.1057440000	-0.5346360000	-0.0075360000
H	-4.9865890000	-0.2030280000	1.7275690000
H	-3.7163750000	1.8067900000	-1.8292220000
C	-2.8362690000	-1.7585090000	2.1153970000
H	-2.6962880000	-2.7722580000	1.7326450000
H	-1.9563630000	-1.5066030000	2.7115980000
H	-3.7030230000	-1.7650710000	2.7765090000
H	-1.7941460000	1.1802640000	-2.9574580000
H	-0.5439520000	1.3838210000	-1.7277320000
H	-0.8027970000	-0.2037860000	-2.4608830000
C	-1.3051470000	0.6972610000	-2.1107310000
C	-5.7919500000	1.6555050000	-0.0993650000
H	-5.6028530000	2.7316630000	-0.1170480000
H	-6.3543230000	1.4073060000	-1.0034220000
H	-6.4171140000	1.4294220000	0.7651650000
S	-0.6163530000	-1.5610560000	0.0611310000
O	-0.4154320000	-2.2116260000	-1.2834130000
N	0.4870910000	-0.2724880000	0.2811660000
C	1.4668080000	-0.2257530000	-0.5754920000
H	1.4658300000	-0.8229700000	-1.4891210000
C	2.3015120000	1.0154180000	-0.6458480000
O	2.9949820000	1.2719880000	-1.6018410000
H	4.0342890000	2.7079490000	0.2986520000
H	2.6900010000	3.6124130000	-0.4143980000
O	2.1846730000	1.7908880000	0.4232020000
C	2.9868250000	2.9886130000	0.4311700000
C	2.7508670000	3.6764830000	1.7536540000
H	3.3403190000	4.5945040000	1.7962920000
H	1.6972180000	3.9348540000	1.8729960000
H	3.0508950000	3.0328690000	2.5828720000
C	3.1946490000	-1.5027530000	0.1660110000

C	2.4001080000	-2.6271690000	0.7480830000
H	1.7885530000	-2.2949150000	1.5905080000
H	1.7673600000	-3.1097590000	-0.0009600000
H	3.0965830000	-3.3871560000	1.1295930000
C	3.9028310000	-0.6326880000	1.1574370000
H	4.4359200000	0.1928990000	0.6792410000
H	3.2159060000	-0.2363640000	1.9092300000
H	4.6512770000	-1.2430680000	1.6829880000
C	3.9054270000	-1.7832990000	-1.1193810000
H	3.2775420000	-2.3449270000	-1.8148970000
H	4.2509380000	-0.8677440000	-1.6035130000
H	4.7912030000	-2.3980510000	-0.9022160000

1 imaginary frequency: −280.15 cm^{-1}

si-TS

Charge: 0

Multiplicity: 2

E = −1341.83971014

EB3LYP-D3: −1342.346615

EwB97XD: −1341.963109

ΔG_{corr} = 0.346454

$\Delta G°$ = −1341.490228

Cartesian coordinates:

C	2.2592250000	1.2987110000	-0.7795730000
C	3.2973770000	1.8187320000	-0.0124400000
C	4.0587860000	1.0147330000	0.8341920000
C	3.7657560000	-0.3430560000	0.8910750000
C	2.7337290000	-0.9269700000	0.1472110000
C	1.9773250000	-0.0762380000	-0.6723240000
H	3.5200810000	2.8792570000	-0.0860950000

H	4.3602470000	-0.9842270000	1.5346900000
C	1.4852700000	2.2261730000	-1.6840060000
H	1.4097880000	1.8318540000	-2.7008110000
H	0.4676920000	2.3724510000	-1.3170250000
H	1.9832770000	3.1946130000	-1.7327460000
H	3.2726980000	-2.8115070000	0.9836250000
H	1.5339420000	-2.6386790000	0.7121860000
H	2.5896190000	-2.9370540000	-0.6505110000
C	2.5193910000	-2.4140340000	0.3025280000
C	5.1645250000	1.6103350000	1.6631620000
H	5.8051310000	2.2529850000	1.0550910000
H	4.7514400000	2.2258430000	2.4672990000
H	5.7821010000	0.8330520000	2.1148810000
S	0.6534450000	-0.6723080000	-1.7719670000
O	0.5579600000	-2.1695120000	-1.7012620000
N	-0.6377580000	0.0763370000	-0.9521590000
C	-1.7374320000	-0.6243640000	-0.8176570000
H	-1.8661930000	-1.6070460000	-1.2727160000
C	-3.0146480000	0.1336630000	-0.6255800000
O	-4.0795870000	-0.2883460000	-1.0057760000
H	-4.4695940000	2.3456730000	-0.7342570000
H	-4.7599230000	1.4513010000	0.7653330000
O	-2.8454890000	1.2950590000	-0.0040000000
C	-4.0373450000	2.0717370000	0.2303230000
C	-3.6296460000	3.2829820000	1.0333040000
H	-4.5072710000	3.9014190000	1.2314350000
H	-3.1940380000	2.9833700000	1.9887220000
H	-2.8989390000	3.8822070000	0.4871140000
C	-1.7677080000	-1.5152720000	1.2206260000
C	-0.6998640000	-0.6914510000	1.8684250000
H	-0.9646790000	0.3683290000	1.8802800000
H	-0.5875900000	-1.0256350000	2.9092370000
H	0.2655090000	-0.8048380000	1.3733420000

C	-1.4120760000	-2.9258480000	0.8589220000
H	-1.1830160000	-3.4753820000	1.7834820000
H	-2.2463400000	-3.4346590000	0.3696180000
H	-0.5392200000	-2.9726700000	0.2058340000
C	-3.1457800000	-1.3361180000	1.7849040000
H	-3.3837590000	-0.2883070000	1.9822170000
H	-3.9160370000	-1.7747520000	1.1478590000
H	-3.1801030000	-1.8649320000	2.7482530000

1 imaginary frequency: −359.06 cm^{-1}

R,R-radical adduct

Charge: 0

Multiplicity: 2

E = −1341.87530755

ΔG_{corr} = 0.350074

$\Delta G°$ = −1341.522206

Cartesian coordinates:

C	-2.9584870000	-1.1819600000	0.6447990000
C	-4.1476940000	-0.4578970000	0.7313810000
C	-4.3178000000	0.7546330000	0.0661930000
C	-3.2628710000	1.2553540000	-0.6976790000
C	-2.0495730000	0.5806500000	-0.8119170000
C	-1.9277610000	-0.6352890000	-0.1271610000
H	-4.9607700000	-0.8568720000	1.3297540000
H	-3.3840260000	2.2006520000	-1.2184740000
C	-2.8215840000	-2.4969100000	1.3708410000
H	-2.5910320000	-3.3130030000	0.6812900000
H	-2.0256400000	-2.4589000000	2.1182740000
H	-3.7539110000	-2.7407240000	1.8798820000
H	-1.3288190000	1.8828410000	-2.3514210000
H	-0.2708900000	1.7575130000	-0.9429110000

H	-0.3346960000	0.4374660000	-2.1305120000
C	-0.9282780000	1.1913650000	-1.6092720000
C	-5.6228870000	1.4991180000	0.1436820000
H	-5.4593190000	2.5781930000	0.1514100000
H	-6.2442830000	1.2649970000	-0.7258340000
H	-6.1820920000	1.2228780000	1.0386280000
S	-0.4253270000	-1.6302360000	-0.2927490000
O	-0.2304730000	-2.0037580000	-1.7325620000
N	0.6595340000	-0.5459660000	0.2953050000
C	1.9164390000	-0.4485570000	-0.4135060000
H	1.8513370000	-0.8503370000	-1.4310890000
C	2.2869480000	1.0256300000	-0.5663990000
O	2.9117350000	1.4408090000	-1.5090090000
H	3.2819770000	3.2917390000	0.3703750000
H	1.8188500000	3.5800970000	-0.5839250000
O	1.8680080000	1.7836280000	0.4399240000
C	2.1948770000	3.1870000000	0.3630540000
C	1.5514700000	3.8607220000	1.5504970000
H	1.7734630000	4.9294260000	1.5267150000
H	0.4677930000	3.7305540000	1.5271280000
H	1.9342840000	3.4476330000	2.4854470000
C	3.0606870000	-1.2356960000	0.3293420000
C	2.6030200000	-2.6880990000	0.4946740000
H	1.7814990000	-2.7719310000	1.2105720000
H	2.2828250000	-3.1155420000	-0.4608870000
H	3.4336060000	-3.2900480000	0.8719550000
C	3.3492900000	-0.6251300000	1.7017830000
H	3.7936200000	0.3700810000	1.6154630000
H	2.4380070000	-0.5439010000	2.2985580000
H	4.0581340000	-1.2620360000	2.2382790000
C	4.3209210000	-1.2058510000	-0.5389550000
H	4.1321540000	-1.6416420000	-1.5241030000
H	4.6973750000	-0.1911980000	-0.6811690000

H	5.1045820000	-1.7923290000	-0.0515210000

There are no imaginary frequencies

R,S-radical adduct

Charge: 0

Multiplicity: 2

E = −1341.87038932

ΔG_{corr} = 0.348572

ΔG° = −1341.518789

Cartesian coordinates:

C	-2.7116400000	1.1329250000	0.7767620000
C	-3.9289100000	1.3931340000	0.1444600000
C	-4.4945370000	0.4938880000	-0.7546320000
C	-3.8141660000	-0.6932990000	-1.0357990000
C	-2.5944380000	-1.0021390000	-0.4423170000
C	-2.0699330000	-0.0686110000	0.4628800000
H	-4.4448910000	2.3213010000	0.3682600000
H	-4.2430110000	-1.3991080000	-1.7410850000
C	-2.1369050000	2.1361260000	1.7448150000
H	-2.0328190000	1.7123150000	2.7470010000
H	-1.1497360000	2.4776810000	1.4240090000
H	-2.7917010000	3.0047150000	1.8123320000
H	-2.5028970000	-2.8987730000	-1.4309800000
H	-0.9607850000	-2.0352950000	-1.3596670000
H	-1.5862640000	-2.8323590000	0.0881910000
C	-1.8722900000	-2.2698700000	-0.8026120000
C	-5.8124690000	0.7837530000	-1.4197570000
H	-5.7001330000	0.7977400000	-2.5068140000
H	-6.5443840000	0.0093430000	-1.1765940000
H	-6.2122810000	1.7472460000	-1.1021660000
S	-0.5357760000	-0.4040270000	1.3384410000

O	-0.6021150000	-1.7243700000	2.0419110000
N	0.5576240000	-0.2059760000	0.1840630000
C	1.9234330000	-0.5950510000	0.5183410000
H	2.0013740000	-1.0694190000	1.5021960000
C	2.7760370000	0.6701600000	0.6149110000
O	3.4767210000	0.9147920000	1.5645750000
H	3.1773890000	3.2539900000	0.4317570000
H	4.5134560000	2.3875560000	-0.3425480000
O	2.6707180000	1.4545110000	-0.4512930000
C	3.4608650000	2.6617590000	-0.4405120000
C	3.1839510000	3.3904070000	-1.7329360000
H	3.7624970000	4.3159770000	-1.7594260000
H	3.4694160000	2.7799360000	-2.5917430000
H	2.1249250000	3.6409960000	-1.8163780000
C	2.4966170000	-1.6162680000	-0.5177400000
C	2.1625790000	-1.2245620000	-1.9588760000
H	2.5682240000	-0.2449970000	-2.2162460000
H	2.5932340000	-1.9653960000	-2.6385260000
H	1.0831620000	-1.1973060000	-2.1224040000
C	1.8803890000	-2.9812990000	-0.1960710000
H	2.2143800000	-3.7216250000	-0.9282810000
H	2.1821740000	-3.3219030000	0.7983670000
H	0.7895690000	-2.9418870000	-0.2215800000
C	4.0158060000	-1.6949270000	-0.3380250000
H	4.5101850000	-0.7675870000	-0.6441890000
H	4.2849210000	-1.9006700000	0.7020190000
H	4.4141110000	-2.5024090000	-0.9579050000

There are no imaginary frequencies

10. *References*

(1) Luo, J.; Zhang, J. *ACS Catal.* **2016**, *6*, 873–877.

(2) Ni, S.; Garrido-Castro, A.F.; Merchant, R.R.; deGruyter, J.N.; Schmitt, D.C.; Mousseau, J.J.; Gallego, G.M.; Yang, S.; Collins, M.R.; Qiao, J.X.; Yeung, K.-S.; Langley, D.R.; Poss, M.A.; Scola, P.M.; Qin, T.; Baran, P.S. *Angew. Chem., Int. Ed.* **2018**, *57*, 14560–14565.

(3) (a) Zhao, Y.; Truhlar, D. G.; *Theor. Chem. Acc.* **2008**, *120*, 215–241. (b) Grimme, S.; Antony, J.; Ehrlich, S.; Krieg, H. *J. Chem. Phys.* **2010**, *132*, 154104. (c) Krishnan, R.; Binkley, J. S.; Seeger, R.; Pople, J. A. *J. Chem. Phys.* **1980**, *72*, 650–654.

(4) Gaussian 16, Revision C.01, Frisch, M. J.; Trucks, G. W.; Schlegel, H. B.; Scuseria, G. E.; Robb, M. A.; Cheeseman, J. R.; Scalmani, G.; Barone, V.; Petersson, G. A.; Nakatsuji, H.; Li, X.; Caricato, M.; Marenich, A. V.; Bloino, J.; Janesko, B. G.; Gomperts, R.; Mennucci, B.; Hratchian, H. P.; Ortiz, J. V.; Izmaylov, A. F.; Sonnenberg, J. L.; Williams-Young, D.; Ding, F.; Lipparini, F.; Egidi, F.; Goings, J.; Peng, B.; Petrone, A.; Henderson, T.; Ranasinghe, D.; Zakrzewski, V. G.; Gao, J.; Rega, N.; Zheng, G.; Liang, W.; Hada, M.; Ehara, M.; Toyota, K.; Fukuda, R.; Hasegawa, J.; Ishida, M.; Nakajima, T.; Honda, Y.; Kitao, O.; Nakai, H.; Vreven, T.; Throssell, K.; Montgomery, J. A., Jr.; Peralta, J. E.; Ogliaro, F.; Bearpark, M. J.; Heyd, J. J.; Brothers, E. N.; Kudin, K. N.; Staroverov, V. N.; Keith, T. A.; Kobayashi, R.; Normand, J.; Raghavachari, K.; Rendell, A. P.; Burant, J. C.; Iyengar, S. S.; Tomasi, J.; Cossi, M.; Millam, J. M.; Klene, M.; Adamo, C.; Cammi, R.; Ochterski, J. W.; Martin, R. L.; Morokuma, K.; Farkas, O.; Foresman, J. B.; Fox, D. J. Gaussian, Inc., Wallingford CT, 2016.

(5) Marenich, A. V.; Cramer, C. J.; Truhlar, D. G. *J. Phys. Chem. B* **2009**, *113*, 6378–6396.

(6) Garrido-Castro, A. F.; Choubane, H.; Daaou, M.; Maestro, M. C.; Alemán, J. *Chem. Commun.* **2017**, *53*, 7764–7767.

(7) Fernández-Salas, J. A.; Maestro, M. C.; Rodríguez-Fernández, M. M.; García-Ruano, J. L.; Alonso, I. *Org. Lett.* **2013**, *15*, 1658–1661.

(8) Halland, N.; Jørgensen,, K. A. *J. Chem. Soc., Perkin Trans. 1* **2001**, 1290–1295.

(9) (a) Becke, A. D. *J. Chem. Phys.* **1993**, *98*, 5648–5652. (b) Lee, C.; Yang, W.; Parr, R. G. *Phys. Rev. B* **1988**, *37*, 785–789. (c) Stephens, P. J.; Devlin, F. J.; Chabalowski, C. F.; Frisch, M. J. *J. Phys. Chem.* **1994**, *98*, 11623–11627. (d) Vosko, S. H.; Wilk, L.; Nusair, M. *Can. J. Phys.* **1980**, *58*, 1200–1211.

(10) Chai, J.-D.; Head-Gordon, M. *Phys. Chem. Chem. Phys.* **2008**, *10*, 6615–6620.

(11) Grimme, S. *J. Comp. Chem.* **2006**, *27*, 1787–1799.

(12) Huang, W.; Ye, J.-L.; Zheng, W.; Dong, H.-Q.; Wei, B.-G. *J. Org. Chem.* **2013**, *78*, 11229–11237.

(13) Matos, J.L.M.; Vásquez-Céspedes, S.; Gu, J.; Oguma, T.; Shenvi, R.A. *J. Am. Chem. Soc.* **2018**, *140*, 16976–16981.